Sveučilište u Zagrebu

Grafički fakultet

Tomislav Hudika

UTJECAJ SASTAVA NANOKOMPOZITNOGA PREMAZA NA SVOJSTVA KARTONSKE AMBALAŽE

DOKTORSKI RAD

Zagreb, 2022.

Sveučilište u Zagrebu

Grafički fakultet

Tomislav Hudika

UTJECAJ SASTAVA NANOKOMPOZITNOGA PREMAZA NA SVOJSTVA KARTONSKE AMBALAŽE

DOKTORSKI RAD

Mentor: doc. dr. sc. Tomislav Cigula

Zagreb, 2022

University of Zagreb

Faculty of Graphic Arts

Tomislav Hudika

INFLUENCE OF THE NANOCOMPOSITE COATING COMPOSITION ON THE CARDBOARD PACKAGING CHARACTERISTICS

DOCTORAL DISSERTATION

Supervisor: Assist. prof. Tomislav Cigula, PhD

Zagreb, 2022

UDK 621.798:62-761:655

Imenovano Povjerenstvo za ocjenu doktorskoga rada:

1. izv. prof. dr. sc. Igor Majnarić, Sveučilište u Zagrebu Grafički fakultet, predsjednik,
2. doc. dr. sc. Tamara Tomašegović, Sveučilište u Zagrebu Grafički fakultet, članica,
3. izv. prof. dr. sc. Živko Pavlović, Sveučilište u Novom Sadu Fakultet tehničkih nauka, Srbija, vanjski član.

Imenovano Povjerenstvo za obranu doktorskoga rada:

1. izv. prof. dr. sc. Igor Majnarić, Sveučilište u Zagrebu Grafički fakultet, predsjednik,
2. doc. dr. sc. Marina Vukoje, Sveučilište u Zagrebu Grafički fakultet, članica,
3. izv. prof. dr. sc. Živko Pavlović, Sveučilište u Novom Sadu Fakultet tehničkih nauka, vanjski član,
4. doc. dr. sc. Davor Donevski, Sveučilište u Zagrebu Grafički fakultet, zamjenski član,
5. izv. prof. dr. sc. Nevijo Zdolec, Sveučilište u Zagrebu Veterinarski fakultet, zamjenski vanjski član.

Mentor:

doc. dr. sc. Tomislav Cigula, Sveučilište u Zagrebu Grafički fakultet

Datum obrane doktorskoga rada: 8. srpnja 2022.

Mjesto obrane doktorskoga rada: Sveučilište u Zagrebu Grafički fakultet

Povjerenstvo za obranu doktorskoga rada donijelo je sljedeću odluku:

„Obranio s ocjenom summa cum laude (*s najvećom pohvalom*) jednoglasnom odlukom Povjerenstva“

Onima u čijoj sjeni hodamo i onima koji dolaze iza nas.

Prije svega hvala mentoru, učitelju i prijatelju doc.dr.sc. Tomislavu Ciguli koji nije dizao ruke od mene, koji me savjetima usmjeravao i objasnio mi kako naći „*gap*“ u kojem egzistira znanost.

Zahvaljujem se doc.dr.sc. Marini Vukoje na prijateljstvu, pomoći i ohrabrenju na svakom koraku izrade ove disertacije. Zahvaljujem se i doc.dr.sc. Tamari Tomašegović na pomoći tokom svih ovih godina i strpljenju.

Hvala svim kolegama, upravi Grafičkog fakulteta, povjerenstvu, kolegama s Univerziteta tehničkih nauka iz Novog Sada, kolegama s Veterinarskog fakulteta, Zakladi za znanost i svima koji su doprinijeli izradi ovog rada te svima koji su sudjelovali u mom obrazovanju.

Najveća hvala mojim roditeljima Zrinki i Damiru na svakom danu, svakoj suzi, kapljici znoja, neprospavanoj noći kako bi me podigli, školovali i odgojili. Hvala što se ste mi uzor i potpora.

Hvala i ostaloj obitelji i prijateljima koji su bili uz mene, nadam se da ću opravdati vašu ljubav.

I na kraju hvala mojoj Ani koja je prolazila svaku stranicu sa mnom, koja je slušala moja razmišljanja, bezgraničnoj potpori i ljubavi. Hvala na svakom savjetu, toploj riječi i na toni strpljenja.

Informacije o mentoru:

Tomislav Cigula rođen je 24. listopada 1979. u Zaboku (RH). 2006. diplomirao je na Grafičkom fakultetu u Zagrebu, gdje je i doktorirao 2011. Od 2006. godine je radio kao asistent i viši asistent na Katedri za tiskovne forme, a 2017. izabran je u znanstveno-nastavno zvanje docenta u grafičkoj tehnologiji. Njegovo polje interesa su tiskarski procesi gdje sudjeluje kao suradnik na nekoliko projekata (domaćih i međunarodnih), a trenutno je voditelj projekta Hrvatske zaklade za znanost pod nazivom „Razvoj modela za povećanje efikasnosti izrade i funkcionalnosti grafičke ambalaže“.

Information about supervisor:

Tomislav Cigula was born on October 24th, 1979, in Zabok. In 2006. he graduated at University of Zagreb, Faculty of Graphic Arts, where he earned his PhD degree in 2011. Since his graduation he works at the Department for printing plates. In 2017 he was elected as an assistant teacher in the field of graphic technology. His field of the scientific research is the graphic reproduction processes where he was associate in several national and bilateral projects. Currently he is working as project leader on a project “Development of the model for production efficiency increase and functionality of packaging” financed by the Croatian Science Foundation.

Abstract

The aim of this research was to compose a nanocomposite coating which will upgrade existing varnish and enable transfer of the visual message and function of the packaging throughout the product's lifespan. To fulfil its role, packaging material is often coated. For this research, lithographic offset printed samples were coated with prepared nanocomposites in various nanoparticle's weight ratios (0.25%, 0.5%, 1% and 2 hybrid types (two types of nanoparticles in same coating)). The base of nanocoating was commercial water-based varnish while chosen nanoparticle were zinc oxide (ZnO), titanium dioxide (TiO_2) and silicon dioxide (SiO_2). The prepared samples were characterised by determining colorimetric values, barrier properties, surface and adhesion properties, resistance to colour fading and antimicrobial effect.

The results showed that ZnO nanocoating will have a smaller initial effect on the colour change of the printed image after coating than the TiO_2 counterpart but will also provide lower protection against induced accelerated ageing (UV radiation) or barrier properties for water vapour. Both nanocomposite types showed that increase of nanoparticle weight ratio leads to higher protection benefits. The hybrids (ZnO + SiO_2 and TiO_2 + SiO_2) provide better barrier to water vapour properties than the nanocomposites with single nanoparticle. All presented nanocomposites will upgrade varnish's antimicrobial properties, where the Hybrid/Z (Zno + SiO_2) showed the strongest inhibition potential overall.

This research provided a new method of possible varnish modification via added nanoparticle that can upgrade the protective benefits of the varnish against outer environmental influence such as UV radiation. The newly formed nanocomposite coatings protected the printed image while having limited effect on the colorimetric values of printed inks. Moreover, the prepared nanocomposite coating provided an inhibition of microbial growth.

Keywords: *cardboard packaging, coatings, nanocomposite, zinc oxide, silicon dioxide, titanium dioxide*

Sažetak

Ambalaža, kao važan segment grafičke industrije, ima značajnu ulogu u vizualnoj komunikaciji te mora biti očekivane razine kvalitete tijekom cijelog vijeka trajanja proizvoda. Kako bi se to postiglo, otisnuti ambalažni materijal se često premazuje. Cilj ovog istraživanja je stvaranje nanokompozitnog premaza koji će unaprijediti funkciju osnovnog premaza te omogućiti prijenos vizualne poruke i funkciju ambalaže tijekom cijelog vijeka trajanja proizvoda.

Ambalaža se dijeli na primarnu, sekundarnu i tercijarnu. Sekundarna je u kontaktu s kupcem i treba osim osnovne uloge – zaštite proizvoda, vizualno privući kupca. To se primarno postiže primamljivim dizajnom ili prijenosom informacija. Problem nastaje kad ambalaža nije standardne odnosno očekivane kvalitete te s vremenom, ako nije prodana, gubi na kvaliteti u smislu degradacije otiska ili smanjenja strukturne čvrstoće materijala. Jedan od primjera je ambalaža koja se nalazi u izlozima te je izložena elektromagnetskom zračenju, što s vremenom uzrokuje degradaciju vizualnih, ali i mehaničkih svojstava. Degradacija se najčešće očituje kao izbljeđivanje boje i postupno gubljenje slikovnih informacija, uključujući barkodove, što može uzrokovati smanjenje prava kupaca na jasnu informaciju. Jedna od mogućnosti zaštite proizvoda, odnosno slikovne informacije je aplikacija specijaliziranih folija i lakova (npr. UV lak koji se suši djelovanjem UV zračenja, vododisperzivni lak – lak na vodenoj bazi te uljni lak).

Za ovo će se istraživanje pripremit će se ofsetni otisci te premazati pripremljenim nanokompozitima. Baza za nanokompozite je lak na vodenoj bazi u koji se dodaju nanočestice titanijevog dioksida (TiO_2), cinkovog oksida (ZnO) u masenim koncentracijama od 0,25%, 0,50% te 1% te kombinacija TiO2/ZnO i silicijev dioksid (SiO_2). Pripremljeni uzorci su karakterizirani određivanjem kolorimetrijskih vrijednosti, barijernih i adhezijskih svojstava, otpornosti na svjetlosnu degradaciju te antimikrobnog djelovanja. Istražena je i optimizacija sastava nanokompozita prema željenom djelovanju.

Metode kojima se vršila karakterizacija podijeljene su u dvije kategorije, vizualni doživljaj i mehanička karakterizacija, a dodatno su ispitana površinska svojstva i antimikrobno djelovanje. Za analizu vizualnog doživljaja korištena je kolorimetrija i denzitometrija kako bi se istražio utjecaj premazivanja otiska nanokompozitima na promjenu tona boje kao i mogu li nanokompozitni premazi umanjiti utjecaj UV zračenja i tako zaštiti otisak. Snimanje i analiza SEM mikroskopskih otisaka poslužila je kako bi se detektirali mogući aglomerati nano čestica na površini otiska, dok je EDS metoda poslužila kako bi se istražio kemijski sastav

mikrovidljivih nakupina. FTIR-ATR metodom kemijski se analizirao sastav i struktura površine prije i nakon premazivanje kao i nakon UV radijacije. Tom metodom ustvrdilo se posljedično stanje unutar strukture laka te analiziralo što se i kako događa kao posljedica ubrzanog starenja.

Izmjerila se i analizirala čvrstoća uzoraka putem testa pucanja, otiranja i savijanja. Površinska svojstva određena su mjerenjem kontaktnog kuta referentnih tekućina čime je omogućeno određivanje slobodne površinske energije odnosno posljedično određivanje sile adhezije.

Kako bi se utvrdila mogućnost inhibicije mikrobioloških kultura, napravljena je detaljna analiza na nekoliko bakterija i gljivica (*Staphylococcus aureus* ATCC 25923, *Yersinia enterocolitica* 4 / O: 3, *Listeria monocytogenes* ATCC 7644, inokulacija enterobakterije (*Citrobacter spp.*) u liofiliziranom obliku te plijesan *Penicillium spp*).

Rezultati su pokazali da dodatak ZnO uzrokuje manju početnu devijaciju za cyan i crnu dok kod žute i magente ima veću u odnosu na premazivanje vodenim lakom, no slabije djeluje u usporavanju degradacije. TiO_2 s druge strane ima veću početnu devijaciju, no uslijed djelovanja UV zračenja pruža bolju zaštitu otiska, ali i bolja barijerna svojstva za propusnost vodene pare. Dokazano je i da povećanje masenog udjela nanočestica povećava i razinu zaštite. Što se tiče antimikrobne zaštite, svaka nanočestica djeluje, no Hybrid/Z ima pruža najbolje rezultate na prikazane mikrobne kulture.

Istraživanje je dokazalo da odabrane nanočestice ZnO i TiO_2 same ili u kombinaciji sa SiO_2 (hibridi) imaju mogućnost usporavanja i smanjenja utjecaja degradacije potaknute UV zračenjem. Isto tako poboljšana su barijerna svojstva otisaka odnosno ambalaže premazane nanokompozitima u odnosu na premazivanje nemodificiranim lakom. Dodatno, modificiranjem laka dodanim nanočesticama postignuto je povećanje antimikrobnog djelovanje.

Ključne riječi: *kartonska ambalaža, premazi, nanokompoziti, cinkov oksid, silicijev dioksid, titanov dioksid*

Contents

1 Introduction

1.1 Preliminary research of consumer's behaviour

Packaging is generally divided into primary, secondary, and tertiary; where primary is in the contact with the product (content), secondary is the one in the contact with the users and tertiary is used for transportation. The secondary, as stated, is in the contact with the customer and protects the product, but it also must visually attract the customer. This can be achieved through graphic design and transfer of needed information. The most problems occur when the packaging does not meet the expected quality level and with time, loses its overall visual and structural feature. This mostly happens with the visual degradation of imprints including images and barcodes (colour fading), which leads to reducing the consumer's legal right to clear information. Furthermore, it leads to unappealing visual appearance which makes it difficult if not impossible to sell.

To find more on the customer's stance on packaging the survey was held with 155 examinees via *Google Survey*. It consisted of the 20 questions relevant to the subject. The examinees were 52.8% female, and 47.2% male. The most examinees were from 18-35 old (75.4%), while 20.8% were from 35-50. The group mostly had high school (43.4%) and university degree (39.6%), most being without children (75.5%), all seen in the Figure 1. From the results, most consumers (60.4%) believe that ink's colour degradation on the outer packaging shell reflects the quality of the content structure.

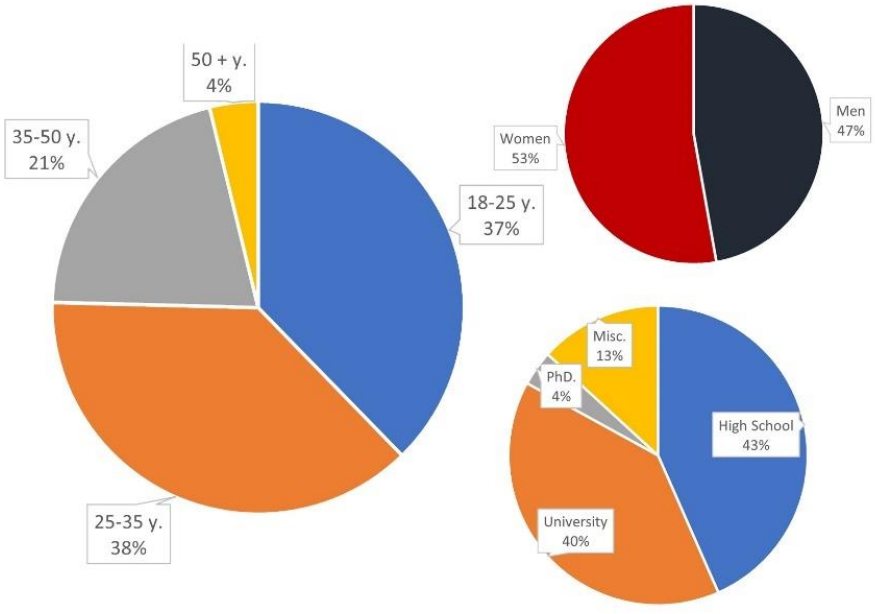

Figure 1 Age, gender and education of the examinees

The 58.5% of people said that if they see the damaged packaging, they think that the product is damaged as well. Moreover, 34% of the people think that the packaging reflects the quality of the product. When it comes to cheaper products, 64.2% of people do not really care about the packaging quality, but when it comes to more expensive items, 38.5% think that packaging is important as they are buying the whole package (product and the packaging). Mechanical wear such as scratches and visual degradation of the image do not worry the most people as they think that the product inside is intact while most find other mechanical wear such as moist and structural damaged a big problem (60.4% in both cases). From obtained results, one can conclude that most people do observe the state in which the packaging is in the time of the purchase. Moreover, they would pay a little extra if they were aware that the packaging is protected from potentially hazardous microbes (34.6%).

1.2 Aim of the research, hypotheses, and the methodology

The aim of this research is to determine the influence of varnish modified with nanoparticles on colour degradation caused by UV radiation, to investigate the barrier properties of the packaging material, coated with nanocomposite coating and its antimicrobial properties. Beside other, it is important to define the optimal compound mixture of nanocomposite regarding ISO standard.

H1:

The addition of nanoparticles in commercial varnish will influence the properties of nanocomposites and of the coated printed samples. However, it will not create significant change of the sample colorimetric.

H2:

The addition of nanoparticles in commercial varnish will lower the overall degradation caused by electromagnetic radiation while improving barrier properties of the packaging material.

H3:

Coatings enriched with TiO_2 and ZnO nanoparticles with the help of the UV light will improve the antimicrobial properties of the packaging material.

To enable determination of nanocomposite influence on prepared printed samples, the following methods were used:

- To investigate the coating's viscosity, rheological analysis of coating before and after adding nanoparticles was performed;

- To enable physical and optical surface characterisation the Scanning Electron Microscope (SEM) analysis will provide an input on nanoparticle behaviour after coating (i.e., whether agglomeration occurred);

- To simulate the exposure to UV light through the glass window (i.e., direct sunlight through shop window to match ASTM 3424-11 2011 standard) after coating process, samples will be put into Cofomegra Solarbox 1500e Xenon Test chamber that simulates;

- To investigate the chemical change to nanocomposite coating after it is exposed to UV radiation and therefore obtain an insight into the degradation process, Fourier-transform infrared spectroscopy (FTIR-ATR) analysis was performed;

- To provide information on overall strength and how the UV radiation influences the material, bursting, rub and bending analysis was performed;

- The adhesion parameters will provide the information on applicability of the nanocoatings;

- To investigate the water-vapour throughput rate of material before and after nanocomposite coating and UV exposure, barrier properties analysis via water vapour transmission rate (WVTR) was performed;

- The microorganism growth inhibition properties before and after nanocomposite coating and UV radiation exposure were tested to assess the antimicrobial potential.

1.3 Background

All industrial areas are generally impacted by two factors, the available technology, and the overall costumer's needs. Printing industry is no exception where some sectors have decreased in volume, leading the overall revenue decrease of the industry in general. The biggest struck sort of speaking came, with the introduction of new media such as internet and desktop publishing. Furthermore, "green" agenda also pushed the graphic industry even further labelling it as the "forest killer". Despite these negative influences, the need for printed packaging is

growing continuously worldwide. The forecast is that the total growth should reach about 269 billion US by the year 2024 [1]. There are different reasons for this kind of growth, for example the development of the new market ventures, increased consumers awareness of consumption (smaller packaging), personalised packaging, overall market globalisation, etc. To answer these consumer's needs, the industry must introduce new materials and processing steps.

Packaging in general is the science, art and technology of goods protection, distribution, sale, and use. It also has a highly significant role in visual communications, and must maintain a certain desired and defined quality level throughout the product's lifespan on the shelf as well. This means that printed packaging must be resistant to various influences before and after purchase where a sustainable packaging disposal plan must be provided. The environmental impact of production must be considered when considering the whole lifespan of a product, not only its production. Beside this parameter, packaging must provide some marketing value in terms of attracting the potential buyers to buy the primary product. The challenge for the packaging lies in the need to reflect quality and price of the primary product.

To tackle issues stated in the *1.1 Preliminary research of consumer's behaviour* chapter, printed packaging must be protected from outer influence. One of the possible methods of protection is the application of special foils and varnishes. Coating process on the printed packaging is much cheaper from its foil counterpart, and there are many available commercial coatings which differ in chemical composition, technology of application, curing and pricing. The common varnishes used in the printing industry are UV based varnishes that cure via UV radiation, water based (WD) and oil-based varnish. Printed industry coatings are also more environmentally friendly which in long turn lowers the CO_2 footprint of the product [2]. Coatings as mentioned, have protective properties as well as visual ones, where the visual effects can boost the level of communication i.e., to highlight the wanted information that can influence the customer to buy the product. Protective purpose can be oriented in couple of directions depending on the needed effect, but mostly it is used towards mechanical damage or/and atmospheric influences, i.e., the protection against ink degradation caused by UV radiation (Sunlight). Coating should minimize the UV radiation influence on ink but at the same time cause minimal change in the products appearance. The offset printing is defined by ISO 12647-2:2013 standard, which defines colorimetric values of primary colours in CIE L*a*b* colour coordinate system. The standard states that ΔE_{ab} colour difference must not exceed tolerance of 5 for the process colours (CMYK). As it is known, any additional layer will affect the colour appearance, especially coatings (varnish) as they are not 100% transparent

substances, mostly due to their composition, curing system, application thickness and surface interaction with the substrate. Therefore, one should take into account the standard designated values when applying the coating. In the recent events regarding COVID-19 pandemic, consumers are more aware of the microbes which can be found on all surfaces. During the early stages of the pandemic, some scientists advised the people that cleaning your items when you bring them home from the shop can prevent spreading of microbes, therefore it could help cope with the pandemic spread [3]. The coating that potentially has the ability to provide certain microbe inhibition potential could be beneficial from marketing as well as the public health point of view. The antimicrobial packaging market was valued as 9.13 billion US dollars in 2020 before the COVID-19 pandemic started and due to it, it is projected to reach 13.86 billion US dollars by the year of 2028. The Compound annual growth rate (CAGR) is 5.4% on the global market [1]. This could also be a powerful marketing tool as it would possibly provide a certain feel of security to know that the packaging you are holding in the shop has better protection against microbes, both bacteria and fungi, than other one. Moreover, it is known that more and more bacteria are getting more resistant as the global antibiotic use grows, therefore, to provide another tool could be a new strategy [4].

Although existing coatings provide many benefits, they can be upgraded by introducing certain compounds in the mixture that are known for their protective potential. In some published papers, those kinds of compounds are in nano size (<100 nm) [5,6,7,14,15]. Nano sized particles are homogenized into commercial varnishes, creating a nano composite mixture. The homogenization process will ensure that nano sized particles do not create any agglomerates which can influence the overall performance of the nano composite.

In those research papers regarding enhancement of the varnish properties, silicon dioxide (SiO_2), titanium dioxide (TiO_2) and zinc oxide (ZnO) were used, each known for some benefit. In one of the papers, used SiO_2 showed that nanocomposite varnish is better absorbed on uncoated than on the gloss coated substrates where they remain mostly on the paper surface [16]. In addition, nanocomposite coatings caused bigger colour change on matte coated than on gloss coated paper substrate. Samples coated with UV nanocomposite showed higher print gloss and mechanical resistance to bending while those coated with water-based varnish nanocomposite coating showed higher resistance to tearing. In both cases, one could not visually detect agglomerates of nanoparticles on the sample surface. Metal oxides, ZnO and TiO_2 are both well known for their ability to absorb UV radiation and are both commonly used as part of inks, colours, coatings, sunscreens, etc. [11,14]. Some research papers used ZnO

nanoparticles homogenized with the commercial aqueous (water based) varnish as base. The result showed that applying the nanocomposite will not create notable colour change with maximum of ΔE_{00}=2.84, but will affect the increase of the tone value at 80% for additional 5%. Moreover, ZnO nanoparticles did upgrade the water-vapour barrier and lower the overall ink's fading [13].

In another research paper, ZnO nanoparticles dispersed in maleic anhydride modified polypropylene (MAPP) were used to protect the rubberwood from degradation induced by the UV radiation. Beside MAPP-ZnO nanocoating, ZnO was also blended with polyurethane (PU). The UV radiation on wooden materials, beside fading, causes the breakdown of wood polymers in the surface layer which leads to creaking. The research showed that both nanocoating mixtures did restrict the colour change and photodegradation of the wood polymers [7].

In the study by Hudika et al. that investigated the TiO_2's nanocomposite influence on antimicrobial properties proved that the TiO_2 in 1% weight ratio is the highest ratio to maintain the colour values in FOGRA PSO designated range. The work also showed that with the increasement of the TiO_2 weight ratio, antimicrobial influence increases [17].

Several studies showed that metal oxide compounds demonstrate antifungal and antibacterial properties against broad range of bacteria [5,6,18,19]. Previously mentioned compounds, ZnO and TiO_2, are known as microbicides. Research of antimicrobial properties was made on wood, using a nanocomposite composed of polyurethane varnish and ZnO nanoparticles, which was exposed to *Staphylococcus aureus*, *Escherichia coli*, *Pseudomonas aeruginosa* bacteria, and *Saccharomyces cerevisiae* fungi. Nanocomposite was made with polyurethane varnish as the base and ZnO was added in designated weight ratios of 0.4% and 0.7%. In both cases, inhibition potential was between 85–100% on all stated bacteria, except *Escherichia coli* [12].

TiO_2 nanocomposite also showed its antimicrobial properties. Bacteria *Pseudomonas aeruginosa* and *Escherichia coli* were both treated with nanocomposite coating containing TiO_2. They were exposed to UV radiation where during the process, the UV induces TiO_2's photocatalysis where oxygen free radical develops. Those radicals lead to inhibition action on bacteria's cell wall which slows the overall bacteria growth [6,9,18] . Moreover, the TiO_2 is interesting since the compound has photocatalytic nature, is chemically stable and it is non-toxic. Furthermore, TiO_2 has the ability to create a strong oxidizing power due to photocatalytic morphology creating free radical generation such as hydroxyl and superoxide anion radicals which leads to growth retardation of microbes [15].

In the study by Hudika et al. that investigated the TiO_2's nanocomposite influence on antimicrobial properties proved that the TiO_2 with the increse weight ratio does influence the antimicrobial properties. The work used the unspecified microbial colonies from the ambient environment [17].

As stated before, in the recent light regarding COVID-19 pandemic, more consumers are more aware of the microbes which can be found on all surfaces. Antibacterial packaging is not a novelty, but it is mostly regarding primary packaging which is in interaction with the product. The main purpose is to reduce, inhibit or retard the growth of spoilage or pathogenic microorganisms on food or other surfaces [20]. Even more, smart and active sensors which can detect change inside the packaging are in use worldwide. There is an important distinction between package sensor function that are smart and those which are active. The active ones create a response to a triggering event such as overexposure to UV light, too big temperature difference in its life cycle, release of CO_2 (when the meat inside the packaging is too old etc.), and it continues to create that response until the process is exhausted. The smart packaging on the other hand, mostly contains a sensor that indicates that the product was or is exposed to some unwanted change that has the potential to be hazardous to the consumer. The time to temperature indicators (TTIs) show irreversible change of the sensor, being colour or shape [21].

More and more people are aware that microbes exist on the outer side of the packaging. According to the survey presented in *1.1 Preliminary research of consumer's behaviour* chapter, 64% of the examinees are aware of the potentially hazardous pathogens living on the packaging surface. With the COVID19 outbreak the common sight was to see buyers wearing surgical gloves when browsing the stores. This was mostly connected with the fear that someone else who is potentially ill have touched the item before. For most people, there is no medical benefit to wearing gloves at the grocery store [22]. Introduction of the antimicrobial secondary packaging could be highly beneficial for customer protection, and it has an important marketing role for the packaging buyers (goods manufactures). Projected growth according to CAGR for antimicrobial packaging is 5.89% or USD 13.86 Billion in the period between 2021–2026. Amidst the pandemic, with the rise of patients suffering with respiratory problems, secondary fungal and bacterial infections are on the rise. According to Lancet, 50% of the patients died from the viruses had secondary infections, which provides the necessity to cope with this issue [23].

2 Theoretical part

2.1 Packaging industry

By simple definition, packaging means wrapping or bottling any kind of products to make them safe for transport, storage and later usable. To ensure the product is marketable, packaging must be easy to distinguish from the competition, easy to identify, describe and promote. Different product type requires different kind of packaging. The biggest evolution of the packaging occurred during the significant times in the human history, mostly in the 20th century. Industrial revolution created a need for better quality products since more goods became available in the trade market. During those time, all kind of material were expensive and scarce, so packaging was mostly limited to luxury goods [24].

The period of the World War 1 was in the packaging terms, a renaissance. The numerous new inventions came to life such as moulded glass, carboard boxes, polymers such as cellophane and metal cans which are still in the use today [25]. With the numerous new materials and inventions, the manufactures had to distinguish themselves, so idea of identity and advertising became very important. Shortly after the World War 1, in the October of 1929 the Great Depression hit the Wall Street market and crashed the economic system creating a new and significantly changed consumption and requirement habits [26]. World War 2 and its post era consumerism created a rise of single use materials. The discovery of aluminium foil and more enhanced polymers – simply called “plastic” made a new manufacturing, scientific and economical breakthrough [27].

Second half of the 20th century and bigger digitalization enabled the expand of the markets from local to global in a very short period. Television came and suppressed radio which resulted in possibility of visual representation of the good through advertising. With all that competition, packaging was the only thing that could present and distinguish the product on the shelf [28].

The terminology is different, but two terms are often simultaneously used, packing and packaging. Packaging means the cover or the sheet that covers, holds, and protects the product from outer influence such as damage, leakage, pollution, UV radiation, contamination, dust etc., while packing means inserting product into previously mentioned covers or sheets. Moreover, packing means putting all the smaller packages into a box, container, crate meant for the purpose of handling i.e., storage or transportation [29].

In the sense of product's identity, packaging is essential. Therefore, packaging can be also defined as a process of providing a protective and informative covering to the product in such way it is beneficial to the manufacturer and consumer as well [30]. From the manufacturer perspective, as mentioned before, packaging has to provide needed protection during handling, storage, movement and also to bring a level of identity to the product [31]. As to consumer, packaging has to distinguish the product from its competition while it has to give a valid and needed information about it, such as content or health regulations [32]. This level of information transport is achieved via both product and graphic design [33]. With the help of shape, size, colour and visualization of information which is formed that gives the product needed visibility. Moreover, due to laws, consumer has the right to information regarding the product. That information is mostly in terms of what volume, colour, size, content or when it comes to food, weight, expiration date, energy values, ingredients content or whether if the food was prepared in certain way i.e., Halal, vegan, Kosher etc. This is controlled in the European Union by Consumer right directive (Directive (EU) 2019/2161) which was amended on the 27$^{th\ of}$ November 2019 by the EU parliament in order to better enforce and modernise consumer protection rules. This amendment is part of EU's consumer law – New deal for Costumers. This basically states that the consumer has the right and the manufacturer/third party is obligated to give all needed information for physical and digital products [32].

There are many important functions of packaging, but the most crucial ones are to protect, unitize and to contain. Protection role is to ensure safe handling, movement, and storage while it minimalizes damage during shifting. Moreover, it should provide protection from outer influence such as heat, cold, moisture or UV radiation [29]. Often, it should provide a safe seal to prevent any kind of tempering with its content. This is done with a printed label or some sort of polymer stripe seal [34]. To ensure a more efficient transportation, packaging is often unitized to optimise storage space and cut down expenses, time and effort in handling and transportation process [35]. To ensure better useability, packaging has to be convenient to store, open and carry as well while its contain should fill the inner packaging volume. This will also ensure better and optimized use of goods needed for production of packaging and cut down the transportation costs [36,37].

Packaging is divided into three types, defined by its purpose: primary, secondary, and tertiary. Primary packaging is the packaging in direct contact with the product itself. It is often referred to as consumer or retail packaging as well. The main and only function is to protect the content and to contain it. In most cases, the inside of the packaging is considered primary, and it extends

its use to most products regardless of if they are food or consumable. Sometimes, primary packaging can also have several components for one product. The best example is a beer bottle or a metal can (fish, meat, soup, beer, or soda). It must function as a container for the product while transferring an information needed for the customer. Carboard secondary packaging can often be found for luxury products such as cosmetics to simulate the sustainability (Figure 2) [38].

Figure 2 Sustainable cardboard packaging [39]

Secondary packaging is referred to the outer shell meant for branding, display, or logistics. It also must protect and collate individual units during storage. In single pack usage it is mostly used by food, beverage, or cosmetics industry for displaying primary packaging on shop shelves. Secondary packaging can be divided into three separate groups, retail-ready packaging (RRP), shelf-ready packaging (SRP), and counter-top display units (CDUs) [36-39]. Secondary packaging in most cases is made of a cardboard substrate with printed image with combination of some other materials, primarily transparent polymer so the content can be seen. It is also common that some type of specialized foil or varnish is used for enhancing visual effect. This packaging type is seen by the consumer [41].

Tertiary packaging is a group packaging set that facilitates protection, handling and transportation of sale units which consists of secondary packaging. This type of packaging is mostly not seen by the consumer. It can have some type of information printed on, such as

products name, unit count, weight etc. This type is often made of a corrugated carboard or wood in the form of a crate [42].

With this in mind, one can conclude that main purpose of all three types of packaging is the same: protection of the product. The term protective function coefficient is numerical value which enables evaluation of packaging [43], the bigger value means better protective features. Mathematical function (1) for that coefficient is:

$$\tau_Z = \frac{\tau_\rho}{\tau_\eta} \quad (1)$$

Where are: τ_z – overall protective function coefficient, τ_p – expiration time of packed product, τ_n – expiration time of an unpacked product.

The usual coefficient value of protective function is 1-2 for fresh products i.e., fruits; 10-100 for dehydrated products i.e., toast bread and 100-1000 for sterilized products i.e., canned meat [44].

2.2 Packaging materials

The choice of materials used for packaging is one of the key elements as it affects many different features [29,43]. The choice will dictate how is packaging going to be handled and stored, in what conditions and for how long. Packaging materials in general, refers to all materials used in the planning and creating the final packaging. The most common ones are metal, glass, wood, paperboard, textile and polymers [45,46].

When constructing and planning the packaging, it is crucial to think about what the purpose is, how is it going to be handled and stored, how it must protect the product, how is it going to be used and how is it going to be disposed later. In short, entire life span of the product must be considered [47]. Although, polymers were introduced due to their lower price than wood or paper, they are slowly being dismissed from general use due various reasons, one of is ecology [27]. New environmental direction of industry and society put the spotlight on biodegradable polymers and bigger industrial market share of recycled paper and other recyclable materials. Plastic straws, plastic eating tools, cups etc., which were in broad use around the world are now

becoming thing of the past [48]. Today it is not uncommon to see companies' marketing strategy stressing the need of environmentally acceptable materials [49].

Packaging material must be mechanically sufficient to withstand chemical, biological and mechanical influence. It is also beneficial if it is resistant to UV degradation as well. Mechanical stability of material has to be enough to resist any deformations or outer mechanical forces that could inflict wear or tear, endangering the product [46].

The packaging surface is, in most cases, constantly under some sort of influence and it basically acts like the first line of protection. Inner surface of the primary packaging interacts with the content. In the case the content is food, it has to be nontoxic, without any specific smell or taste, has to be impermeable to liquids and grease [50]. When it comes to permeability of material it can be mechanical (resistant to moist), optical (resistant to light) and chemical (resistant to chemical influence) [46]. Every packaging material has its advantages and disadvantages, so choosing the right one is a crucial matter. Polymers are relatively easy to produce, they have great mechanical and barrier features, they are lightweight and cheap but not all can be recycled or composted after use [48]. The biggest disadvantage of all is the interaction with the food content and higher price than paperboard [51].

European Union's directive about packaging and packaging waste, 94/62/EC from December of 1994, has the wide goal to minimize the impact of packaging and its waste on the environment and to open the free trade of goods [52]. In the May of 2018, the EU modified the Directive limiting use of plastic bags and introducing a obligatory use of sustainable packaging in the future [53].

According to the directive 94/62/EC, by the 31st December of 2008, all Union members had to ensure that recycling for materials is consisted of 60% paper, 60% glass. 60% metals, 22,5% polymers and 15% wood. After due date, Union members had to set even bigger recycling goals for themselves and fulfil them on an annual rate [54]. The part of the directive that states that manufacturer of over 50 tons of packaging materials per year is responsible and must pay the pollution fee, shifted the industry's focus on new materials and technologies. Some hazardous materials and compounds used in the manufacturing process such as Hg, Pb, Cr^{6+} and Cd have also been banned [52]. According to the new revised directive 2018/852 of the EU parliament, amending the 94/62/EC new goals have been set, with the target dates of 31st December 2025 and 31st December 2030. The overall waste must be at least 70% recycled with some specified materials such as glass (75%), plastic (55%), aluminium (60%), metal (80%) etc. [53].

2.3 Branding and packaging design

When thinking about the packaging design one must tackle two issues at the same time. The design that must be easily noticed and be innovative while it must be as optimal to accommodate the transportation requirements [55]. For packaging to stand out, designers and engineers often use new structural forms which in the long term can increase the handling and transportation price, and if it's not well engineered, can endanger the structural form of the entire packaging [56]. On the other hand, if design is made to accommodate the transportation requirements, designers must find new solutions for packaging to stand out. The packaging shape can help with protection from mechanical influence such as impact, can help as well with the ability to stock it more efficiently in the storage or on the shelf [37]. Beside protection, shape has also an important function of communicating with the consumer. The shape can tell the customer how to handle it, open it and use it. Best example for that is the boxed milk from who's shape one can tell how to open and pour milk.

On the other hand, branding is oriented to marketing of the product and sales. Branding of the product mostly involves the packaging due to fact that consumers buy either by the brand/product name or by the looks. Therefore, product and its packaging work in a joint venture in terms of sale [49].

The brand identity mostly depends on two separate components, visual and structural. Both components communicate with the customer on visual and perceptual level as they combine and form the story around the item. This is achieved through colour, typography, images, shapes, materials, and size [56].

2.4 Paperboard

As a results of COVID-19 pandemic, economic impact, and transition to an “on-line world” in 2020 resulted that multiple paper producers dismiss capacity of graphic paper production, up to 40%. Some paper mills reorganised paper machines to paper packaging grades [57]. In the year later, 2021, the market bounced back as the entire market re-opened. Although the market is back, mill cost, wood pulp, fuel and energy skyrocketed which increased the paper prices worldwide [58]. According to the DAT Freight & Analitys report, in the USA alone, Load-to truck ration (number of loads posted for every truck posted) is at 6:1, which is double the norm of the normal paper demand [59].

In 2019, pulp and paper market was valued at 348.83 billion US dollars and according to the forecasts by the year of 2027 that market has the potential to expand up to 370 billion US dollars increase of CAGR [60].

Paper, as the basic material in the printing industry can be defined as a substance made from wood pulp, straw, rigs, or other material. It is usually in thin pre-cut sheets or rolls, used for writing, wrapping, or printing. Paperboard is a thicker paper-based material. Beside name, there is no rigid distinction between paper and paperboard as most people refer to both as either paper or paperboard.

Industry on the other hand, classed those two terms according to the grammage, therefore paper is considered all paper-like material below 250 g/m^2. The paper can also be classed more accurately by its grammage, purpose, finish, structure, thickness, smoothness, barrier properties, whiteness etc. Paper grammage refers to how does the paper sheet weights in grams per m^2. In general, paper is divided and defined by ISO standards [61]. In the Table 1, the denomination of paper by its grammage according to Klemm [62].

Table 1 Paper classification by its grammage according to Klemm

GRAMMAGE (g/m^2)	**TYPE**
6-150	paper
250-500	paperboard
600-5000	cardboard

In Table 2, the denomination of paper according to its purpose can be seen [63]:

Table 2 Paper classification to its purpose

GRAMMAGE (g/m²)	**TYPE**	**PURPOSE**
80-100	office	flyers, brochures, documents, inner pages, notes
110-120	letterhead	general stationary
130-170	durable	posters, leaflets
170-200	halfway	brochure covers, double side flyers
200-250	quality paper	quality printing (more luxurious)
300-400	paperboard	printed packaging, business cards
400+	cardboard	high-end business cards, luxury goods

The corrugated cardboard is not stated in the table above as it described by the different parameters such as number of layers, thickness in millimetres or flutes (USA) [64].

Corrugated cardboard is thicker and heavier than paperboard thus it is used for box making and packaging that requires higher level of protection. Usually, corrugated type packaging (Figure 3) is not visible to the customer so it rarely has some type of image printed on beside the handling instructions [42].

Figure 3 Corrugated transport boxes [65]

The advantages to the cellulose-based materials are that they are cheap, easy to handle with, they are biodegradable, can be recycled rather easy. When compared with polymer materials, the main advantage is that cellulose-based material production is sustainable and eco-friendlier. Most of the cellulose-based material such as cardboard is recycled after use [66].

One of the important features regarding the production, costs, printing, and finishing is the fibre direction of the paper or paperboard. This also dictates the production price of printed product due to desired format that must be “cut out” from the paper sheet. For printing process, the

fibres must be aligned with the printing cylinder of the printing press. This will lower the dimension change when it gets wet. The paper is hydrophilic material due to its porous surface. When the liquid or moisturise reaches paper, paper fibres attract the liquid and swell creating this phenomenon [67].

2.5 Packaging printing process

In general, packaging printing process can be done with all printing techniques but five are the most dominate ones: offset (lithography), flexography, screen, digital (inkjet and electrophotography), gravure and pad printing. All five techniques have their advantages and limitations, i.e., offset printing can achieve high reproduction quality but the substrate has to be flat cardboard and it has limitations do to sheet's thickness; flexography can print on corrugated cardboard but it lacks the offset quality; screen can achieve thicker layers of colour but it lacks the speed; pad can print of curved surfaces but it is limited by the printing pad's size, etc. [67]. Choosing the right printing techniques is crucial when constructing and designing the packaging. Some techniques are controlled via ISO standards that guarantee that all samples are the same throughout the printing process.

For instance, offset (lithography) printing is controlled by ISO 12647:2-2013, that dictates the process for four colour (CYMK) printing [68]. Today, almost all printing products including packaging are printed with combination of standard printing technique and some sort of protective coating. This technique hybrids are made to achieve the wanted result in terms of visual and protective purpose [69].

Offset printing is an indirect printing technique that involves transfer of the image from a metal printing plate to a rubber blanket roller and from there to the substrates surface. In this method, the substrate itself does not come in the contact with the printing plate. In some literature offset is also known as an offset lithography printing.

The predecessor to modern day offset was the stone litography printing technique. This technique was direct but used the similar chemistry techniques to create the image. The stone surface was drawn on with a greasy ink or chock. The stone was coated with a special gum-arabic solution where the parts without the greasy ink were prepared to adhere the water.

In lithography, the printing and the non-printing elements are at the same level [70]. The common reproduction process today includes motive development and creation of portable document format (PDF). The PDF file is then process by RIP (Raster Image Processor) to create 4 achromatic separated colour channels, CMYK, or cyan, magenta, yellow and black (Key), (Figure 4). The channels are created as a 1-bit TIFF.

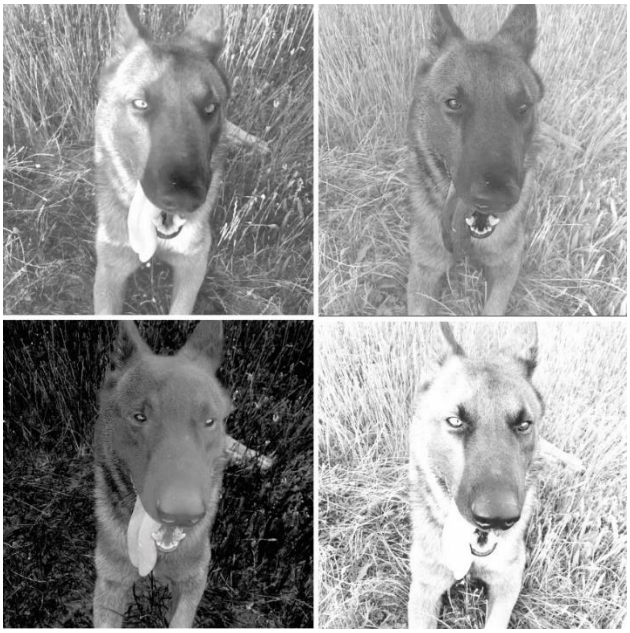

Figure 4 CYMK separated image

The 1-bit files are sent to the computer-to-plate (CTP) unit where it is, depending on the printing plate and the CTP type are chemically developed to create a printing motive. This process creates the similar effect as in the older lithographic technique. The finished printing plate is put into the printing press.

The printing process starts with fountain solution dispersed on the printing plate's surface where it adheres only on the non-printing elements. The ink is then transferred to the printing plate where it only adheres on the printing elements, i.e., the surface without fountain solution. The image is then transferred on the rubber sheet roller (blanket) and from then onto the substrate surface (Figure 5).

Figure 5 Offset printing process (plate to rubber (red) image transfer) [71]

Figure 6 presents an offset printing scheme.

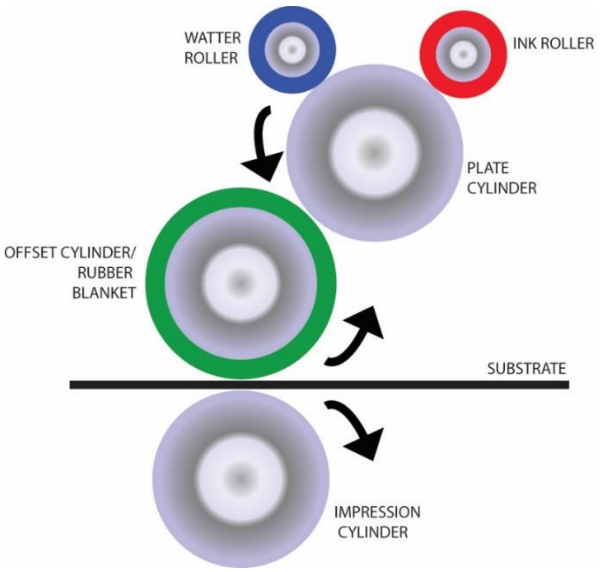

Figure 6 Offset printing process

2.6 Coatings

"Coating" as verb is used when describing finishing layer in the printing process, but to be accurate, coating as noun is defined as a liquid coating material – varnish, that is made of some sort of resin that dries into a hard transparent film. In some literature, varnish is explained as a coating that is applied to the printed piece during or after printing [72].

Most varnishes are a mixture of drying oil, resin, drier and volatile solvent which can be simply described as ink without pigment. The varnishing mostly depends on the technology available or needed for the process and can be done by hand with the brush, roller, by air with the airbrush or by printing press with some type of coating unit. In the printing industry, varnish can be applied via multiple ways, but most common ones are by means of offset printing, screen printing and flexography. All application processes depend on the varnish type [73]. Moreover, some design features can be done by coating from the most popular being spot coating, motion coating, raised dimensional coating etc [72]. Coating types can also be referred to by their curing method instead of their components i.e., UV based cures via UV radiation.

Coatings, as mentioned before, are applied to enhance the visual effect and mechanical resistance of the printed sample [67]. The visual finish depends on the coating's composition, and it can be high gloss, gloss, matte, strike-through matte, and satin.

UV cured varnish can be applied in sheet-wide or segment spread. It is mostly used as a high-gloss finish, as it has the highest gloss of all mentioned varnishes. They are usually composed of polyethylene, calcium carbonate and kaolinite. To achieve curing, UV light is used to harden the coating where UV photo initiators added to the composition activate the curing process [72].

Oil-based varnish also referred to as offset varnish is the cheapest to produce as it is basically printing ink without pigment and it has the ability to be applied without the printing plate [74,75]. This type of varnish can only be applied via printing press as it needs the same run parameters as printing ink.

Water-based varnish (WB) also referred to as aqueous coating is the most environmentally acceptable as there is no aggressive solvent in the mixture. Therefore it is also safe for the printing press operator [67]. By its composition, water based overprint varnish is usually composed of polyvinyl acetate (PVAc) polymer as the binder component [72]. It is usually a clear, fast drying solution that can range from high gloss to matte finish.

In recent studies, some researchers are adding different nano sized compounds to improve the printing coating's performance, either based on biodegradable polymers or commercial varnishes [10,11,13,76,77].

2.7 Nanoparticles

In general, all materials that are in the size smaller than 100 nanometres (nm) can be called nanomaterials [78]. They mostly come from natural resources although there are synthetic kinds as well. Nanoparticles are in use from the beginning of the 20th century and can be found in various products people use today. They are used in the pharmaceutical chemistry, material industry, food technology etc. for variety of benefits [79]. Some nanoparticles can be harmful to common health due to their size as they can penetrate the human skin so protective gear is highly recommended when handling them [80].

Use of nanoparticles also extends to printing industry as well. Beside enhancing existing systems, some compounds can cope with microbic migration and inhibition which is especially important in the packaging industry [81]. The risk assessment of nanoparticles is well regulated in order to avoid any risks to general health [82].

It is also known that metallic compounds such as ZnO and TiO_2 are capable of slowing the growth of the microbes with the strong oxygen free radicalization process that affects the cell wall, therefore killing the bacteria or fungus [83,84]. The oxygen free radicalization process starts when cells use oxygen to generate energy after free radicals are created as consequence of adenosine triphosphate (ATP) production, as well as reactive nitrogen species (RNS). That results in the cellular redox process. Very high concentrations of RNS will generate oxidative stress which will damage the cell structure. The free radicals in general include hydroxyl ($OH^{\bullet}$), superoxide ($O_2^{\bullet -}$), nitric oxide ($NO^{\bullet}$), nitrogen dioxide ($NO_2^{\bullet}$), peroxyl ($ROO^{\bullet}$) and lipid peroxyl ($LOO^{\bullet}$). Oxidants such as hydrogen peroxide (H_2O_2), ozone (O_3), nitrous acid (HNO_2) etc., can easily lead to free radical reactions in living organisms [85].

2.7.1 Zinc-oxide (ZnO)

ZnO is an inorganic compound, a white powder that is insoluble in water but when it is combined with acid it creates salts. It has a high melting point at around 1975 °C. It is used as part of variety of products such as food, cosmetics, drugs, polymers, rubber, cement, glass, adhesives, sealants, fire retardants, bandages, paints etc. In nature, it comes as mineral zincite, but most commercial ZnO is produced synthetically. It can also be found as part of sunscreens as it can absorb, and scatter UV radiation. ZnO is a versatile phosphor that can change colour

as well it can convert UV lights, X-rays and television cathode in various colours. ZnO crystals create wurtzite structures in which the oxygen ions are hexagonally close packed, and half of the tetrahedral interstices are filled with zinc ions [76,86].

2.7.2 Titanium-dioxide (TiO_2)

Titanium (IV) dioxide or titania (TiO_2) is the naturally occurring oxide of titanium. TiO_2 is a bright white substance used as a vivid colourant (whitener) in wide array of products. When used as a pigment, it is referred to as titanium (titan) white, Pigment White 6 or CI77891. It comes in couple of modifications such as brokite, ilmenite, rutile and anatase. As a photocatalyst, TiO_2 can be added in paints, varnishes, cements, glass, ceramics to decompose environmental pollutants. It has the ability to absorb UV radiation and it is also used in the protective coatings, where the rutile shows better UV absorbance while the anatase shows better antimicrobial properties [87,88]. Although it was used as a food colorant known as a E171, in 2021 the European Commission defined it as no longer safe for that purpose [89]. On the worldwide scale, in 2014, production of TiO_2 exceeded 9 million. The value of the TiO_2's market in 2020 was around 16.98 billion US dollars and its estimated to growth of 8.3% overall in the period of 2021-2028 [90]. With that being said, the antimicrobial potential of TiO_2 is vast and it favours inactivation of microorganisms due to its strong oxidizing power by free radical generalization, such as hydroxyl and superoxide anion radicals which can slow or even stop microorganism's cell development [83].

2.7.3 Silicon-dioxide (SiO_2)

Silicon dioxide (SiO_2) also known as silica is an oxide of silicon mostly found in the nature as quartz. It is a natural compound of silicon and oxygen found around the World as part of sand. SiO_2 has many forms but there are three main crystalline varieties: quartz, tridymite and cristobalite. SiO_2 compounds can be divided into two main groups: crystalline (c-silica) and amorphous (a-silica). All forms of silica are odourless solids and can be combined with other metallic elements and oxides such as TiO_2 or ZnO [13]. SiO_2 is also found naturally in many plants such as oats, rice, beets etc. and is also added in many foods and supplements, while as a food additive, it serves as an anticaking agent (E551) which was proved to be nontoxic despite

many public concerns [91]. Although safe in food, inhaling crystalline SiO_2 can lead to severe inflammation of the lung tissue or cancer. Inhalation of amorphous silica is also dangerous due to possible inflammation but all effect will heal throughout time [92]. Orally, SiO_2 is essentially nontoxic with LD_{50} of 5000 mg/kg. SiO_2 also has a very high melting point at 2230 °C, while fumed silica (pyrogenic) is prepared by burning $SiCl_4$. It is an ultrafine powder that consist of amorphous spherical particles which is mostly used as an anti-aging agent. Hydrophobic silica is used as a defoamer component found in most electronic packaging. Typical SiO_2 application include antireflection coatings for near-UV laser optics, all-dielectric mirrors, beam-dividers and polarizers [93].

3 Experimental

The experimental phase has several phases which are separated into two main types of measurements (non-destructive and destructive). The scheme of the experiment is presented in the Figure 7. The first phase is the industrial offset (lithography) printing of the samples and preparation of the nanocomposites in the laboratory. The second phase is coating and preparing the samples for the AcA. Third phase involves separation of the coated and AcA samples for characterization with planed methods (colorimetric and densitometric analysis, SFE and adhesion properties, barrier properties, FTIR-ATR, SEM and EDS, strength analysis and antimicrobial properties). For the destructive methods, samples were also divided for mechanical measurements and SFE and antimicrobial ones.

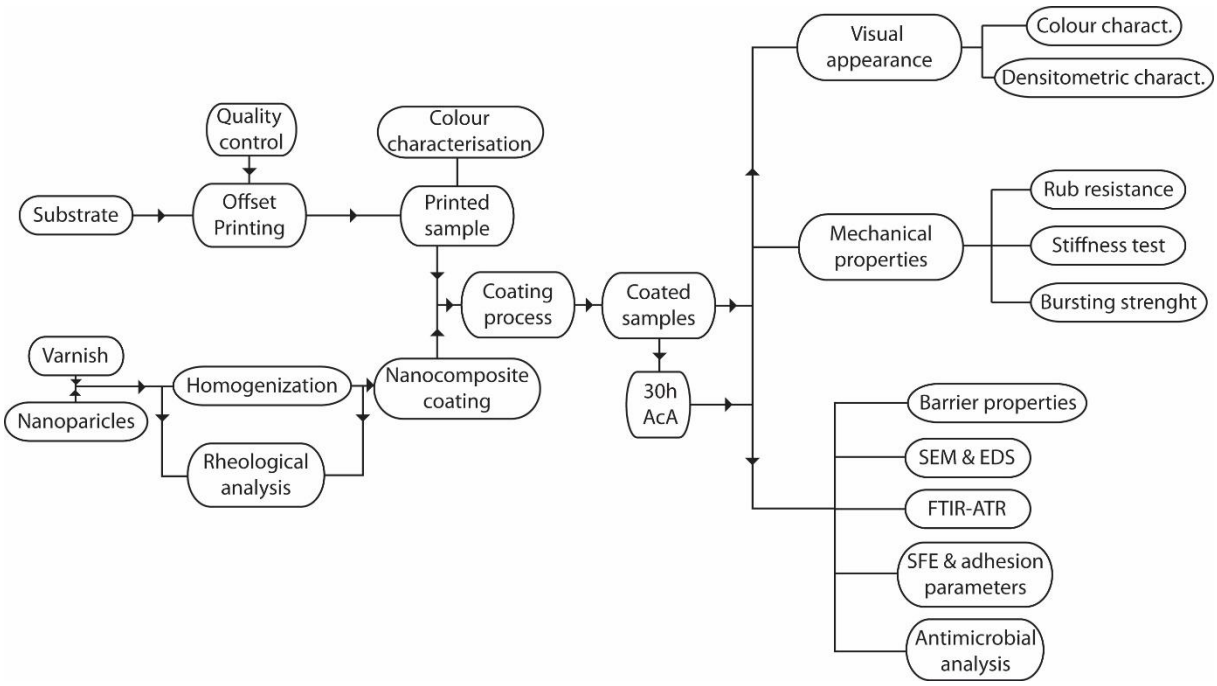

Figure 7 Scheme of the experiment

3. 1 Materials

3.1.1 Paperboard

For this research, UPM Finesse white gloss paper WFC (Woodfree coated) grade with gloss coating and grammage of 300 g/m^2 was used (Table 3). The paper and a its grammage used for this research was a commonly used industrial printing paper. Paper was conditioned and stored in environment at temperature of (23 ± 1) ◦C and (50–55) % relative humidity before the printing process.

Table 3 UPM technical datasheet

Category	Sheet fed offset paper
Grade	Woodfree coated (WFC)
Finish	Gloss
Basic Weight (ISO 536) g/m^2	300
Thickness (ISO 534) µm	0.75
Brightness D65 (ISO 2470-2) %	98
CIE Whiteness (ISO 11475:2017)	125

3.1.2 Offset printing ink

The four colour CYMK offset printing was done with Novavit F918 Supreme Bio inks made by Flint Group. The ink's base is a vegetable oil [94]. Ink's technical datasheet is presented in the Table 4.

Table 4 Novavit F918 technical datasheet

NovaVit F918	Lightfastness (by ISO 12040)	Alcohol	Solvent mixture	Hot calendaring	Alkali
C	5	+	+	+	+
M	5	+	+	+	-
Y	8	+	+	+	+
K	8	+	+	+	+

3.1.3 Varnish

The prepared prints were varnished using water based coating (denoted as WB) with production name Terra High Gloss Coating G9/285 by Actega USA [95,96]. The coating is compliant with the EU's Framework Regulation No. 1935/2004 and EU Plastic Directive No. 10/2011 (Table 5) [97,98]. As the varnish's composition is protected under patent laws, in general, most of the water based varnishes for the flexographic printing are composed of polyvinyl acetate, acrylic binders and additives such as polyethylene or polypropylene waxes [72].

Table 5 Terra High Gloss Coating G9/285 technical datasheet

Delivery viscosity	40 sec. and 60 sec. (20°C, DIN 4mm cup)
Solid	37 – 42%
Specific weight	1.03 g/ml

3.1.4 Nanosized compounds

As mentioned before, nanoparticles according to the definition given by the European Commission states that the particle must be measured 100 nanometers (nm) or below [99]. Nanoparticles can be classified into different classes based on their properties, shape, purpose and size. They can be roughly divided into four groups; fullerene, metal NPs, ceramic NPs and polymer NPs [100]. For this research, three compound in nano size were chosen; zinc oxide (ZnO), titanium dioxide (TiO_2) and silicon oxide (SiO_2).

ZnO used in this research was by NanoArc with the production name ZN-0605[101]. The technical sheet can be found in the Table 6.

Table 6 ZnO datasheet (NanoArc, ZN-0605)

CAS	1314-13-2
Linear Formula	ZnO
Molecular weight (g/mol)	81,379
Melting point	1975 °C
Physical size	40 – 100 nm

TiO_2 used in this research was from Sigma Aldrich with the production code EC 2015-282-2 [102]. The technical sheet can be found in the Table 7.

Table 7 TiO_2 datasheet (Sigma Aldrich, EC 2015-282-2)

CAS	1317-80-2
Linear Formula	TiO_2
Molecular weight (g/mol)	79,87
Melting point	1840 °C
Physical size	< 100 nm
Form	Rutile

SiO_2 used in this research was by Evonik with the production name Aerosil 200. It is hydrophilic fumed silica [103]. The technical sheet can be found in the Table 8.

Table 8 SiO_2 datasheet (Evonik, Aerosil 200)

CAS	112945-52-5
Linear Formula	SiO_2
Molecular weight (g/mol)	60,08
Melting point	170 °C
Physical size	< 100 nm
Form	Fumed

3.2 Sample preparation

3.2.1 Offset lithography printing process

For this research printing was done in accordance with the ISO 12647-2:2013 standard, i.e., FOGRA PSO. The standards sets the CIE L*a*b* values of each primary colour and defines the tolerance level is $\Delta E_{ab}=5$ [68]. The sheetfed offset printing was done with industrial printing press KBA 105 PRO-5+L FAPC (Figure 8) [104]. The printing production was conducted by *Kerchoffset LCC* in Zagreb, Croatia.

Figure 8 KBA 105 PRO litho. offset printing press [105]

For the printing a test form was created which included large patches (50 x 200 mm) with full tone of primary colours and tone value (TV) patches (10 x 10 mm) from 0 – 100% with the step of 2% (0 – 10%) step of 5% (10 – 20% and 80 – 100%) and step of 10%.

3.2.2 Nanocomposite preparation

Nanoparticles used in the nanocomposite mixture were weighed using Mettler Toledo XS205DU Dual range Analytic Scale. The varnish was weighted in the mixture cup.

To dilute the overall relative density of the varnish, 5% of demineralized water was used. This lowered viscosity to approx. need 0.7 Pa•s.

The nanocomposites were prepared by homogenization of nanoparticles into water-based varnish using ultrasound dispenser Hirrlscher UP100H (Figure 9) from 20 to 40 minutes depending on the nanoparticles weight ratio (%) in the varnish (Table 9).

During the course of homogenization process the mixture was cooled down in the water bath with the temperature of 5°C. The cooling console was specially designed for this experiment and can be also seen in the Figure 9. This console allows the constant emersion of the lower part of the cup in the cooled water bath.

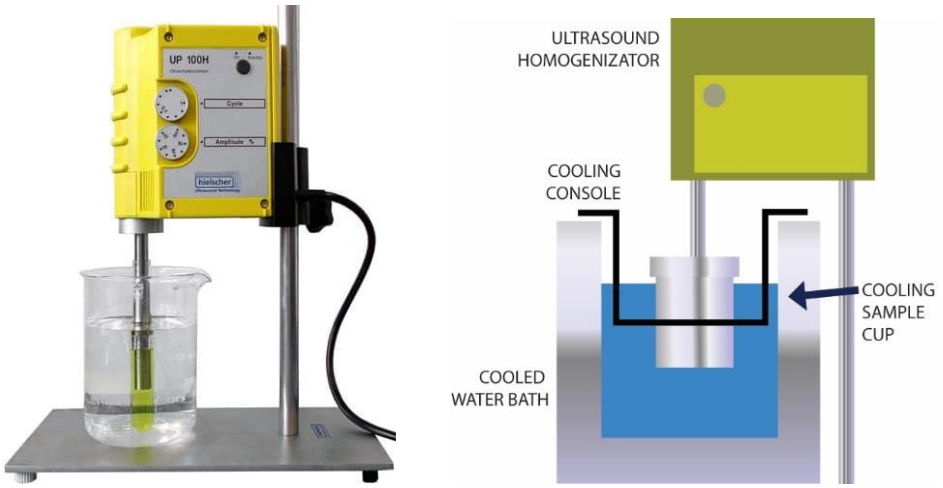

Figure 9 Hirrlscher UP100H and the cooling console [106]

The homogenization time of the nanocomposites can be found in the Table 9. Time differs depending on the weight ratio and its was assessed during the preliminary research that included similar weight ratios of the nanoparticles.

Table 9 homogenisation time for each noncompound

Compound	Weight ration (%)	Homogenization time (min.)
ZnO	0.25	20
ZnO	0.5	30
ZnO	1	35
TiO_2	0.25	20
TiO_2	0.5	30
TiO_2	1	35
SiO_2-*ZnO*	0.5 + 0.5	40
SiO_2-TiO_2	0.5 + 0.5	40

3.2.3 Nanocomposite coating application

To apply the nanocomposite coating, IGT F1 printability tester for flexography was used (Figure 10). To create an even coating layer, flexography was used as varnishing technique. The anilox used was IGT 402-258 roller with 90 l/cm screen line and 18 ml/m^2 cell volume. The flexographic polymer printing plate used was Kodak Flexcel NX with DigiCap NX patterning. The printing plate had 100% TV coverage, used for varnishing. The DigiCap NX pattering is a software-based feature for the entire Kodak Flexcel NX system that ensures the enhanced ink/varnish transfer through micro-texturized pattern on the plate's surface [107]. The IGT F1 settings can be seen in the Table 10.

Figure 10 IGT F1 [108]

Table 10 IGT F1 settings

Anilox force	200 N
Printing force	300 N
Speed	0,30 m/s
No. of revolutions	1

The IGT F1 production stripe is only 5 cm wide while some analytic methods i.e., bursting test, folding and rub test require wider samples. Therefore, some samples were coated using the Control Coated K 202 with the coating rod 1 (Figure 11), that gives a 1µm of wet deposit layer, which is similar thickness to the flexography coated samples [109].

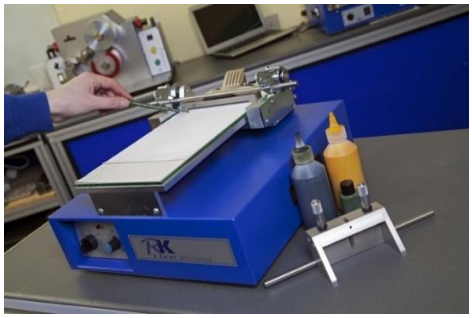

Figure 11 K202 rod coater [105]

3.2.4 UV induced degradation

To simulate the accelerated aging (AcA) or degradation by UV radiation the Solarbox 1500 e chamber was used (Figure 12). Xenon light exposure in the solar chamber with the indoor filter simulates the sunlight rays hitting the surface through a glass or shop window. In this research, an indoor filter S208/S408 (artificial daylight) was used. This was done to assess the level of visual and physical degradation of the samples which were meant to be kept in an indoor environment during their lifespan. Irradiation in the chamber was set to 550 W/m^2 and the temperature of 50 °C. The experiment was done in accordance with the ISO 4892-2 standard [110]. The samples were exposed to 30h of AcA, i.e., to electromagnetic energy of 59 MJ/m^2.

Figure 12 Solarbox 1500 e chamber [111]

4. Sample characterisation

4.1. Rheological analysis

Printing inks and coatings are liquids with their required viscosity variating from one printing technique to another. Their printability is defined by the viscosity and to modify the coating properly, rheological analysis must be conducted. To do so, rheometer is used. Rheometer is a laboratory device that measures the liquid, slurry or suspension flows in response to applied force. It is commonly used in printing industry to modify the inks or coating to match the proscribed viscosity set by the manufacturer of printing press. There is sometime a confusion regarding difference between viscometer and rheometer, where viscometer measures mere viscosity of fluid i.e., one type of viscosity analysis is how it flows (liquid) through from a testing cup in the unit of time. The rheological analysis was conducted via Anton Paar Rheolab QC rotational rheometer [104]. The rheometer's testing cup was cooled down to 20°C.

4.2 Scanning electron microscopy analysis

Scanning electron microscope (SEM) is the type of electron microscope that produces sample image by scanning the surface with a focused beam of electrons. The electrons interact with the atoms from the sample and they create a response that contains various information about the topography of the scanned surface as well the composition of the sample. The electrons penetrate the sample at various depths and different signals are emitted including secondary electrons (SE), reflected back-scattered electrons (BSE), characteristic X-rays and cathodoluminescence (CL) [112,113].

Figure 13 JEOL JSM-6460 scanning electron microscope [114]

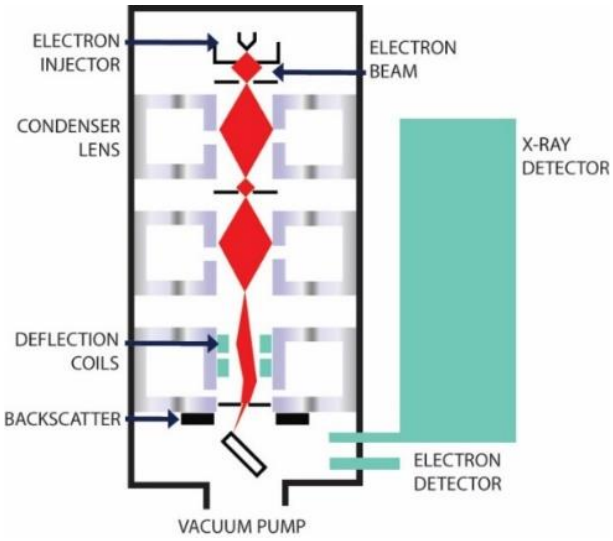

Figure 14 schematic representation of SEM microscope

The SEM microscope principle is presented in

Figure 14. The samples must be small enough to fit on the specimen holder or stub using a conductive adhesive. For conventional SEM scanning, sample must be electronically conductive on the surface and electronically grounded to prevent the accumulation of electrostatic charge. Metal samples, as being conductive, do require little preparation. To prepare non-metal samples, surface is coated with ultrathin layer of conductive material such as gold, gold-palladium alloy, platinum, tungsten, iridium, chromium, osmium, or graphite. Samples that undergo energy dispersive x-ray spectroscopy (EDS) analysis are often carbon coated.

For this research, SEM micrographs were obtained by JEOL JSM-6460 scanning electron microscope, (Figure 13). To assure uniform electronic properties, the samples were gold coated via Baltec SCD 005 sputtering unit.

JEOL JSM-6460 was also used for EDS. EDS is used to determine the element composition of sampled volume, moreover EDS is used to identify the portion of some characteristic elements present in the sample. The same method for sample preparation was done for SEM and EDS.

4.3 Visual appearance

4.3.1 Colorimetric characterisation

To express the colours numerically, the International Commission on Illumination “CIE” recommended two alternative spaces, CIE 1976 or L*a*b*, also known as CIELAB and CIELCH or L*C*h°.

Both scale systems are based on the opponent-colour theory of colour vision. CIELAB is presented by three coordinates which define (L*) lightness, (a*) red/green values and (b*) yellow/blue values [115]. The CIELAB (L*a*b*) colour space and its coordinated system is presented on the Figure 15.

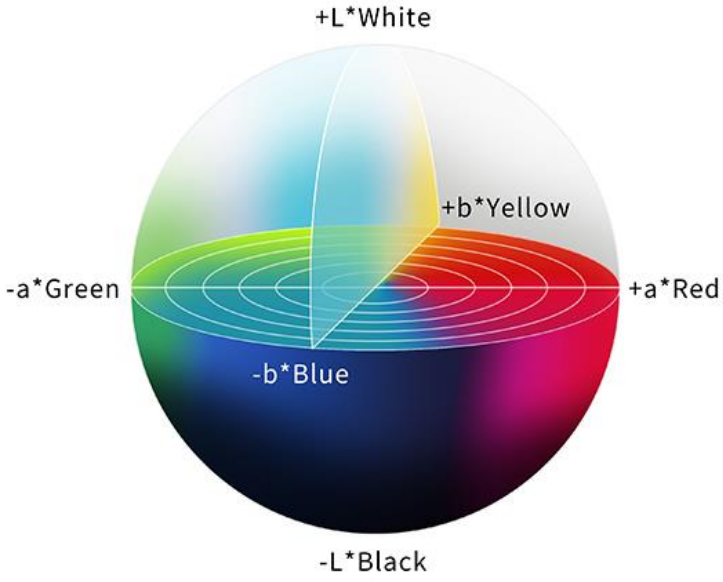

Figure 15 CIELAB colour space [116]

The quality control of the printing processes is defined by ISO 12647 family of standards. This standard consists of seven parts and the part which is referred to in this research is the ISO 12647-2:2013, from where FOGRA PSO was developed [68,117]. This standard consists of many of parameters and defined values which are allowed when preparing CYMK separation, printing plates for offset printing as well as when printing. The standard excludes cold-set offset on newsprint. The parameters and designated values cover the typical production process for commercially available printing substrates.

In quality control for hard copy prints, standard refers to colorimetric values of CMYK separation according to CIELAB colour space. The allowed tolerance is $\Delta E_{ab}=5$, where ΔE_{ab}* refers to colour difference and the letter "E" stands for *Empfindung*, or German for "sensation". The difference between two colours in the three-dimensional coordinate system is known as ΔE_{ab}. This term was created by Hermann von Helmholts and Ewald Hering [115]. For this research a control wedge was created in Adobe Illustrator and printed in accordance with ISO 12647:2-2013. It features all four process inks (CMYK), with halftone patches and 100% tonal value stripe (Figure 16). The halftone wedges were created for density control of halftones while the 100% TV stripe is for colorimetric control.

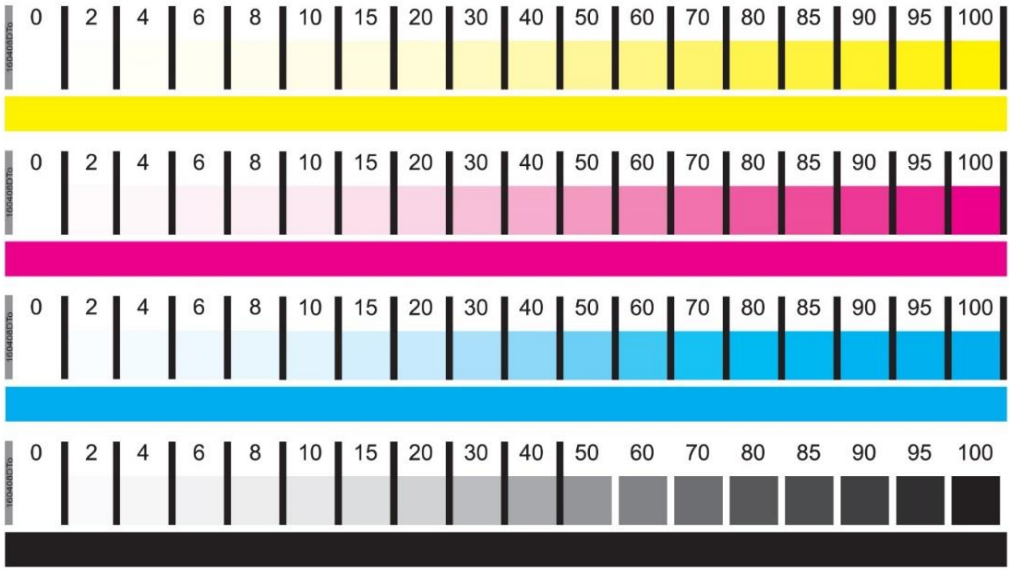

Figure 16 FOGRA PSO control wedge

The colour control was conducted by measuring full tone patches with the use of Techkon SpectroDens spectrophotometer (Figure 17), [118]. The setting for the colorimetric measurements is presented in the Table 11.

Figure 17 Techkon SpectroDens [116]

Table 11 spectrophotometer settings

Illuminant	D50
Standard observer angle	2°
Polarization filter	No
Measuring mode	M1
Calibration	Absolute white

The standard ΔE_{ab} equation can be seen in the equation 2:

$$\Delta E_{ab} = \sqrt{(L^{*\prime} - L^{*})^2 + (a^{*\prime} - a^{*})^2 + (b^{*\prime} - b^{*})^2} \quad (2)$$

Where are: L'^*, a'^*, b'^* - second measured colour, L^*, a^*, b^* - first measured colour.

The two most notable ΔE formulas are CIE76 (ΔE_{ab}) and CIEDE2000 (ΔE_{00}) [119].

The ΔE_{00} equation can be seen in the equation 3 [119]:

$$\Delta E_{00}^{*} = \sqrt{(\frac{\Delta L'}{k_L S_L})^2 + (\frac{\Delta C'}{k_C S_C})^2 + (\frac{\Delta H'}{k_H S_H})^2 + R_T \frac{\Delta C'}{k_C S_C} \frac{\Delta H'}{k_H S_H}} \quad (3)$$

Where are: R_T- hue rotation term (to deal with the problematic blue region), S_L- Compensation for lightness, S_C- Compensation for chroma, S_H- Compensation for hue , k_L, k_C, k_H – parameters weighting factors in terms of computing the colour difference.

4.3.2 Densitometric characterisation

Ink density (D) in offset printing is calculate according to the measured light that is reflected or transmitted from/through an ink. It is essentially the measurement of how dark and ink is [67]. To measure ink density, the light reflectance of ink is used, meaning that the more ink on the surface the less light is reflected. This is true to the one point where adding more ink will not darken the image [67].

The equation (4) to describe ink density is:

$$D = log_{10} 1/R \tag{4}$$

Where is: R – reflectance.

The reflectance density is a function of light amount that reflects from the surface. The ink density was measured before and after UV exposure to better assess the ink fading [120,121].

The measurement was performed with Techkon SpectroDens spectrophotometer with the setting presented in the Table 12.

Table 12 densitometer settings

Illuminant	D50
Density status	E
Polarization filter	No
Calibration	Paper sample

Densitometry was used to investigate the dot gain (also known as tone value increase , TVI), which is defined as the difference between the actual printed dot and nominal (ideal) digital dot (%), i.e., a dot could indicate 50% TV, but after printing it measures 65%. This means that dot gain is 65-50=15% [122]. For the tone value control Murray-Davies equation [123] (5) was used to calculate tone values (G):

$$G = \frac{1-10^{(D_0-D_N)}}{1-10^{(D_0-D_{100})}}\ x\ 100 - N \tag{5}$$

Where are: D_0 – measured density of 0% TV (i.e., unprinted white substrate), D_{100} – density of 100% TV, D_N – density of measured sample (i.e., 60% TV). To investigate the density change (ΔD), equation 6 was used:

$$\Delta D = D_b - D_{AcA} \tag{6}$$

Where are: ΔD – density difference, D_b – density before AcA, D_{AcA} – density after 30h AcA.

4.4 Mechanical characterisation

4.4.1 Rub resistance test

Abrasion or rub damage commonly occurs on the packaging during storage, handling, and transport. This results in decrease in visual appearance of the product as well as in decreased readability of product information. Rub resistance test measures the ink bonding with the printing substrate. The test itself was conducted via Hanatek RT4 Rub and Abrasion tester which can be seen in the Figure 18.

Figure 18 Hanatek RT4 Rub and Abrasion tester [116]

The resistance of the printed samples to rub was determined on a dry print by assessing the degree of ink layer removal due to the friction. This was created by rubbing the tested printed paper and white paper as seen in the Figure 19.

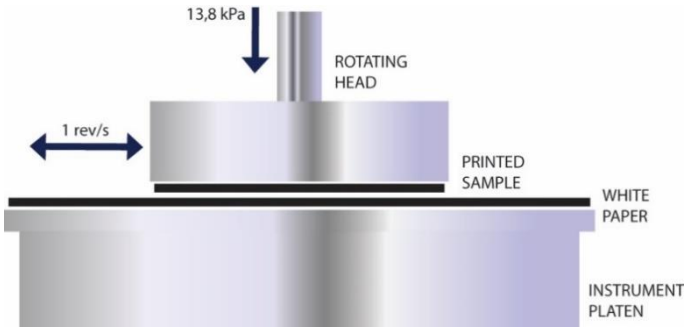

Figure 19 Schematic representation of Hanatek RT4

Powered by an electric motor, the felt disc with the face-down attached printed sample and the disc with white paper substrate rotate at the same angular speed of 1 rev/sec. The pressure between them was 13.8 kPa, and 50 revolutions were induced, since lower number of revolutions did not result with visible rub marks on the white paper for most samples.

Rating of rub resistance is performed by assigning the grades (1-5), depending on the visible amount of ink particles on the white paper during rub rotation under pressure. This is done according to the BS 3110 standard [124]. Lowest grade (1) means that no ink was transferred to the white paper, while the grade 5 the lowest, meaning that the transfer of ink was significant.

4.4.2 Bending stiffness test

The paper's resistance to angle torque force or flexural rigidity is called paper stiffness and it is one of the important parameters when choosing the packaging material. It can be influenced by many factors, such as paper grammage or thickness, etc. This physical characteristic is also related to the economic value of the paper since it is also directly influenced by the amount of fibre used in the papermaking process and hence to its cost, it can be used as a quantitative value that interests both the manufacturer and the user/buyer. For example, some papers have to be flexible but firm i.e. wrapping paper used for gifts.

Bending testers work on the principle presented in Figure 20; a rectangular sample is used, clamped at one end in the testing unit. The force is used under an angle to the free end of the sample while the clamped end is fixed. The resistance results are then presented in Taber stiffness units or millinewtons (mN/m) [125]. Taber stiffens units are defined as the bending

moment of 1/5 of a gram applied to 38 mm wide sample at 50 mm test length at 7.5°. One Taber unit is equal to 0,098066 millinewton. The equation (7) for calculating the bending moment is:

$$bending\ moment = F * l \tag{7}$$

Where are: F – torque force applied, l – overall length of the sample.

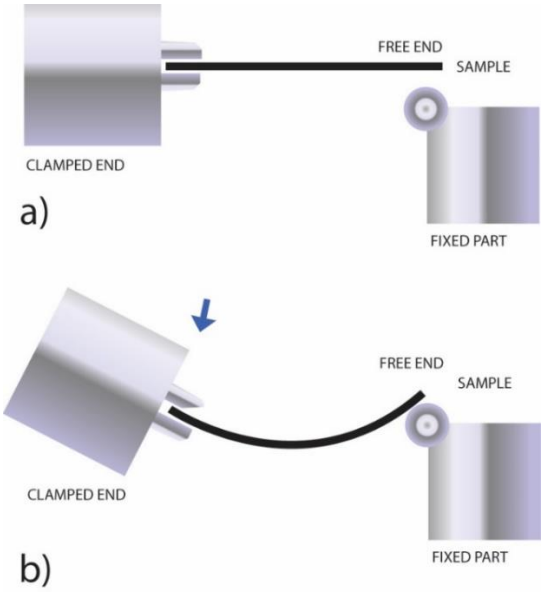

Figure 20 Schematic representation of Taber bending resistance tester; a) starting position, b) testing position

The samples were cut to the needed size via Lorentzen & Wettre sample puncher. The sample punch is a device that is run by compressed air which lowers the knife to cut paper into rectangular 38 x 80 mm pieces.

The bending test was conducted by Loretzen & Wettre bending tester code 160, (Figure 21). The pre-cut samples are placed in the clamp that holds the sample while the other end is free, as described earlier. The head with the clamped sample is rotated in a specific angle measuring the paper's resistance to bending. The measurement was done in ordinance with ISO 2493-1:2010, that describes the method of determination of bending resistance for paper and board [126]. The standard specifies the force measurements for the sample size of 38 x 80 mm at 5°, 7.5°, 15° or 30° angle (on the longer edge). The testing device itself can measure from 20 to 10000 mN. The results are presented in Taber units as the testing device

calculates the applied force with the Taber constant. The technical datasheet of the device can be found in the Table 13 [127].

Figure 21 Lorentzen & Wettre stiffness tester code 160 [128]

Table 13 Lorentzen & Wettre stiffness tester code 160 technical datasheet

Strength measurement range	50-5000 mN
Bending angle	5°, 7.5°, 15°, 30°
Bending length	5, 10, 15, 20, 25 ,50 mm
Bending speed	5°/s
Max. sample thickness	3 mm
Standards	APPITA/AS 1301.453s, ISO 2493, NFQ 03048, SCAN P29, TAPPI T 556, DIN 53121

4.4.3 Bursting strength test

During packaging, transporting, and handling, packaging is subjected to different stresses that can damage the surface and the overall structure of the packaging as well as the products inside. The paper or paperboards resistance to rupturing is called the bursting strength and it is defined as the hydrostatic pressure that is needed to burst the paper's surface under a uniformed force. With the use of fillers, paper can become more resistant to bursting. Bursting strength is an important parameter in choosing the packaging material, in this case paperboard. The carboard packaging is prone to blunt force-induced damage that occurs when a blunt force strikes the surface creating a dent or a hole which can damage the inner product and create problems in handling or selling. The aftermath of the burst test can be seen in Figure 22.

Figure 22 Burst test aftermath with visible holes in the substate's surface

To determine the bursting strength of the surface, Mullen bursting test was conducted. The paper sample is placed under the glass bell (dome) which lowers itself onto the testing sample, while the hydraulic press inflates a rubber diaphragm. The diaphragm expands, creating a force that stretches the sample. The measurement continues until the sample breaks, creating a "pop" or a "popping sound", meaning the inflated rubber diaphragm created a hole, (Figure 23). The test itself consists of an assessment of the protective properties i.e., force that is used to create break or puncture on the face of the surface. To determine that, the testing force is applied on the flat side.The test measures the total hydraulic pressure needed to inflate the diaphragm to the breaking point of the sample. The units can be expressed both in pounds per square inch and kilopascals.

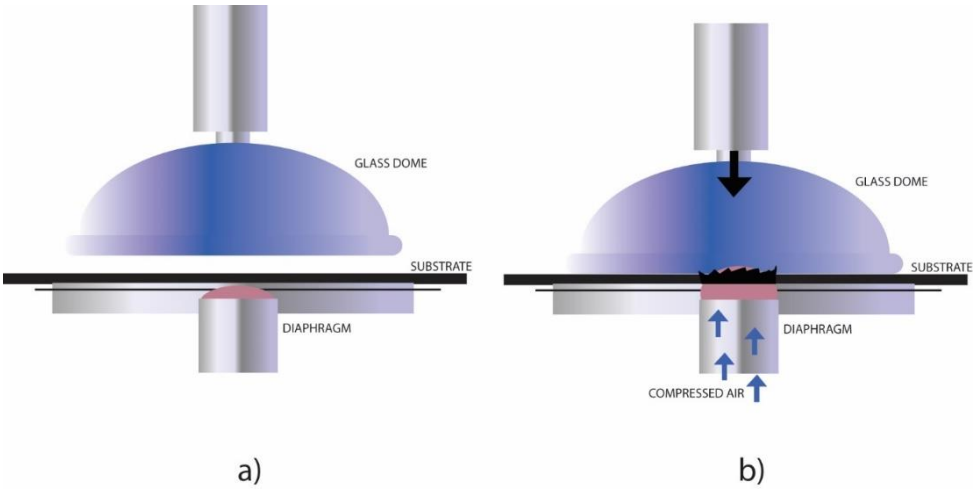

Figure 23 Schematic representation of Lorentzen & Wettre Bursting strength tester; a) elevated position, b) testing position

The measurements for this test were conducted by means of Lorentzen & Wettre Bursting Strength Tester (Figure 24). The tested samples were cut to ø=100 mm, while the testing area was ø=50 mm. The rubber diaphragm is ø=33.1 mm. Under the diaphragm, the pressure in the Lorentzen & Wettre burst tester rises from 70 kPa up to 1400 kPa in accordance to the ISO 2759-2001 standard.

Figure 24 Lorentzen&Wettre Bursting Strength Tester [128]

The technical data sheet of the L&W Bursting strength tester can be found in the Table 14.

Table 14 L&W Bursting Strength Tester datasheet

Strength measurement range	50-2000 kPa
Max. sample thickness	9 mm
Measurement standards	ISO 2759, DIN 53149, FEFCO No.4, TAPPI T807, T810, APPITA AS 1301.438

4.5 Fourier Transform Infrared spectroscopy - Attenuated Total Reflection (FTIR-ATR)

Fourier Transform Infrared spectroscopy - Attenuated Total Reflection (FTIR-ATR) is an analytical method to better understand the structure of individual molecules and composition of molecular mixtures. To obtain the information, FTIR-ATR uses modulated, mid-IR energy to investigate the sample. The IR light is absorbed at specific frequencies directly related to atom-to-atom vibration bond energies in the molecule. When equivalent of bond energy of the vibration and mid-IR energy, the bond can absorb that energy. Different bonds vibrates at different energies meaning that they absorb different wavelengths of IR radiation (Figure 25) [129,130]. FTIR analysis was performed by Shimadtu IRAffinity-1 FTIR-ATR Spectrophotometer.

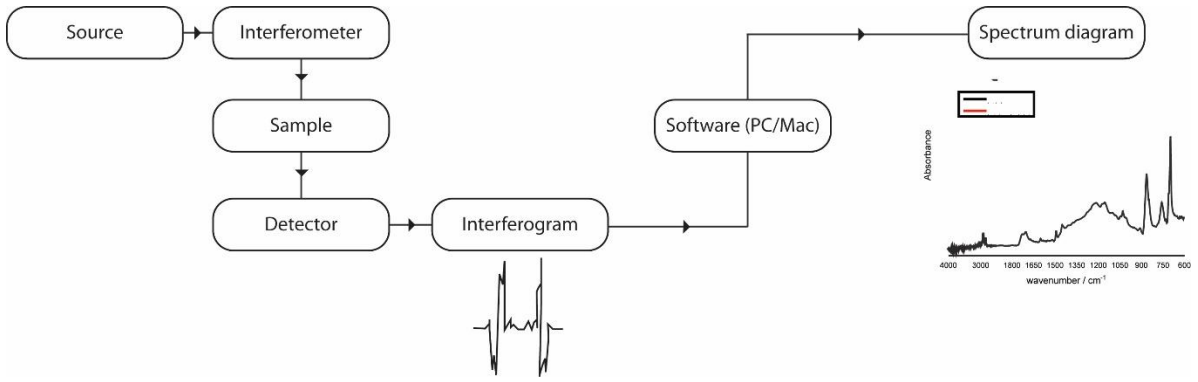

Figure 25 Schematic representation of FTIR [123]

4.6 Surface free energy and adhesion parameters

The surface free energy (SFE) can be also referred to as the surface tension of a solid. The SFE is presented in mN/m in the SI system or dynes/cm in the metric system. In terms of physics, the interaction in the solid-liquid system is important as it determines the adhesion force. This is an important feature in the printing industry as the paints, varnishes and variety of solvents are used with on solids such as paper, foils, metal and polymer surfaces i.e., wall painting, printing, cleaning, etc. To calculate SFE, contact angle (CA) must be obtained.

Contact angles were measured using sessile drop method, ten times per sample, at different sample positions. The droplet shape was a spherical cap, and the volume was set to 1 µl. The

schematic representation of the contact angle via droplet as seen in the Figure 26. Everything over 90° angle has a high wettability.

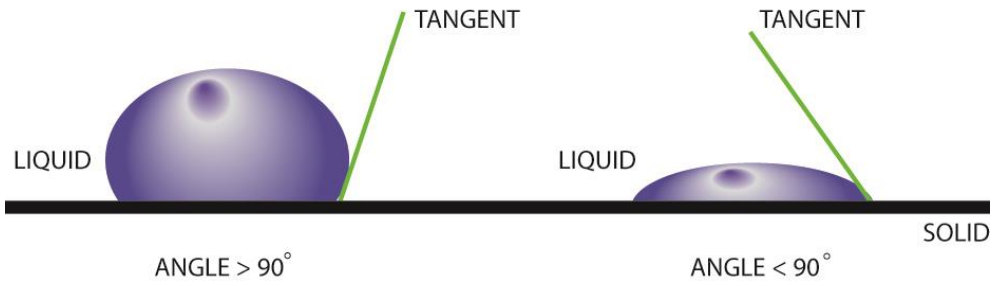

Figure 26 Schematic representation of contact angle

All measurements of the contact angles were performed with the first frame being when the drop touched the surface, and the measurement frame was 2 seconds later and Laplace-Young fitting was used. From the CA results, SFE is calculated. When SFE is high, the solid is easily wetted. To obtain the optimal approximation of the SFE in the Owens, Wendt, Rabel and Kaelble (OWRK) method [131], a minimum of three liquids with known SFE values have to be applied. SFE of the test liquids and their contact angles were recalculated into sample's SFE. The adhesion parameters were than calculated from the calculated SFE values.

The SFE was calculated using the OWKR method equation (8) [132]:

$$\frac{(1+\cos\theta)*\sigma_s}{2\sqrt{\sigma_l^D}} = \sqrt{\sigma_s^P}\sqrt{\frac{\sigma_l^P}{\sigma_l^D}} + \sqrt{\sigma_s^D} \qquad (8)$$

Where are: γ_s – surface tension of the solid, γ_l – surface tension of the liquid, γ^d – dispersive part of surface tension, γ^p – polar phase of surface tension, Θ- contact angle.

To obtain the SFE using a CA, four liquids with known properties were used: water, diiodomethane, formamide and glycerol, according to the values presented in Table 15.

Table 15 Liquids used for contact angle measurements

Liquid	SFT (total)	SFT (disp.)	SFT (polar)
Water *[Ström et al.]*	72.80	21.80	51.00
Diiodomethane *[Ström et al.]*	50.80	50.80	0.00
Glycerol *[Ström et al.]*	63.40	37.00	26.40
Formamide *[Van Oss et al.]*	58.00	39.00	19.00

To analyse adhesion between print and prepared coating, adhesion parameters were calculated. The thermodynamic work of adhesion W_{12} between two phases was calculated using equation (9):

$$W_{12} = \gamma_1 + \gamma_2 + \gamma_{12} \tag{9}$$

Where are: γ_1 – refers to SFE of the first layer, γ_2 – refers to SFE of the second layer, i.e., printed sample and coating, γ_{12} – refers to interfacial tension between first and second solid.

Using the Owens-Wendt model, the SFE of the interface was determined according to the equation (10):

$$\gamma_{12} = \gamma_1 + \gamma_2 - 2(\sqrt{\gamma_1^d * \gamma_2^d} + \sqrt{\gamma_1^p * \gamma_2^p} \tag{10}$$

Where are: γ^d– dispersive component of surface tension, γ^p– polar component of surface tension, while index 1 and 2 mean first and second material.

The adhesion parameter of wetting S_{12} was calculated using equation (11):

$$S_{12} = \gamma_1 - \gamma_2 - \gamma_{12} \tag{11}$$

Optimal adhesion is achieved if the following conditions of the adhesion parameters are fulfilled: thermodynamic work of adhesion must be maximal, interfacial tension must be minimal and close to zero, and wetting must be equal to or greater than zero [77].Surface free energy (SFE) and contact angles on samples were obtained and analysed using the Data Physics

OCA 30 goniometer and calculations were done using the DataPhysics OCA 20 unit and Dataphysics SCA 20 software, (Figure 27) [133].

Figure 27 Data Physics OCA 30 goniometer [128]

4.7 Water Vapor Permeability Test

One of the most important features of printed packaging is to keep products from outer influence by its barrier properties. The water transfer rate test (WVTR) was done via permeability cups made by TQC Sheen with the production name VF 2201 in accordance to the ASTM D1653 standard [134]. Test cup consists of a cup, seal and a cover ring. The seal is designed to prevent turning when closing the cup while the cover ring secures the sample in place. The cup is than filled with 25 ml demineralized water and weighted with analytic weight. The WVTR was calculated using equation (12):

$$WVTR = \frac{\Delta m}{\Delta t * A} \tag{12}$$

Where are: Δm - change of the glass container mass in grams, Δt - time between sample weighing given in days, A - area of the sample in m^2.

For this test, conditions were temperature 22 ± 1 °C and RH of 60 ± 2%. Weighting of samples was performed at 0h, 24h, 48h and 72h.

4.8 Antimicrobial properties

Antimicrobial property is the ability to kill or inhibit the growth, development or spread of microbes such as bacteria, fungi, protozoans, or viruses. Often, some products have some sort of antimicrobial protective agents of their surface which does not interact with the human skin. To determine antimicrobial potential of presented nanocomposite coating, two methods were used:

a) Testing of microbial contamination of samples in ambient conditions

- aerobic mesophilic bacteria count
- yeasts and molds count

b) Testing the growth of pathogenic bacteria and mold on the surface of samples after artificial inoculation.

To determine size of microbial contamination of samples in ambient conditions the aerobic mesophilic bacteria count had to be set. For this research, samples were cut into 4 x 10 cm stripes and left exposed at the room temperature (approx. 21 °C) for 10 days, (3 replicates), assuming ambient air contamination and sample manipulation. Aerobic mesophilic bacteria count on the sample surface was determined by first disinfecting the lower part of the sample with alcohol to create sterile conditions. The sample was then cut with scissors into smaller pieces (sample weight was 1g), and they were put into sterile sample bags. Nine ml of buffered peptone water was added and homogenized for 1 minute. Serial decimal dilutions were then made, and 1 ml of dilution was plated with nutrient agar (Plate Count Agar, PCA) [135] and incubated for 72 hours at 30 °C.

To determine size of microbial contamination of samples in ambient conditions the yeasts and molds count had to be set. For this research, samples were cut into 4 x 10 cm stripes and left exposed to natural contamination for 10 days at room temperature. Yeasts and molds count was tested by contact plates (figure 28) which were incubated for 48 hours at 30 °C.

Figure 28 Sampling for determination of yeast and molds count

Staphylococcus aureus ATCC 25923

Staphylococcus aureus ATCC 25923 was propagated in Brain Hearth Infusion (BHI) broth and inoculated on Baird Parker agar [136,137]. Five colonies were applied to the surface of the samples (strips 4x10 cm; 1 g). The strips were then incubated for 48 hours at 37 °C. After incubation, the count of *S. aureus* ATCC 25923 on the sample surface was determined by first disinfecting the lower part of the sample with alcohol to create sterile conditions. The sample was then cut with scissors into smaller pieces (sample weight was 1g) into sterile sample keeping bags, 9 ml of buffered peptone water was added and homogenized for 1 minute. Serial decimal dilutions were then made and 0.1 ml of dilution was plated on Mannitol Salt Agar (MSA) and incubated for 24 hours at 37 °C. The experiment was repeated three times [138].

Yersinia enterocolitica 4/O:3

Yersinia enterocolitica 4/O:3 strain was propagated in Peptone Sorbitol Bile (PSB) broth and streaked on Cefsulodin-Irgasan-Novobiocin (CIN) agar [139,140]. Five colonies were applied to the surface of the samples (4 x 10 cm strips). The strips were then incubated for 24 hours at 30 °C. After incubation, the number of *Y. enterocolitica* on the sample surface was determined by first disinfecting the lower part of the sample with alcohol under sterile conditions. The sample was then cut with scissors into smaller pieces (sample weight was 1g) into sterile sample keeping bags, 9 ml of buffered peptone water was added and homogenized for 1 minute. Serial decimal dilutions were then made, and 0.1 ml of dilution was plated on CIN agar and incubated for 24 hours at 30 °C. The experiment was repeated three times.

Listeria monocytogenes ATCC 7644 (serogroup 1/2c)

Listeria monocytogenes ATCC 7644 (serogroup 1/2c) was propagated in BHI broth and inoculated on *Listeria Chromogenic Agar Base according to Ottaviani and Agosti* (ALOA) agar [140–142]. Five colonies were applied to the surface of the samples (4 x 10 cm strips). The strips were then incubated for 48 hours at 37 °C. After incubation, the number of *L. monocytogenes* on the sample surface was determined by disinfecting the lower part of the sample with alcohol to create sterile conditions. The sample was then cut with scissors into smaller pieces (sample weight was 1 g), then put into sterile sample keeping bags, 9 ml of buffered peptone water was added and homogenized for 1 minute. Serial decimal dilutions were then made, and 0.1 ml of dilution was plated on ALOA agar and incubated for 24 hours at 37 °C. The experiment was repeated three times.

Inoculation of Enterobacteria (*Citrobacter spp*.) in lyophilized form

Citrobacter spp. multiplied in buffered peptone water (PPV) [143]. The number of cells in ml was determined and 10 ml was lyophilized. One gram of lyophilisate contained 10^9 cells of Citrobacter spp. of which 0.01 g (10^7/g; 7 $\log_{10}$ CFU/g) was weighed and applied to the surface of each sample (4x10 cm; 1 g). The samples were then incubated for 24 h at 37 ° C. Each sample was cut with scissors into smaller pieces (sample weight was 1g) into sterile sample keeping bags, 9 ml of buffered peptone water was added and homogenized for 1 minute. Serial decimal dilutions were then made and 1 ml of inoculum was poured by Violet Red Bile Glucose (VRBG) agar and incubated for 24 hours at 37 °C [144].

Mold of *Penicillium* spp.

The mold was grown on Yeast Glucose Chloramphenicol (YGC) agar and applied to the surface of the samples (4x10 cm strips) [145]. Contaminated samples were incubated in a thermostat at 25 °C for 10 days with elevated humidity (RH of 80%). The number of molds on the sample surface was determined by first disinfecting the lower part of the sample with alcohol to create sterile conditions. The sample was then cut with scissors into smaller pieces (sample weight was 1g) into sterile sample keeping bags, 9 ml of buffered peptone water was added and homogenized for 1 minute. Serial decimal dilutions were then made and 0.1 ml of dilution was plated on Yeast Glucose Chloramphenicol (YGC) agar and incubated for 5 days at 25 °C.

5. Results and discussion

5.1 Viscosity of nanocomposites

The samples are denominated as ZN/NC, TI/NC and SI/NC to illustrate which nanoparticle is mixed into the water-based varnish (WB). Furthermore, denomination of Hybrid/Z and Hybrid/T is used for the nanocomposites including two nanoparticles, zinc oxide and silica and titanium dioxide and silica, respectively.

First evaluation of samples was to determine their applicability in the proposed coating technology. Chosen coating technique is flexography where ink viscosity ranges from 0.05 – 0.5 Pa•s and forms an ink layer up to circa 1 μm [67]. Same applies to coatings as well.

To investigate the prepared coating applicability, first batch of nanocomposite coatings were homogenized according to Table 16 and their viscosity was measured via rheometer Anton Paar RheolabQ, the measurement was at 20 °C and determined after 10 minutes of rotation. The time interval was enough to establish the stable measuring values regardless of the viscosity.

Table 16 Nanocomposite viscosity report

H_2O (%)	Nanoparticle	Weight ratio (%)	Homogenization time (min)	Viscosity (mPa•s)	Shear modulus (τ) (Pa)
0	Pure WB	-	-	394	19.7
0	ZnO	0.25	15	640	32
0	ZnO	0.5	20	880	44
0	ZnO	1	30	1499	75
0	TiO_2	0.25	15	565	28
0	TiO_2	0.5	20	610	30.5
0	TiO_2	1	30	770	38
0	SiO_2	0.5	20	1280	64

As it can be seen in Table 16, viscosity of nanocomposites such as 0.5% ZN/NC and 1% ZN/NC, 1% TI/NC as well as 0.5% SI/NC exceeds 0.7 Pa*s. This means that initial varnish must be modified with added demineralised water to lower the viscosity values.

In Table 17 viscosity of the samples with 5% added water is presented with exception of 0.5% SI/NC which was replaced with nanocomposite hybrid made of 0.5% SiO_2 + 0.5% TiO_2 weight ratio. As it can be observed, all presented samples are in the viscosity limits for flexographic printing.

Table 17 Modulated nanocomposite viscosity report

H_2O (%)	Nanoparticle	Weight ratio (%)	Homogenization time (min)	Viscosity (mPa•s)	Shear modulus (τ) (Pa)
5	Pure WD	-	-	105	5.5
5	ZnO	0.25	15	168	10.5
5	ZnO	0.5	20	272	13.5
5	ZnO	1	30	376	18.8
5	TiO_2	0.25	15	213	16.8
5	TiO_2	0.5	20	310	15.5
5	TiO_2	1	30	357	17
5	SiO_2 +TiO_2	0.5+0.5	40	690	34.5
5	SiO_2 +ZnO	0.5+0.5	40	710	35.2

5.2 SEM and EDS analysis

The two peaks visible in EDS spectra (Figure 29) which are not designated to chemical substance, at 0 keV and 2.1 keV belong to electronic noise and gold (removed as it is consequence of gold sputtering). The presented samples are chosen randomly to illustrate that these peaks are present on all samples.

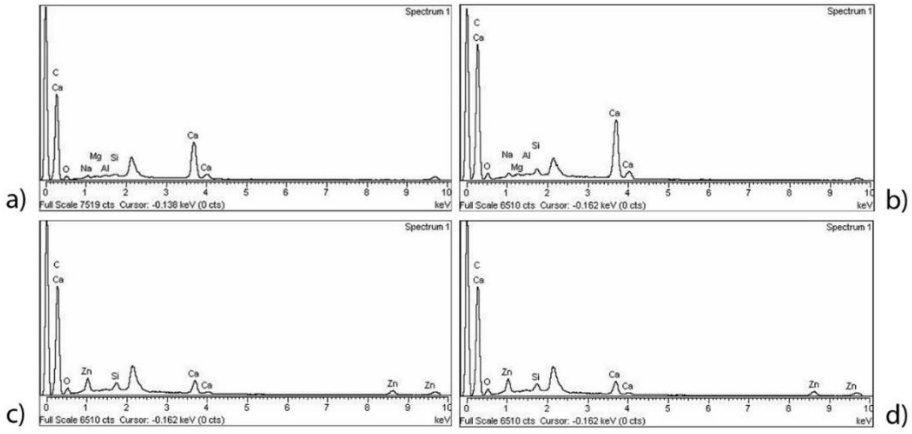

Figure 29 EDS showing the same peaks at 0keV and 2.1 keV on a)WB, b)0.25% TI/NC, c) Hybrid/T, d)1%ZN/NC

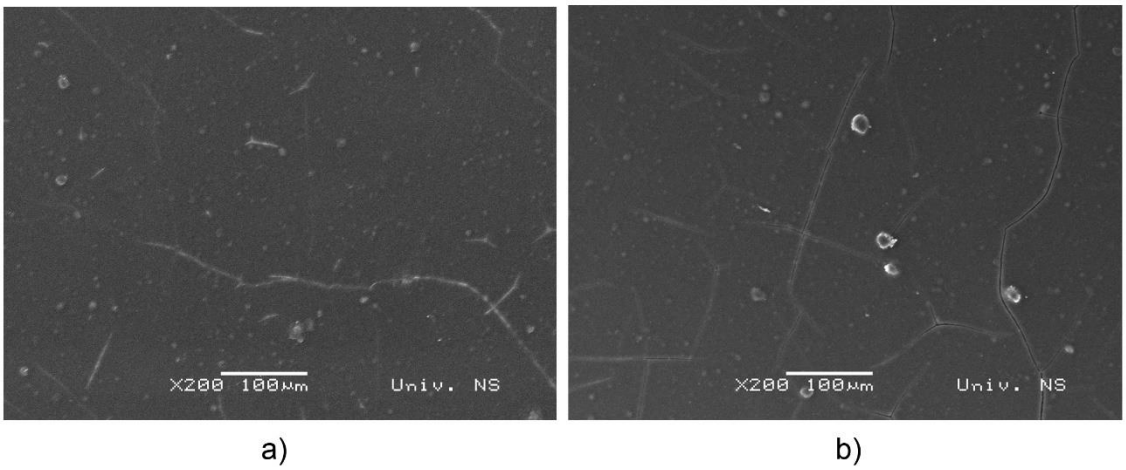

Figure 30 SEM image of (a) 0.25% and (b) 1% ZN/NC

The Figure 30 is showing SEM image of 0.25 and 0.5% ZN/NC. One can note from the figure that with the increase of nanoparticle weight ratio the surface morphology does not change significantly, meaning that the "lumps" that are visible on the surface do expand or grow with the higher weight ratios. The white lines across both SEM images are result of cracking that occurred when the samples were cut. The impurities that can be seen on the 1% ZN/NC are analysed via EDS (Figure 31) where visible clusters are not agglomerates of ZN/NC, but other compounds such as calcium ($CaCO_3$, $CaSO_4*2H_2O$) which are often used as a filler in paper production and used in offset printing as an anti set-off powder to avoid unwanted transfer of ink from one printed sheet to another [146,147].

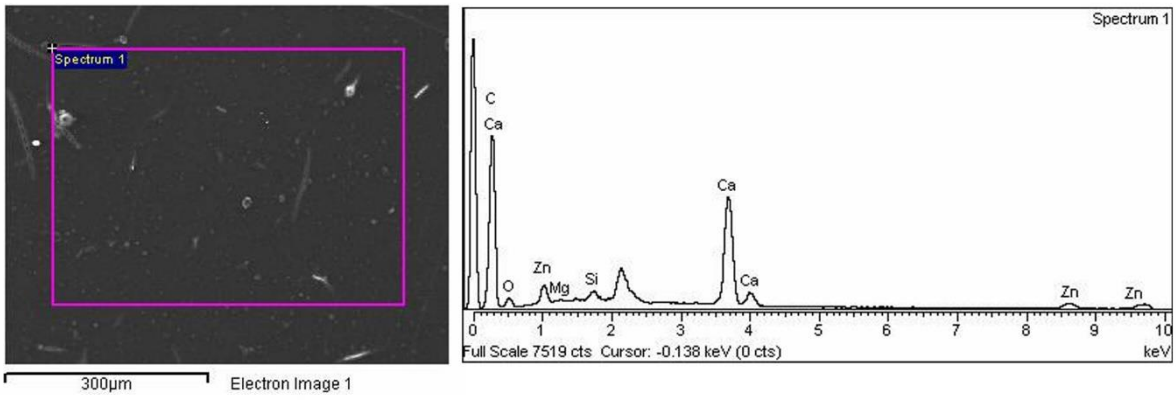

Figure 31 EDS analysis of 1% ZN/NC

The Figure 32 shows SEM image of 0.25 and 0.5% TI/NC. One can note that same to the Zn/NC that with the increase of nanoparticle weight ratio the surface morphology do not change significant, meaning that the “lumps” that are visible on the surface do expand or grow with the higher weight ratios. As this also occurred on ZN/NC samples, we can determine that the homogenization of composites were good enough to result with optimal spread of nanoparticles. The clusters are more profound on the 1% TI/NC where EDS was analysis was made (Figure 33). As on ZN/NC those clusters are not agglomerates of ZN/NC, but other compounds such as calcium, used in the papermaking and in offset printing as an anti set-off powder to avoid unwanted transfer of ink from one printed sheet to another.

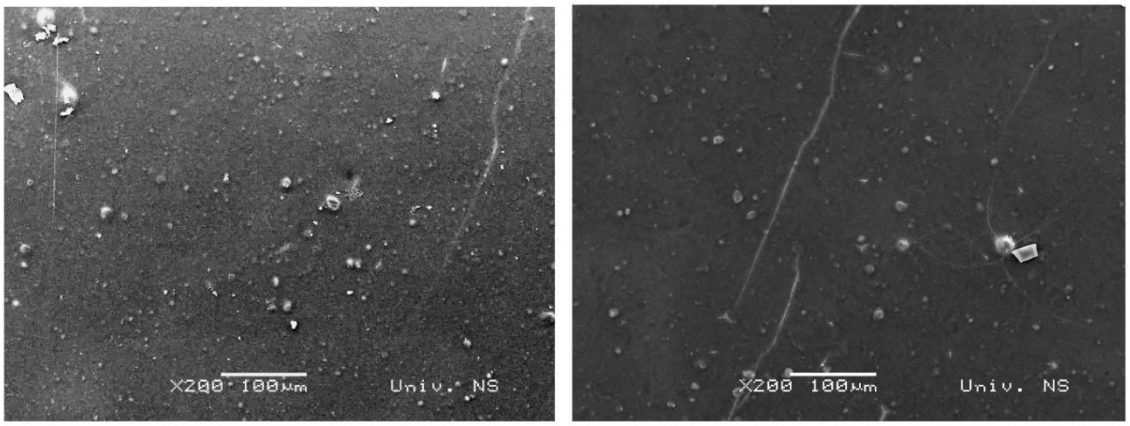

Figure 32 SEM image of (a) 0. 5% and (b) 1% TI/NC

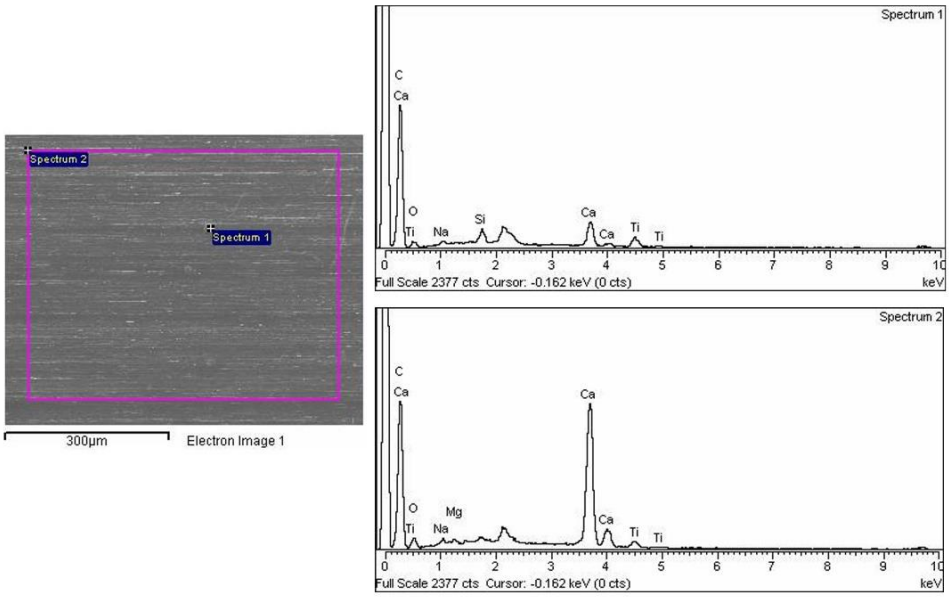

Figure 33 EDS of 1%TI/NC with 2 spectrum points

The Figure 34 show SEM images Hybrid/Z and Hybrid/T nanocomposites. One can note from the figure that surface morphology is much smoother than it was on ZN/NC or TI/NC (Figure 30 and Figure 32). Again, the white lines are from cutting the samples. In both hybrids, the clusters are dust fragments on the surface as seen on the EDS (Figure 35).

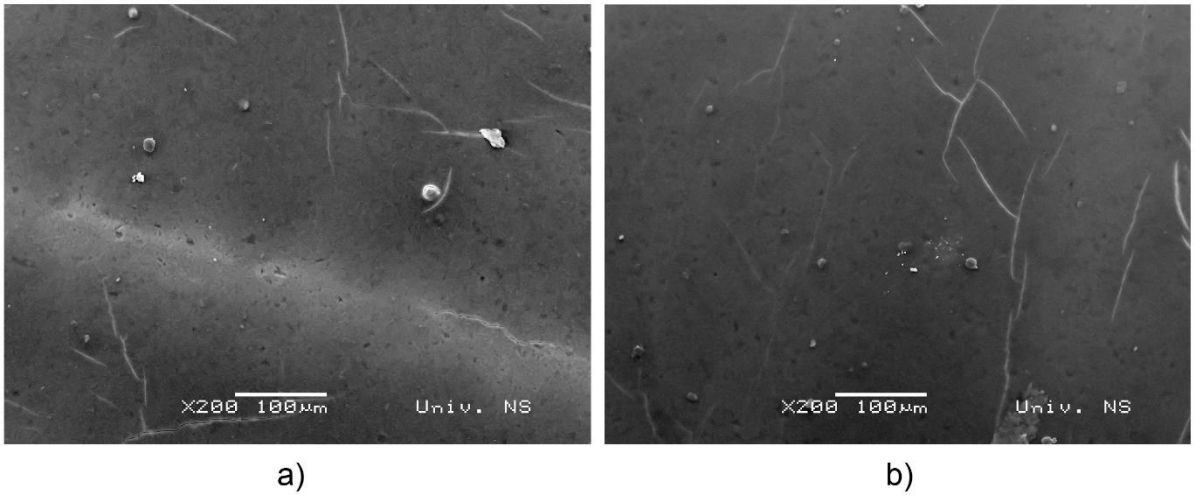

Figure 34 SEM image of (a) Hybrid/Z and (b) Hybrid/T

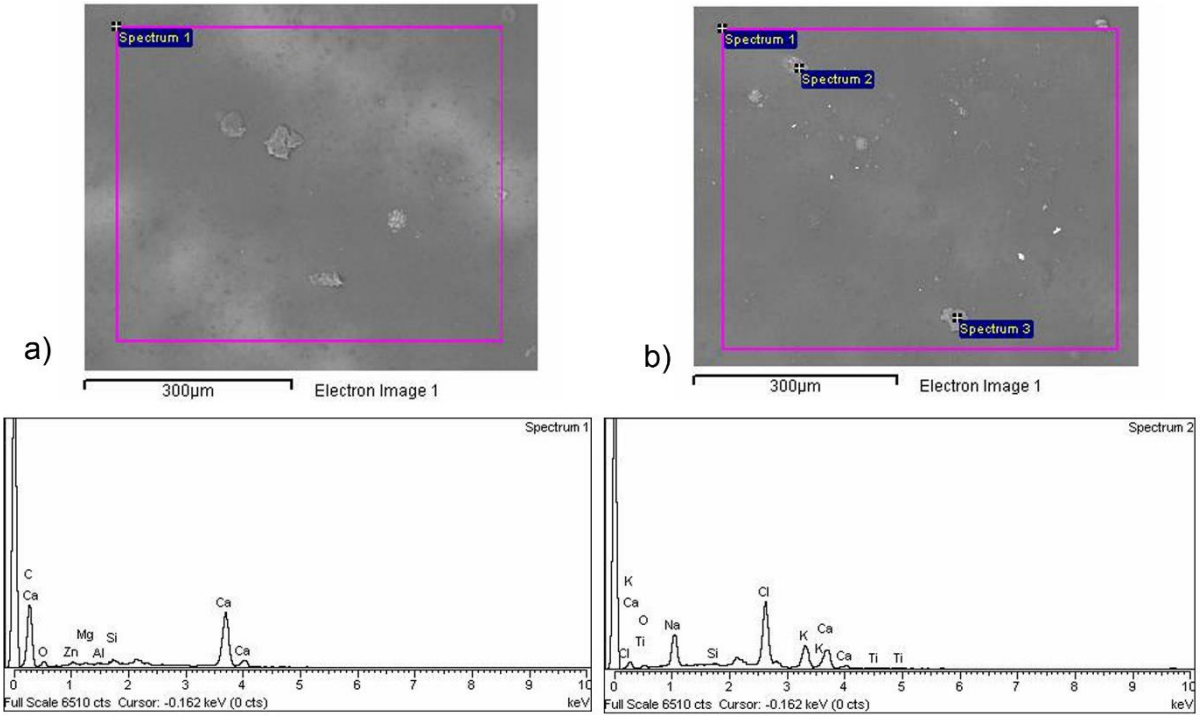

Figure 35 EDS of (a) Hybrid/Z and (b) Hybrid/T

5.3 Appearance analysis

5.3.1. Colorimetric Measurements

After homogenization of ZN/NC and TI/NC, colorimetric analysis was conducted in two ways; first determining the difference between sample and colour target set by FOGRA PSO (ΔE_{ab}) and second, between the initial unaged sample and sample after 30h AcA (ΔE_{00}). The calculation of ΔE_{ab} was done using equation 2 while the calculation of ΔE_{00} was done using equation 3. The FOGRA PSO target values are presented in Table 18.

The colorimetric measurements (ΔE_{ab}) were conducted on six samples and in Figure 36 and Figure 39 average values are presented The values represent difference between measured values and colour targets set by ISO 12647-2:2013 (Fogra 51 PSO, Table 18) [68].

As mentioned in *4.3.1 Colorimetric characterisation,* the tolerance is ΔE_{ab}=5, and in Table 19initial values of uncoated CMYK printed samples can be seen. The ΔE_{ab} values of M (ΔE_{ab}=3.74) and K (ΔE_{ab}=3.05) are sightly high where Y (ΔE_{ab}=4.28) is very close to the tolerance limits. It could be noted that due to increased ΔE_{ab} values on the uncoated samples one can also note that ΔE_{ab} values of WB (Figure 36 and Figure 39), value M ink is close to the tolerance limits (ΔE_{ab}=4.45).

Table 18 FOGRA PSO target values

Colour	***L****	***a****	***b****
C	55	-34	-52
M	47	74	-5
Y	87	-4	90
K	16	0	0

Table 19 ΔE_{ab} of uncoated CMYK printed samples

Colour	***C***	***M***	***Y***	***K***
ΔE_{ab}	1.97	3.74	4.28	3.05

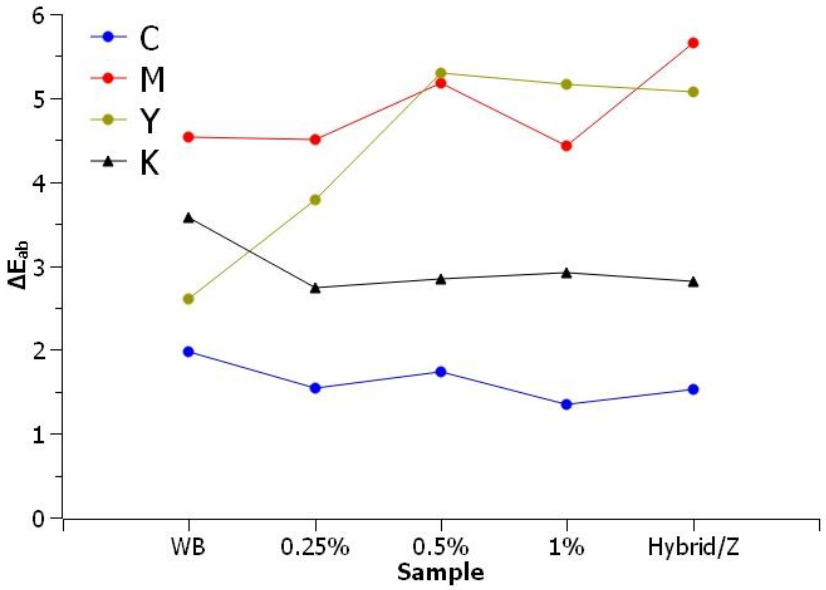

Figure 36 ΔE_{ab} of ZN/NC in regards to FOGRA PSO colour target

In Figure 36, ΔE_{ab} of ZN/NC is presented. Adding the nanoparticles led to the biggest change on the Y samples. The 0.5% and 1% ZN/NC as well as the Hybrid/Z sample on Y exceeds the ΔE_{ab}=5 tolerance. To better evaluate this change, CIELAB coordinates of Y can be observed in Table 20. Moreover, the 0.25% ZN/NC also has the increase of ΔE_{ab}=1.18 when compared to the WB. The biggest change is in the b* coordinate, meaning that with increase of nanoparticle weight ratio the print becomes more yellowish (+b*). There is also a slight change in the a* coordinate as well, where colour saturation shifts slightly towards red. The ZnO in nature occurs as the rare mineral zincite, which usually contains manganese and other impurities that confer a yellow to red color [148]. Moreover, ZnO can turn yellow by heating it (above 800 °C) and reverse to white upon cooling, but this was not the case here, as the temperatures were not as high. The Y colour is most likely to fade the first as it was proven in multiple researches [11,149,150]

Table 20 CIELAB of Y ink for ZN/NC

Sample	***L****	***a****	***b****
WB	**88.24** ± 0.18	**-4.49** ± 0.43	**92.33** ± 1.02
0.25%	**87.91** ± 0.12	**-4.37** ± 0.24	**94.29** ± 0.7
0.5%	**88.40** ± 0.16	**-4.56** ± 0.23	**94.49** ± 0.87
1%	**88.38** ± 0.16	**-4.70** ± 0.21	**94.62** ± 0.87
Hybrid/Z	**87.87** ± 0.1	**-4.16** ± 0.08	**95.16** ± 0.5

In Table 21 0.5% ZN/NC coated samples, also had swift above ΔE_{ab}=5 (ΔE_{ab}=5,18) When observing Table 21 one can see that with the incensement of the NPs weight ratio (%), the value in the b* coordinate rise towards positive [151]. The Hybrid/Z has the most notable change in the b* coordinate, meaning that M slightly losses its blueish hue.

Table 21 CIELAB of M ink for ZN/NC

Sample	***L****	***a****	***b****
WB	**47.67** ± 0.19	**76.99** ± 0.22	**-1.64** ± 0.27
0.25%	**47.31** ± 0.12	**76.83** ± 0.1	**-1.22** ± 0.24
0.5%	**47.45** ± 0.13	**76.83** ± 0.21	**-0.36** ± 0.22
1%	**47.43** ± 0.15	**76.60** ± 0.26	**-1.12** ± 0.22
Hybrid/Z	**47.47** ± 0.06	**76.62** ± 0.5	**0.26** ± 0.02

To determine the AcA influence on the coated samples and its colour perception, colour difference (ΔE_{00}) was calculated from measured CIELAB values. In the Figure 37, diagram showing colour difference (ΔE_{00}) between coated samples before and after 30h AcA. Most notable difference can be seen on the Y samples. With increase of nanoparticles in the nanocomposite coating, the effect of UV exposure decrease. Similar result, although less significant can also be seen on the M.

One must consider that all ΔE_{00} changes occurred under ΔE_{00}=1. The notable change occurred on the Y samples coated with Hybrid/Z. The SiO_2 causes insignificant colour change [152], but as seen on the 0.5% ZnO, ΔE_{ab} is 5.29. Magenta samples also showed similar result to those coated with plain 0.5% ZnO (ΔE_{ab} = 5.18). To get a better assessment, CIEALAB results for Y must be observed closely. It can be seen that the b* coordinates values shifts positive with Hybrid/Z application meaning this shift is towards more yellowish hue.

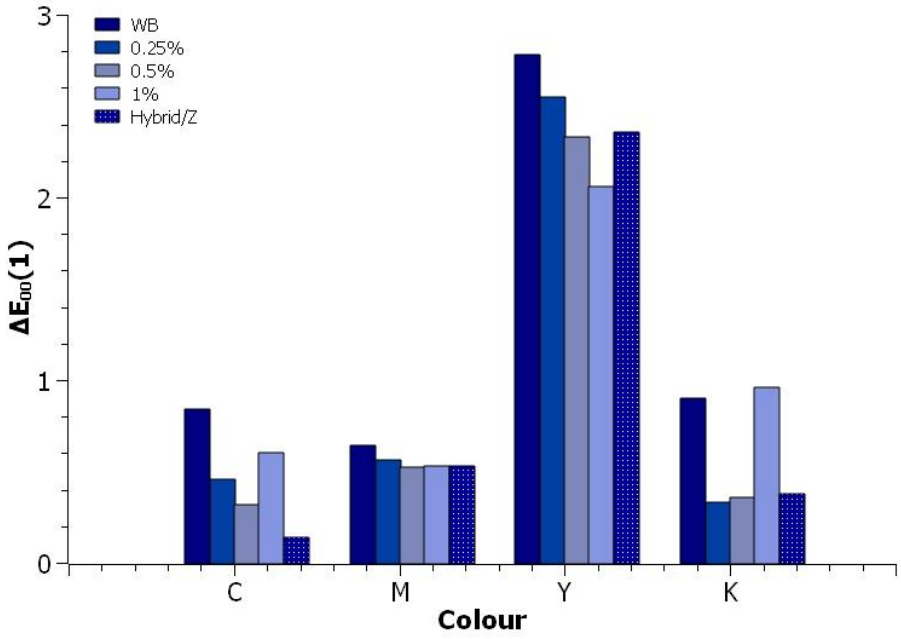

Figure 37 Colour difference (ΔE_{00}) of ZN/NC coated samples

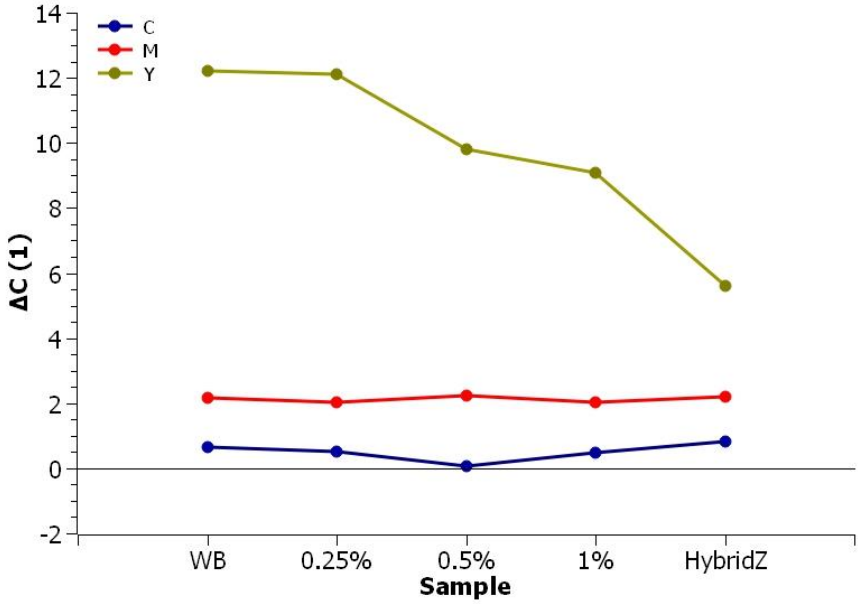

Figure 38 Chroma difference (ΔC) of ZN/NC coated samples

Yellow samples had the biggest chromatic change as well (Figure 38). Chromatic values or chroma refers to purity or intensity of colour [153]. This leads to conclusion that with the increase of nanoparticles weight ratio, chromatic value difference, due to the AcA, decreases.

The ZnO and TiO_2 nanoparticles can absorb the part of UV radiation. The gap band of ZnO is similar to the one TiO_2, although the ZnO gap is somewhat wider. The ZnO absorbs UV radiation up to 374 nm (almost all visible spectral radiation was scattered by the ZnO), while the TiO_2 absorbs UV radiation up to 329 nm. This leads to ink samples coated with either ZnO or TiO_2 to appear darker, as less light is reflected [154]. The same research steps were conducted with TI/NC samples. In the Figure 39, ΔE_{ab} of TI/NC is presented.

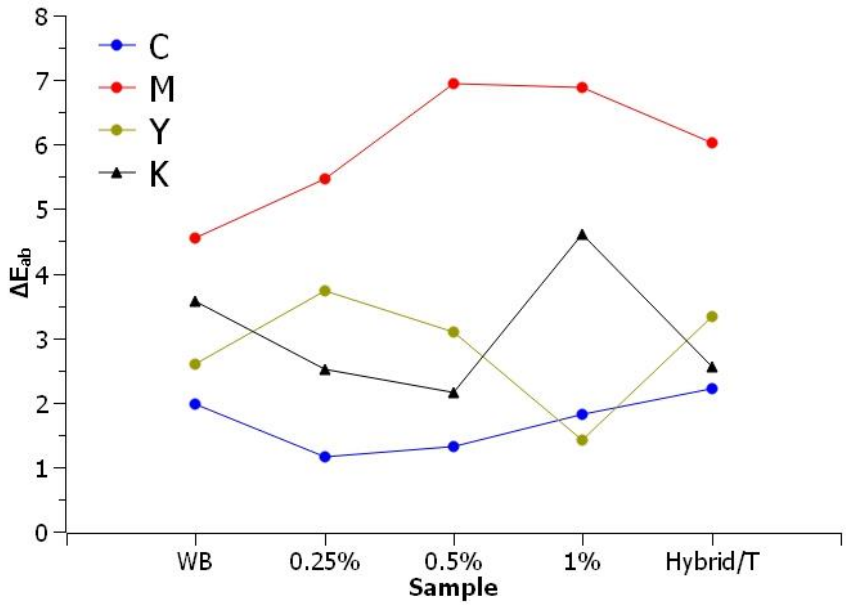

Figure 39 ΔE_{ab} of TI/NC in regards to FOGRA PSO colour target

The nanocomposite application caused most notable change on the M, Y and K samples. The 0.25% TI/NC and higher weight ratios on M samples exceeds the ΔE_{ab}=5 as on ZN/NC samples, but one must consider that the initial ΔE_{ab} of WB coated M samples was near border tolerance value (ΔE_{ab}=4.54). In the Table 22, measured CIELAB values of M are presented. With increase of TiO_2 nanoparticles, a* values decrease while the b* coordinate's values increase.

Table 22 CIELAB of M ink for TI/NC

Sample	*L**	*a**	*b**
WB	**47.70** ± 0.18	**77.01** ± 0.22	**-1.64** ± 0.28
0.25%	**47.53** ± 0.13	**76.49** ± 0.11	**0.04** ± 0.23
0.5%	**47.72** ± 0.1	**75.90** ± 0.08	**2.01** ± 0.17
1%	**48.06** ± 0.08	**74.46** ± 0.16	**2.09** ± 0.36
Hybrid/T	**48.12** ± 0.3	**75.75** ± 0.21	**0.65** ± 0.5

As for the Y samples coated with TI/NC (Table 23), the values in the b* coordinate also oscillates as in the ZN/NC, i.e. first added weight concentration increased the b* coordinate but further increase of the added nanoparticles caused decrease of the b* coordinate. The overall biggest shift is with the 0.25% TI/NC and with the Hybrid/T. Lowering the b* coordinate can be attributed to the TiO_2's whiteness.

As mentioned in the 2.7 Nanoparticles, TiO_2 is used as white pigment in various types of paints [155]. For paint to appear whiter it must have a bluish hue.

Table 23 CIELAB of Y ink for TI/NC

Sample	*L**	*a**	*b**
WB	**88.24** ± 0.18	**-4.49** ± 0.43	**92.33** ± 1.02
0.25%	**88.20** ± 0.21	**-4.15** ± 0.02	**95.23** ± 0.5
0.5%	**88.56** ± 0.1	**-4.49** ± 0.36	**92.68** ± 0.46
1%	**88.15** ± 0.72	**-4.26** ± 0.11	**90.60** ± 0.31
Hybrid/T	**88.84** ± 0.01	**-5.06** ± 0.4	**92.54** ± 0.33

To determine the influence of AcA to the TI/NC coated samples and its colour perception, colour difference (ΔE_{00}) is presented in Figure 40. Most notable difference can be seen on the Y samples. With increase of nanoparticles in the nanocomposite coating, the effect of UV exposure decreases.

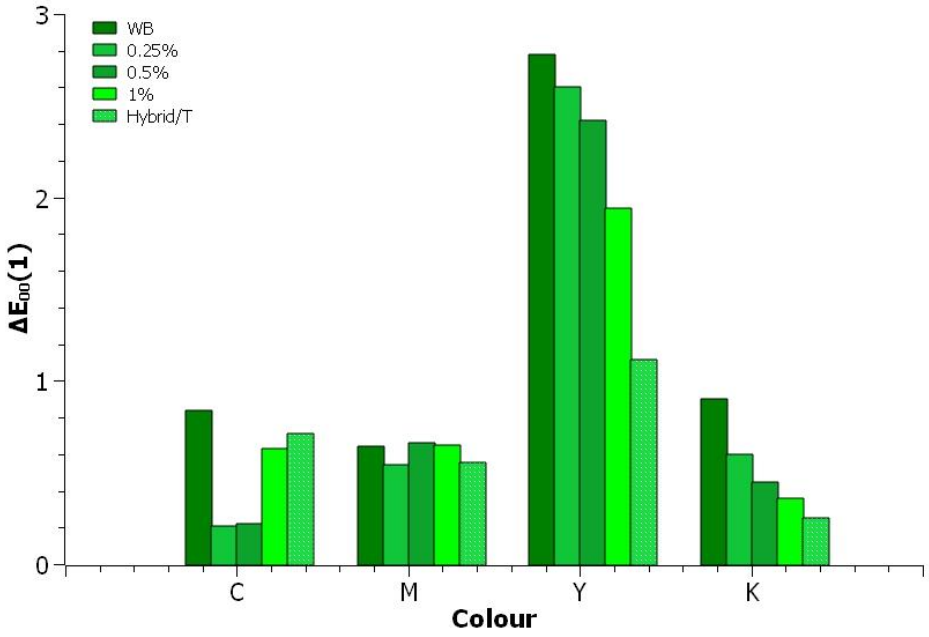

Figure 40 Colour difference (ΔE_{00}) of TI/NC coated samples

Y samples had the biggest chromatic change as well, as seen on the diagram in Figure 41. This leads to conclusion that with the increase of nanoparticles weight ratio chromatic value difference decreases. Meanwhile, the ΔC for C dropped belove 1 for 1% od added TiO_2, meaning that the colour became more intensive. This can be attributed to TiO_2 compound's colour of the natural state. TiO_2 as mentioned before is used also as white pigment but in its natural state it is blue [156].

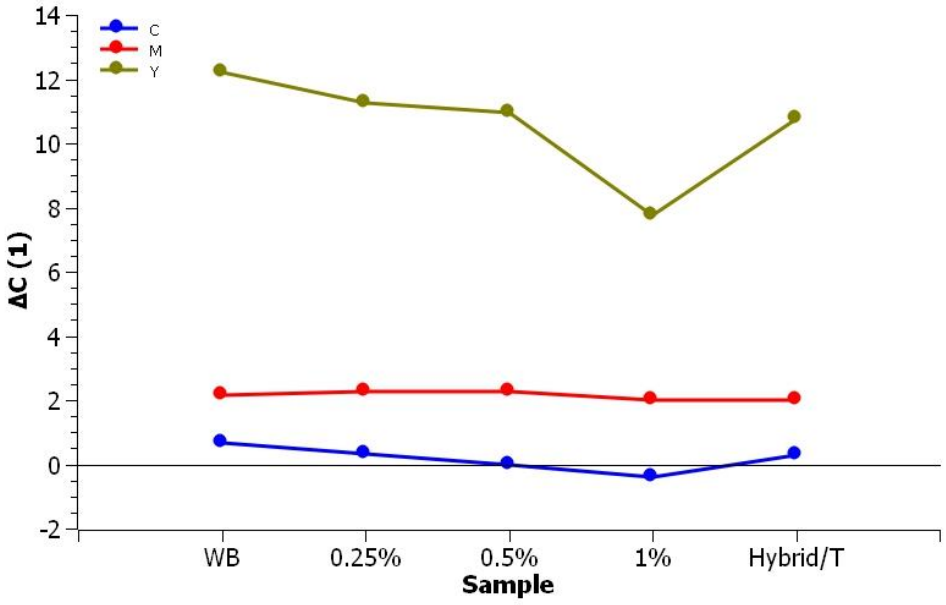

Figure 41 Chroma difference (ΔC) of TI/NC coated samples

The compared nanocomposite systems, ZN/NC and TI/NC did increase the resistance to AcA induced by the UV radiation on colour appearance. ZN/NC have the initial colour difference to FOGRA PSO target values smaller than the TI/NC. After 30h AcA, TI/NC showed higher resistance to UV radiation, where the ΔE_{00} values are lower.

As to Hybrid/Z and Hybrid/T nanocomposites, they did upgrade the WB varnish's resistance to AcA. One can note that Hybrid/T performed better in terms of lightfastness than its counterpart.

5.3.2 Densitometry of the prints

Density measurements were performed on the wedge patches of different nominal tone values (TV, Figure 16) before and after 30h AcA. The first measurement set was performed on 100% TV and second one on half tones. Tone values (TV) were calculated using Murray-Davies equation (5). In Table 24, density changes of the full tone or ΔD between 0h and 30h AcA are presented for ZI/NC, this was done using equation 6. It is visible that Y samples have the biggest density change, although the change lowers with increase of added nanoparticles. The C and K proved to be the most resilient to AcA, resulting with small density difference.

Table 24 ΔD between 0h and 30h AcA of ZN/NC

Sample	**C**	**M**	**Y**	**K**
WB	-0,02	0,09	0,31	-0,03
0,25%	0,01	0,09	0,31	0,01
0,50%	0,01	0,09	0,29	0,01
1%	0,02	0,08	0,28	-0,05
HybridZ	0,01	0,09	0,30	0,02

To enable better assessment of coating influence and UV exposure, half-tone patches (20%, 30%, 40%, 50% and 60% nominal values) were analysed as those are the spots where change is most likely to occur. Yellow being the most sensitive process colour, there is where that change is most notable (Figure 42).

It can be noted that with increase of nanoparticle weight ratio (%) overall density difference changes where the best result is with 0.5% and the poorest is with 1% ZN/NC . As expected, the half-tones from 40% up to 50% are very sensitive, while 20% remains almost unchanged.

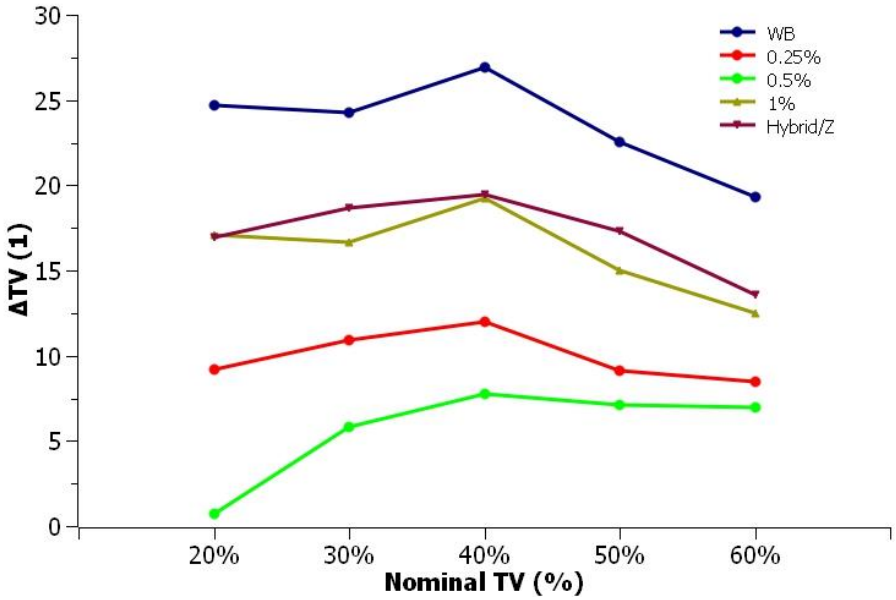

Figure 42 ΔTV of Yellow for ZN/NC sample

For samples coated with TI/NC, density measurements were performed in the same way as on the ZN/NC samples. In the Table 25, ΔD between 0h and 30h AcA of 100% TV are presented for TI/NC. It is evident that Y samples have the biggest density difference. Although the difference is notable, it lowers with increase of TiO_2 nanocomposite weight ratio (%). The C and K proved to be the stable, i.e., almost no change can be noticed.

Table 25 ΔD between 0h and 30h AcA for TI/NC

Sample	**C**	**M**	**Y**	**K**
WB	-0,02	0,09	0,31	-0,03
0,25%	0,00	0,11	0,32	0,03
0,50%	0,01	0,10	0,29	0,04
1%	-0,03	0,10	0,22	0,02
Hybrid/T	0,01	0,11	0,12	0,08

On the diagram presented in Figure 43, half-tone values of Yellow are presented. It can be noted that with increase of nanoparticle weight ratio (%) overall density lowers. The 1% TI/NC proved to be the most resistant to change in the half-tones. Overall, the samples coated with the TI/NC are more resistant to chance during AcA from their ZN/NC counterpart. It is also interesting to see that the 0.25% TI/NC has almost same affect as the 1% ZN/NC. This can be attributed to the lower UV absorption edge of the TiO_2 compound (329 nm) than the ZnO (374 nm), leading to TI/NC being more resistant and stable after the UV induced AcA [154].

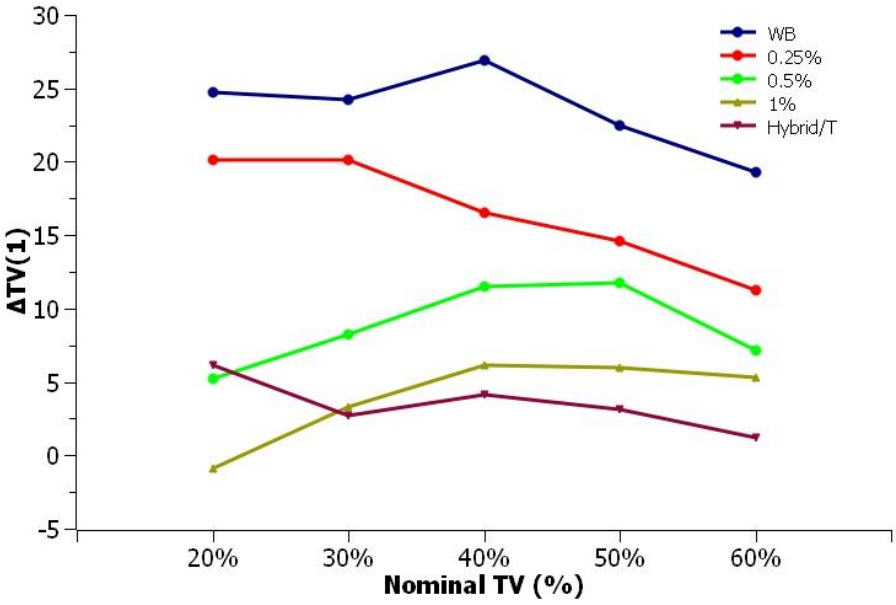

Figure 43 ΔTV of Yellow for TI/NC sample

5.4 Material characterisation

5.4.1 Rub resistance analysis

The rub resistance test provides an insight in the protective capabilities of the coating enriched with the tested nanoparticles and their weight ratios (%) to the mechanical wear. Rub resistance is determined by assigning the grades (1-5), depending on the visible amount of ink particles on the white paper during rub rotation under pressure. This is done according to the BS 3110 standard [124]. Highest grade 1, represents that no ink was transferred to the white paper, while the grade 5 the lowest, meaning that the transfer of ink was significant. The rub white paper used was Navigator office 80 g/m^2 [157]. In the Table 26 the rub resistance results are presented for ZN/NC. The values are all grade 1.

Table 26 rub resistance grades for ZN/NC samples (unaged and AcA)

Sample	Unaged samples	Aged samples (AcA)
WB	1	1
0,25%	1	1
0,5%	1	1
1%	1	1
Hybrid/Z	1	1

As for the TI/NC samples, they also show great rub resistance. The grades are all graded with 1, seen in the Table 27.

Table 27 rub resistance grades for TI/NC samples (unaged and AcA)

Nanocomposite	Unaged samples	Aged samples (AcA)
WB	1	1
0,25%	1	1
0,5%	1	1
1%	1	1
Hybrid/T	1	1

5.4.2 Stiffness analysis

Stiffness analysis provides the analysis of force needed to bend the substrate. The measurement was conducted in pairs of samples, coated unaged and AcA coated. Every sample was measured 10 times. Diagram presented in the Figure 44 diagram is shows stiffness of the ZN/NC samples with and without 30h AcA's influence.

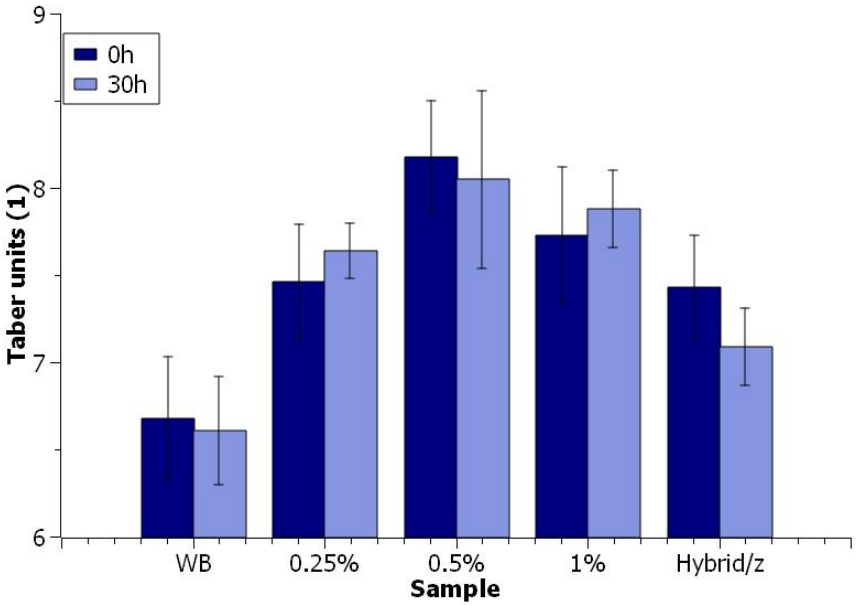

Figure 44 Stiffness test diagram for ZN/NC coated samples

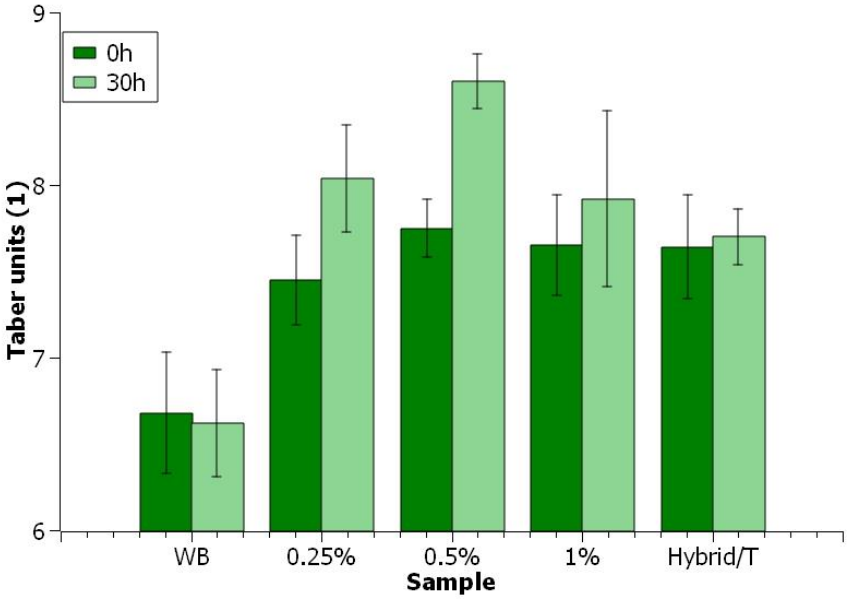

Figure 45 Stiffness test diagram for TI/NC coated samples

It can be noted that the AcA slightly influences stiffness of the samples and even more, adding nanoparticles cause slight increase of the initial stiffness values approx. 1.2 Taber units.

The TI/NC coated samples showed similar behaviour as the ZN/NC samples (Figure 45). The aged samples showed slightly higher values meaning the sample got more rigid after exposure. Again, the WB coated sample showed lower values than the 0.25% TI/NC coated sample which leads to conclusion that in both cases, nanoparticles will increase the initial stiffness values. The sample after UV exposure show slightly higher values.

5.4.3 Bursting strength analysis

The test was designed to simulate the outer force of possible damage to the surface of the sample (packaging). The measurement was conducted in pairs of samples, coated unaged and coated AcA. Every sample was measured 10 times, diagram in the Figure 46 shows average values and standard deviation. It can be noted that the overall bursting strength of the sample's surface is unchanged, with exception in 0.25% ZN/NC sample. The values after exposure remain under 5kPa of measured strength. The WB sample underwent change of approx. 16 kPa (from 266.25 kPa to 250.4 kPa), which is significantly larger change than in the other tested ZN/NC samples. The reason could be that the ZnO nanoparticles due to their ability to absorb UV radiation and the increased degree of polymerisation that preserved the tensile strength more as the WB sample became stiffer therefore more likely to break easily, as later proved by FTIR. The

Hybrid/Z showed no notable change before or after 30h AcA. Hybrid/Z, has the SiO_2 in its composition, meaning that the overall surface strength have increased due to fact that it is used (approx. 95% of commercially available) in the enforcing of the concrete [158].

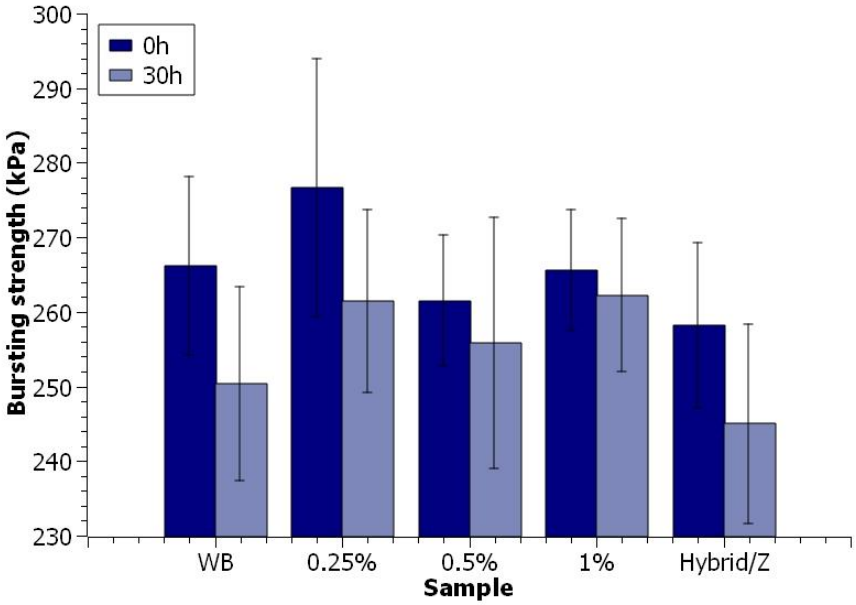

Figure 46 Bursting strength diagram for ZN/NC nanoparticles

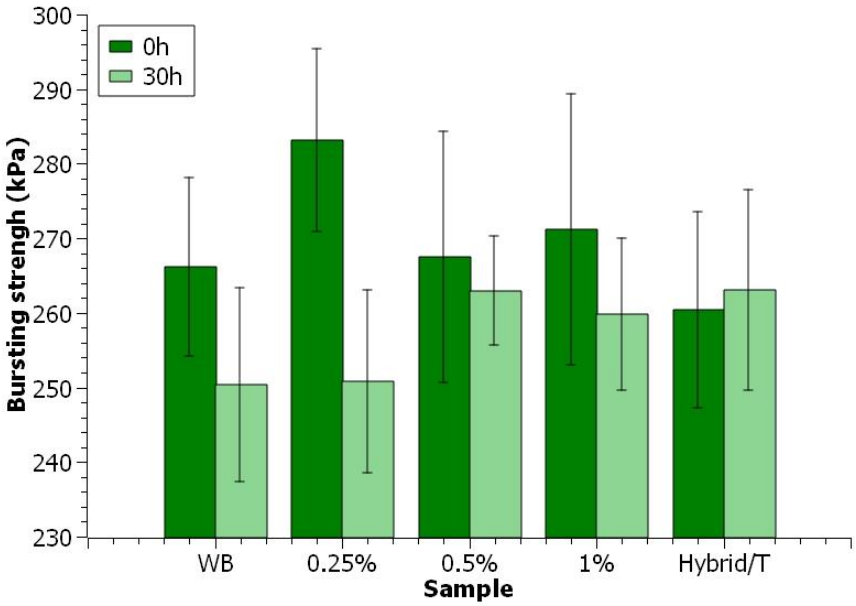

Figure 47 Bursting strength diagram for TI/NC nanoparticles

In the Figure 47 bursting strength diagram for TI/NC samples is presented. It can be noted that TI/NC samples have slightly higher values than the WB in the start, but the difference is not

significant. The results after 30h AcA show higher values than the WB one, which can also be attributed to the TiO_2 ability to absorb the UV radiation. The increase of the TiO_2 nanoparticle's weight ratio did not show any significant upgrade to the sample performance. On the 0.25% TI/NC sample, the change is notable before and after 30h AcA (approx. 32 kPa). The Hybrid/T showed no significant change before or after UV exposure time.

5.4.4 Adhesion parameters analysis

The surface free energy (SFE) and other adhesion parameters were determined as presented in 4.6 Surface free energy and adhesion parameters. Based on the measured values of contact angles, surface properties of samples can be assessed. The contact angles of four liquids (Table 15), with know SFT were measured and used for SFE calculations. In Table 28, the calculated SFE of samples without nanocomposite coatings with four liquids are presented. From the presented table it can be noted that the plain paper after 30h AcA has some change in the polar component because of forming new oxidation products which are less polar from its -OH group. Kaolin, also one of the ingredients of the paper is a very hydrophilic substance as well [159]. The ink, as stated before, contains vegetable oil in its composition, which is influenced by the UV radiation where ester bounds are destroyed, therefore the polarity has risen [160]. With exposure to the 30h AcA the hydrophilic properties of ink are lowered. WB samples, after 30h AcA have lower polar component but higher total SFE values. This can be attributed to the acrylic resin that is a common ingredient in water based varnishes and it tends to become more hydrophobic after exposure to UV or ozone [161].

Table 28 SFE calc. of samples without nanocomposite coating

	SFE (γ (mJm^{-2}) – OWRK)		
Sample	**SFE (Total) / (γ)**	**Dispersive SFE /(γ^d)**	**Polar SFE/ (γ^p)**
Paper	27.06	20.27	6.81
AcA-Paper	28.01	22.32	5.69
Ink	32.41	30.83	1.57
AcA-InK	35.03	30.58	4.45
WB	33. 68	28.61	5.08
AcA-WB	30.85	26.45	4.41

In Table 29, SFE values of ZN/NC nanocoated samples are presented. The ZnO as such is hydrophilic, mostly due to the presence of -OH groups on its surface [76,163]. With the UV exposure, the polar component rises (0.25% and 0.5%), turning the ZnO into more hydrophilic where with the 1% as the polar component lowers the surface turns more hydrophobic [76].

Table 29 SFE calc. of samples with ZN/NC nanocomposite coating

	SFE (γ (mJm^{-2}) – OWRK)		
Sample	**SFE (Total) / (γ)**	**Dispersive SFE /(γ^d)**	**Polar SFE/ (γ^p)**
0.25%	34.31	32.14	2.17
(AcA)-0.25%	28.89	23.1	5.79
0.5%	34.97	32.5	2.47
(AcA)-0.5%	33.52	30.78	2.74
1%	37.06	34.76	2.3
(AcA)-1%	31.82	29.76	2.07

The SFE values of TI/NC samples are presented in Table 30. It can be noted that with the increase of TiO_2 nanoparticle weight ratio (%), the wettability of TiO_2 coated samples also increases but after the AcA it lowers. According to the Stevens et al., with UV exposure, the surface properties in terms of SFE change, increasing the hydrophilic properties of TiO_2 [164].

Table 30 SFE calc. of samples with TI/NC nanocomposite coating

	SFE (γ (mJm^{-2}) – OWRK)		
Sample	**SFE (Total) / (γ)**	**Dispersive SFE /(γ^d)**	**Polar SFE/ (γ^p)**
0.25%	33.59	29.15	4.45
(AcA)-0.25%	28.82	22.69	6.13
0.5%	37.03	34.94	2.09
(AcA)-0.5%	36.18	33.24	2.94
1%	38.08	37.07	1
(AcA)-1%	34.55	28.66	5.89

The SFE results of SiO_2 combined with ZnO and TiO can be seen in Table 31. Hybrid/Z has higher hydrophilic properties that Hybrid/T. Interesting to see that in both cases, after 30h AcA,

the samples follow the similar behaviour meaning that the ZnO becomes more hydrophobic after AcA (γ^d =35.11 mJm^{-2}/ γ^p=1.62 mJm^{-2}), while TiO_2 becomes more hydrophilic (γ^d =29.45 mJm^{-2}/ γ^p=5.5 mJm^{-2}).

Table 31 SFE calc. of samples with Hybrid/Z and Hybrid/T nanocomposite coating

	SFE (γ (mJm^{-2}) – OWRK)		
Sample	**SFE (Total) / (γ)**	**Dispersive SFE /(γ^d)**	**Polar SFE/ (γ^p)**
Hybrid/Z	36.59	33.55	3.04
(AcA)- Hybrid/Z	36.73	35.11	1.62
Hybrid/T	37.14	33.1	4.03
(AcA)- Hybrid/T	34.95	29.45	5.5

By observing the presented results, it can also be noted that the dispersion component has a higher contribution to the SFE. The polar component is highest for the plain paper samples, which was expected since the paper substrate itself is made from cellulose, which is highly hydrophilic. With the addition of WB and nanoparticles, the polar component lowers, with the most overall (before and after AcA) stable results in the 0.5% weight ratio.

The optimal adhesion is crucial for the optimal interaction between the printed samples and nanocomposite coatings in terms of the mechanical properties and overall quality of the printed product. For the adhesion to be optimal, the SFE of interphase (γ_{12}) should be minimal (close to zero), while work of adhesion (W_{12}) should be maximal and wetting coefficient (S_{12}) should be positive.

In the Table 32 calculated adhesion parameters are presented. To evaluate results, all three parameters (γ_{12},, *and* S_{12}) should be observed together as a whole. From the presented, the best adhesion was achieved using 0.25% ZN/NC and 0.25%TI/NC in the nanocomposite coating.

The highest work of the adhesion was achieved between the print and the coating with 1% TI/NC (70.12 mJ/m^2). According to some authors, only interphase dispersion interaction are important for the work of the adhesion i.e., 0.25% TI/NC (γ^d =29.15 mJm^{-2} / γ_{12} =0.06 mJm^{-2}) [165,166]. Furthermore, the increased concentration of nanoparticles in the varnish resulted with the increased work of adhesion, pointing to the increased work necessary to separate the two layers and improved adhesion. From SFE of the interphase and wetting coefficients one can also note that SFE of interphase generally lowers as the wetting coefficient increase 0.25% TI/NC / 1% TI/NC (S_1 = - 1.94 mJ/m^2 / S_1 = - 6.04 mJ/m^2).

However, SFE of the interphase is close to zero for all samples, which is favourable for the optimal adhesion. Wetting coefficients are negative for all coatings but are closer to zero for the nanocomposite coatings with 0.25% ZN/NC and 0.25% TI/NC. One can conclude that the increased concentration of the nanoparticles added to the varnish impairs the spontaneous spreading of the coating on the printed substrate.

Table 32 adhesion parameters between the plain print and - nanocomposite coatings

	Adhesion parameters (mJm^{-2})		
Sample	***γ_{12}***	***W_{12}***	***S_{12}***
WB	1.13	66.64	-2.71
0.25% ZN/NC	0.06	66.65	-1.97
0.5% ZN/NC	0.12	67.25	-2.69
1% ZN/NC	0.19	69.27	-4.85
0.25% TI/NC	0.75	65.24	-1.94
0.5% TI/NC	0.17	69.26	-4.80
1% TI/NC	0.36	70.12	-6.04
Hybrid/Z	0.30	68.69	-4.49
Hybrid/T	0.62	68.92	-5.36

5.4.5 FTIR analysis

From the obtained IR spectra of used printing substrate (paper), print and coated print, the vibrational bands of paper are masked with the vibrational bands of printing ink (Figure 48). The contribution of paper vibrational bands can be seen in the spectral region 1500 – 1100 cm^{-1} of print IR spectra. Moreover, the bands of paper and print are covered with the vibrational bands of used varnish.

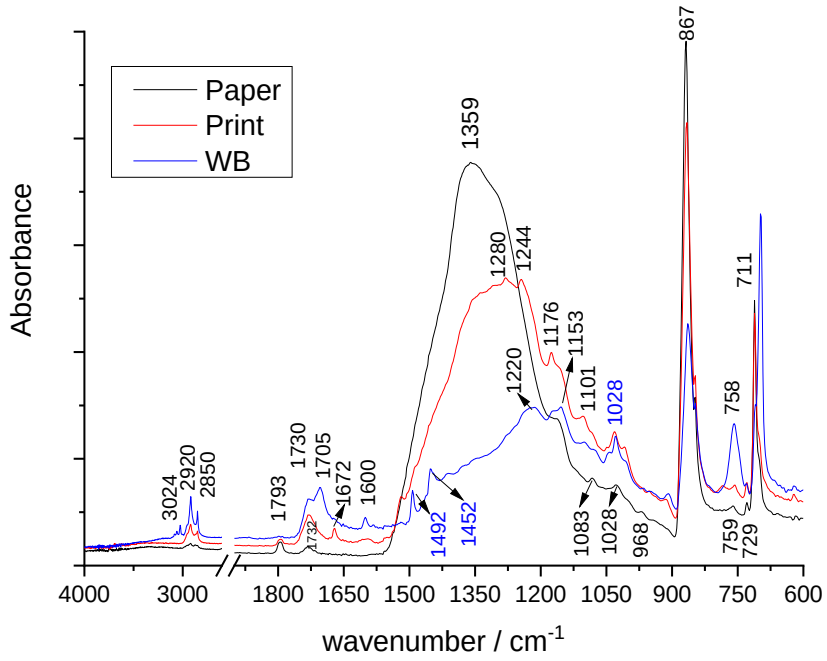

Figure 48 IR spectra of substrate, printed sample and WB coated sample

The substrate used in this research is coated paper. In the IR spectra, in the fingerprint region, a broad band centred at about 1359 cm^{-1} is detected, followed by the peaks around 1083, 1028, 1001, indicating the presence of kaolin in the coating formulation. The bands observed at 867 and 711 cm^{-1} can be attributed to the out-of- phase CO_3 bending vibration and the in-plane CO_2 bending vibration of calcium carbonate [167].

The used printing ink dries by the oxypolymerization. That means that the ink binder is composed of pigment, additives and ink binder based on the vegetable oil. In the IR spectra of print, bands characteristic of vegetable oils, common components of the ink binders, were observed. The bands at 2921 and 2852 cm^{-1} were assigned to the stretching modes of CH, CH_2, and CH_3 groups in aliphatic chains of fatty acids, while the carbonyl stretching band at 1732 cm^{-1} accompanied by the bands at 1244, 1176 and 1101 cm^{-1} pointed to the ester group.

The common water-based varnishes available on the market are of unknown chemical composition, due to the patent rights or intellectual rights. But in general, most of the water based varnishes for the flexographic printing are composed of polyvinyl acetate, acrylic binders and additives such as polyethylene or polypropylene waxes [168]. With the absence of information related to the composition of the used WB, but strong claim cannot be given about

the WB composition based on the IR spectra, although some assumptions can be made. In addition, differences between the functional groups can be observed.

The infrared spectrum of the WB can be characterized by several sharp and intense peaks. The most dominant band is related to the double C=O carbonyl stretching vibration associated to acetate groups with a molecular vibration at 1730 cm^{-1} and 1705 cm^{-1}, complemented by two less intense peaks at 1492 and 1435 cm^{-1} due to the CH3 asymmetric and symmetric bending vibration, respectively. The peak at 1220 cm^{-1} can be attributed to the asymmetric stretching mode of (C–O–C) linkages of the ester groups, followed at lower wavelengths by a double peak with the maximum at 1028 cm^{-1}. Additionally, different less intense peaks such as the doublet of the CH_3 and CH_2 antisymmetric stretching vibration at 2920 and 2850 cm^{-1} were detected [169,170].

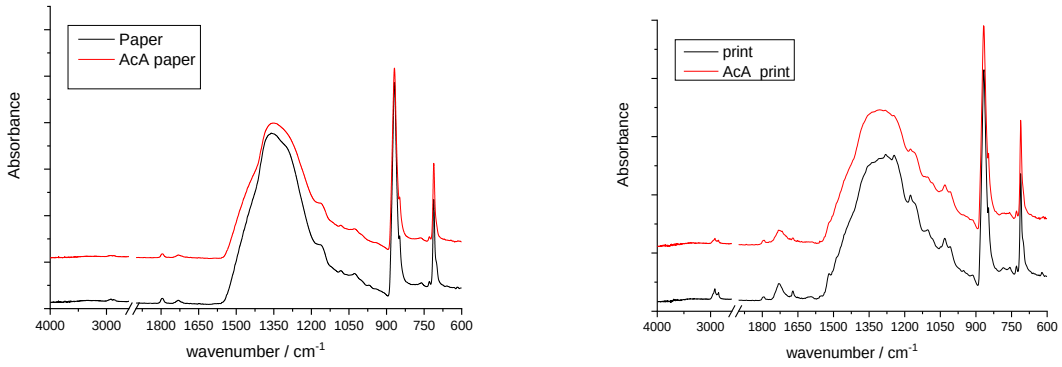

Figure 49 IR spectra of paper/AcA and print/AcA

With the ageing, no significant changes occurred in the IR spectra of paper (Figure 49). Moreover, it is important to emphasize that 30h AcA is probably very small period of time in which significant changes can occur. In the case of print, changes in the spectral range from 1300 – 1000 cm^{-1} can be noticed. Those vibrational bands are mainly attributed to the (C–O–C) linkages of the ester groups. After the exposure to UV radiation, the loss of ester groups can be noticed, i.e., the changes of the characteristic ester bonds and consequently the broadening of carbonyl vibrational band, which can be attributed to the formation of new oxidation products. In addition, differences of the CH_3 and CH_2 antisymmetric stretching vibration at spectral range 2920 - 2850 cm^{-1} were detected pointing to the changes in polymer structure.

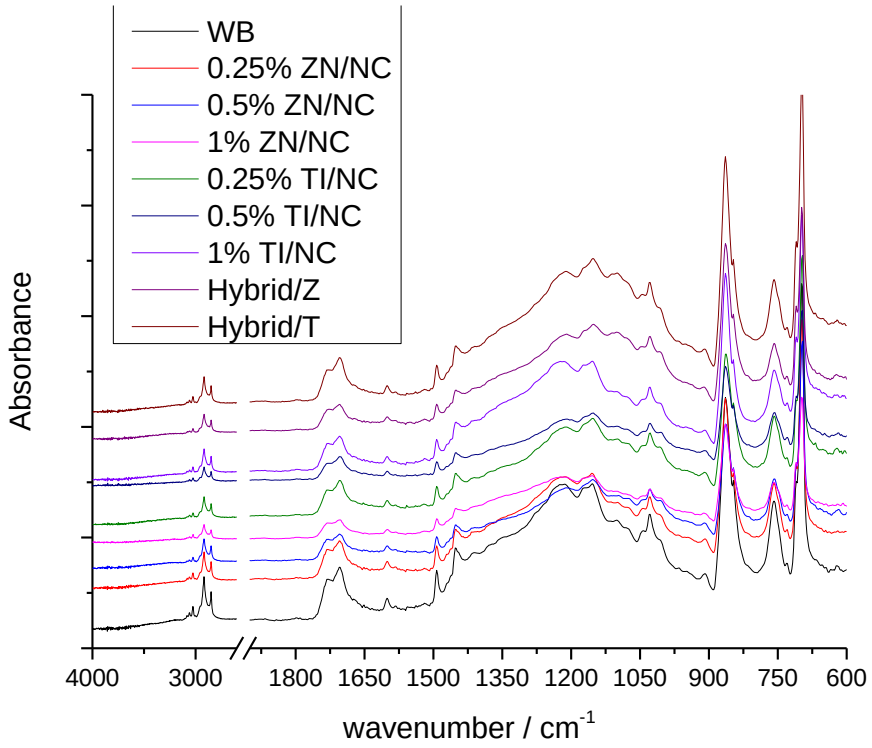

Figure 50 IR spectra of the presented nanocoatings

The incorporation of the nanoparticles in the polymer structure does not cause any significant changes in the IR spectra, as seen in the Figure 50. The changes in the intensities of the vibrational bands correspond to the ATR sampling performance not to any changes in chemical structure. For the samples made with the incorporation of the Hybrid systems, a significant changes and formation of new vibrational band at 1101 cm^{-1} can be noticed, with more pronounced peak in the case of Hybrid/T system. This can be attributed to the ester crosslinking which in the end can stabilize the whole polymer [171].

The influence of the ageing process can be noticed in the case of 0.25% and 0.5% ZN/NC, mainly in the case of C=O vibrational band. The broadening of the carbonyl stretching band can be attributed to the formation of newly oxidative products. In the case of 1% ZN/NC, no significant changes occurred in the IR spectra.

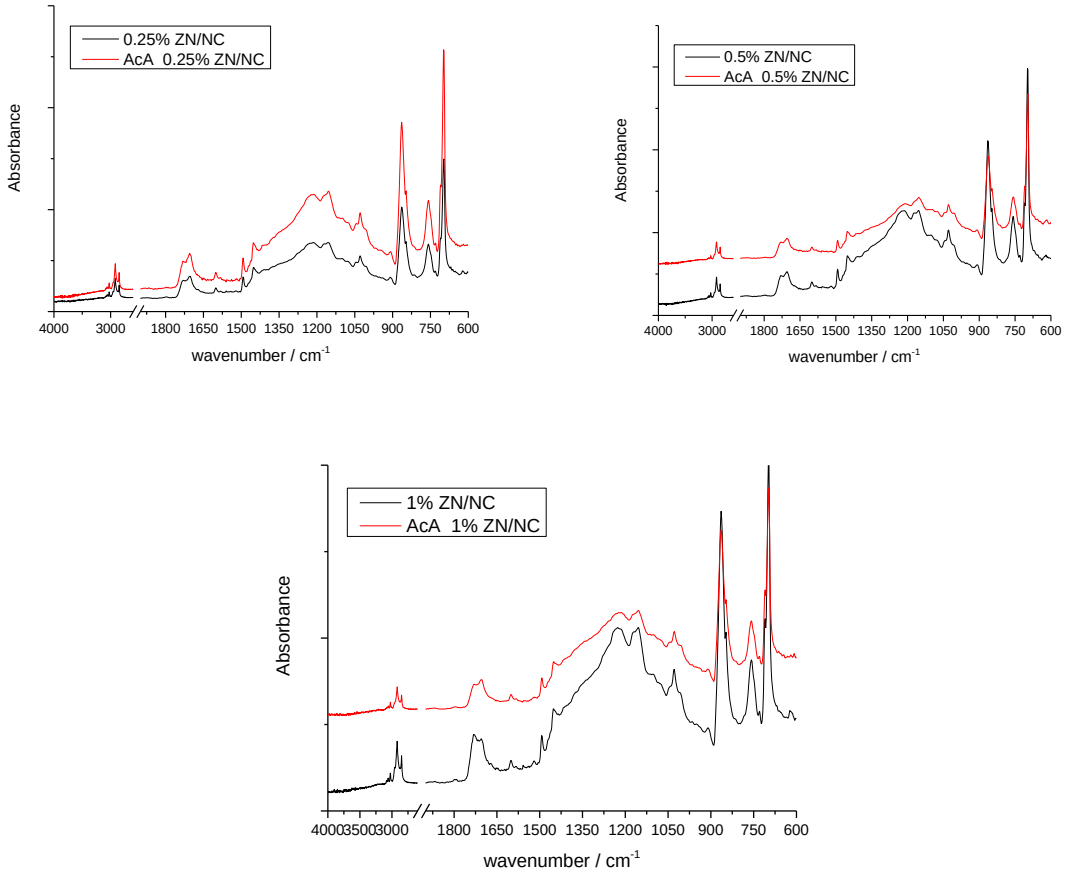

Figure 51 IR spectra of ZN/NC coated samples

In the case of TI/NC, no significant changes occurred in the IR spectra (Figure 52). This implies that WB is stabilized by the addition of nanoparticles. The results of the FTIR-ATR spectroscopy indicate a significant improvement of the UV stability of the nanomodified WB. The presence of the nanoparticles in the WB formulation slows down the formation of oxidative products during the aging process.

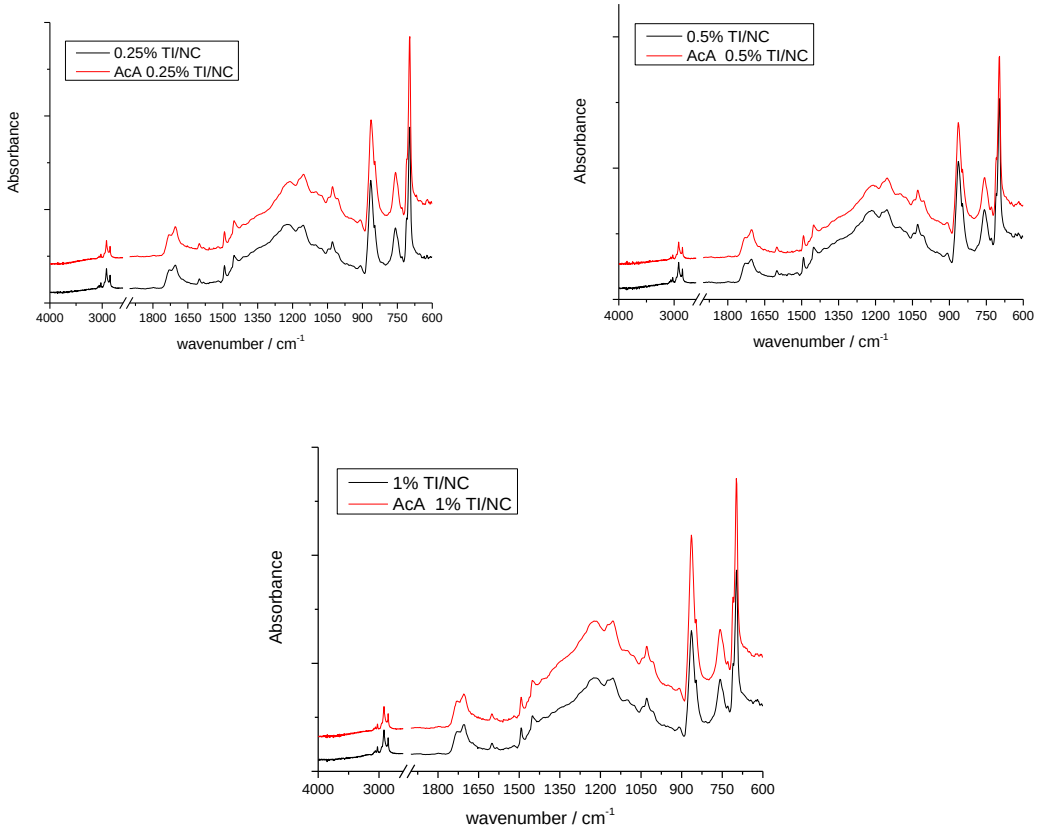

Figure 52 IR spectra of TI/NC coated samples

The same behaviour can be noticed in the case of the ageing of Hybrid/T system in which formation of new bands (at 1101 cm^{-1}) was observed (Figure 53). With the ageing process, slight changes occur in the case of Hybrid/Z system, mainly related to the carbonyl peak at 1730 cm^{-1} and increase of the band at 1600 cm^{-1} which can be attributed to the formation of new oxidative species.

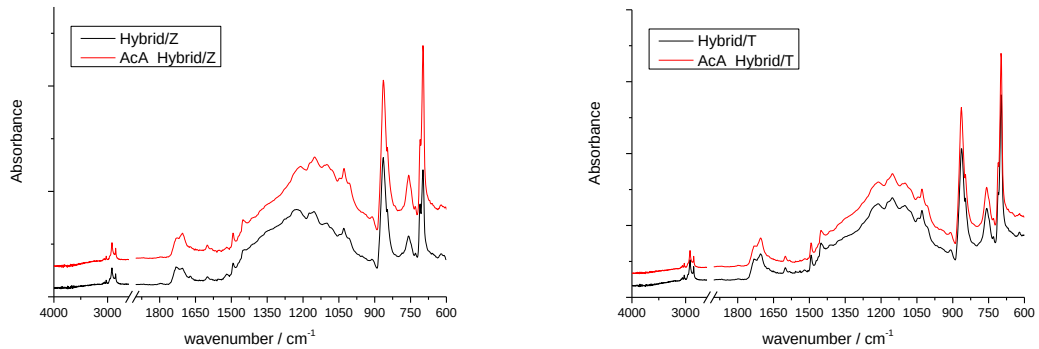

Figure 53 IR spectra of Hybrid/Z and Hybrid/T coated samples

5.4.6 WVTR analysis

Barrier properties of substrates can be upgraded by lamination or by coating, where coating can be even more upgraded by introducing the various compounds that could help with surface impregnation. As mentioned before, those compounds are in nano size. Unfortunately, there could be some limiting factors such as dispersion of NPs in the mixture and of course the limitations of the varnish itself. The investigation of barrier properties was conducted in two phases; one set of coated samples with 0h UV exposure time and one set of coated samples that were exposed to UV radiation for 30h. The samples were weighted, and results were recalculated with *WVTR* equation (12) from the chapter *4.7*. On diagram in Figure 54, WVTR results for ZN/NC are presented.

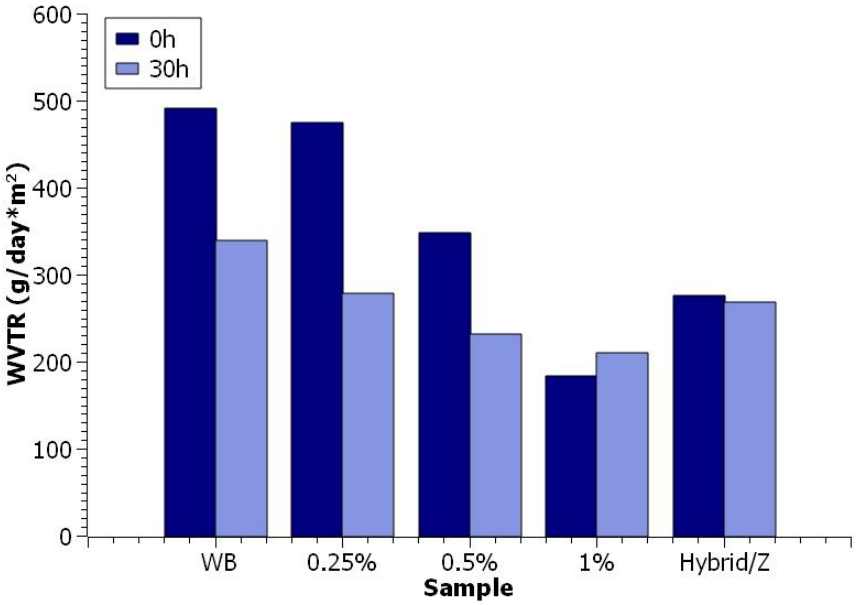

Figure 54 WVTR diagram for ZN/NC

The ZnO compound has a semi ion and semi covalent features, meaning it is very difficult to establish whether the H_2O vapour is absorbed as the whole molecule or just its dislocated parts [76,172]. The water absorption takes mostly place in the dissociated form where H_2O molecules are absorbed on ZnO compound for all temperature differences in form of $OH^{\cdot}$ and $H^{\cdot}$ radicals. Adsorption of $OH^{\cdot}$ radicals takes place at the Zn^{2+} location on the ZnO surface [173]. The unpaired $OH^{\cdot}$radical electrons bind to free electrons that are bound to Zn^{2+} location, therefore the strong homopolar bonds are formed [174]. In the case of metal oxides (ZnO and TiO_2) absorption occurs on dissociated parts of water and this is more the rule than the exception [76].

Diagram also shows that with increase of TiO_2 nanoparticles weight ratio, water permeability does decrease significantly. After 30h AcA the water permeability lowers.

The TiO_2, also a metal oxide is a compound that is found to have good water permeability features in various bulk studies [175–177]. In Figure 55, diagram is showing TI/NC. Oppose to the water-based varnish, lowest weight ratio of 0.25% TI/NC reduced water permeability by 56%. The *WVTR* results of 0h remained more or the less unchanged regardless of the NPs weigh ratio (%).

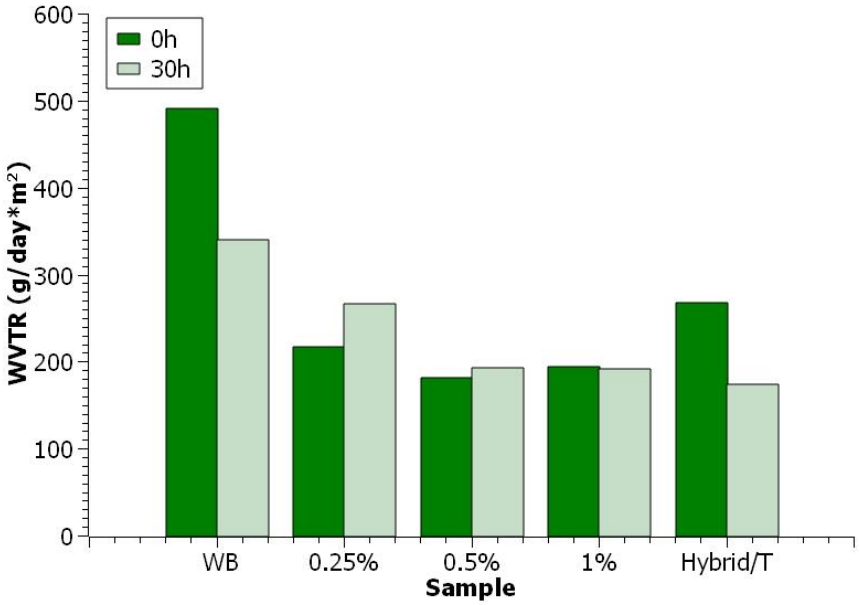

Figure 55 WWTR diagram for TI/NC

Coatings containing SiO_2 also decreased water permeability drastically, where Hybrid/Z 44% (Figure 54) and Hybrid/T (Figure 55) by 46% compared to WB. The SiO_2 nanoparticles with dissociative mechanism of water adsorption, primarily form Si-OH bonds, thus creating a layer that slows down the permeability process [13,172]. The 30h AcA on Hybrid/Z coated samples did no effect while on Hybrid/T coated samples it decreased the water permeability. The results of WVTR determination are in accordance with the SFE as well as FTIR results approximation.

5.4.7 Antimicrobial properties analysis

In Table 33., results for samples containing aerobic mesophilic bacteria, yeasts and molds can be seen. The sample coated with water-based varnish did inhibit more overall bacteria growth than the sample without coating. The problem related to the growth of various microorganisms occurs in almost all water-based inks. Since water-based varnishes used in printing have similar composition as printing inks, only without pigment, this problem can be related to them as well. In order to prevent or inhibit microbial growth, different biocides and fungicides can be added in their formulation [178].

When it comes to printing inks, additives in a function of biocides/fungicides are added in proportion of <0.5%, based on the total quantity of the ink formulation. The problem with ambient condition method is the uncertainty of the initial microbial count on the sample surface, meaning that the overall result between nanocomposite coated samples may oscillate regardless of the provided conditions [178]. The sample with 0.25% ZN/NC and Hybrid/Z showed the highest inhibition properties from the test batch.

Table 33 Testing of microbial contamination of samples in ambient conditions (ZN/NC)

	Aerobic mesophilic bacteria		***Yeasts and molds***
Sample	**$\log_{10}$ cfu/ml**	**cfu/cm^2**	**cfu/10cm^2**
No coating	2.47	7.5	1
WB coating	2.06	2.9	2
0.25%	1.60	1	2
0.5%	1.93	2.1	1
1%	1.93	2.1	2
Hybrid/Z	1.60	1	1

The TI/NC did not affect the contamination rate of samples by aerobic mesophilic bacteria, while Hybrid/T showed the best results overall (Table 34).

Table 34 Testing of microbial contamination of samples in ambient conditions (TI/NC)

	Aerobic mesophilic bacteria		***Yeasts and molds***
Sample	**log_{10} cfu/ml**	**cfu/cm^2**	**cfu/10cm^2**
No coating	2.47	7.5	1
WB coating	2.06	2.9	2
0.25%	2.51	8.1	2
0.5%	2.14	3.5	2
1%	2.35	5.6	1
Hybrid/T	2.00	2.5	1

The results of the growth test of pathogenic bacteria and mold on the surface of samples after artificial inoculation are presented in Table 35 and Table 36, for *S. aureus* and *L. monocytogenes*. The water-based coating performed better than the non-coated sample against *S. aureus* (Figure 56).

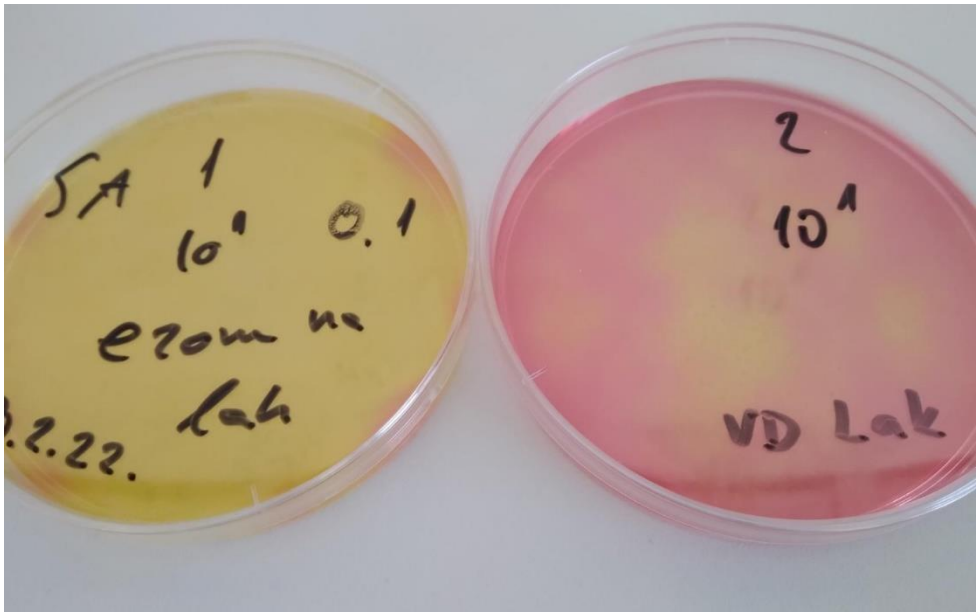

Figure 56 *Staphylococcus aureus* after incubation on WB samples

Samples contaminated with *L. monocytogenes* showed lower inhibition potential. In Figure 57 the inhibition of *L. monocytogenes* after incubation can be seen.

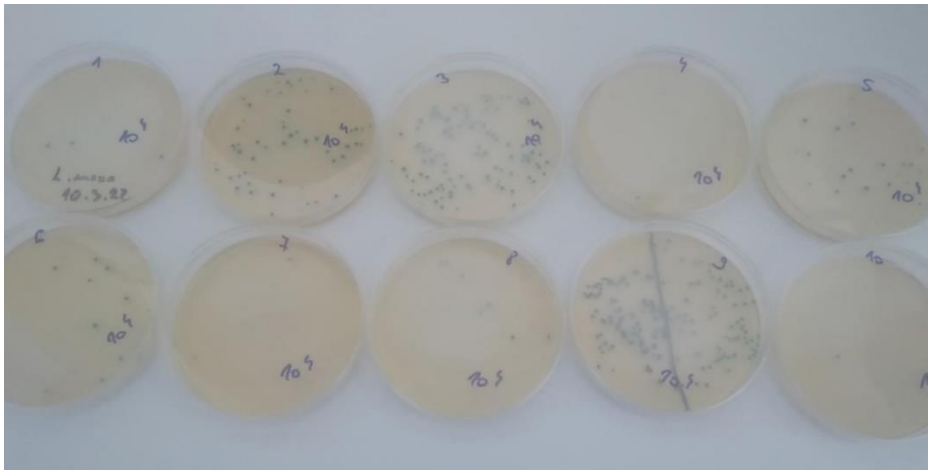

Figure 57 inhibition of *Listeria monocytogenes* after incubation (various samples)

The ZN/NC did not upgrade the water-based varnish's antimicrobial mechanism against *S. aureus* (Table 35, Figure 58). On the other hand, ZN/NC provided better results against *L. monocytogenes*. From the presented results, antimicrobial activity of the WB varnish was not present against *L. monocytogenes*, where ZN/NC showed the antiliteral potential [12]. The samples coated with Hybrid/Z nanocoating performed the highest antimicrobial properties toward both *S. aureus* and *L. monocytogenes*.

Table 35 Testing of microbial contamination of samples by *Staphylococcus aureus* and *Listeria monocytogenes* (ZN/NC)

	***Staphylococcus aureus* ATCC 25923**	***Listeria monocytogenes* ATCC 7644**
Sample	**$\log_{10}$ cfu/ml**	**$\log_{10}$ cfu/ml**
No coating	6.16 ± 0.42	5.77 ± 0.34
WB coating	5.23 ± 0.95	6.59 ± 0.17
0.25%	5.72 ± 0.13	5.49 ± 0.07
0.5%	5.1 ± 0.62	6.17 ± 0.18
1%	5.7 ± 0.61	5.8 ± 0.09
Hybrid/Z	5.03 ± 0.09	5.56 ± 0.32

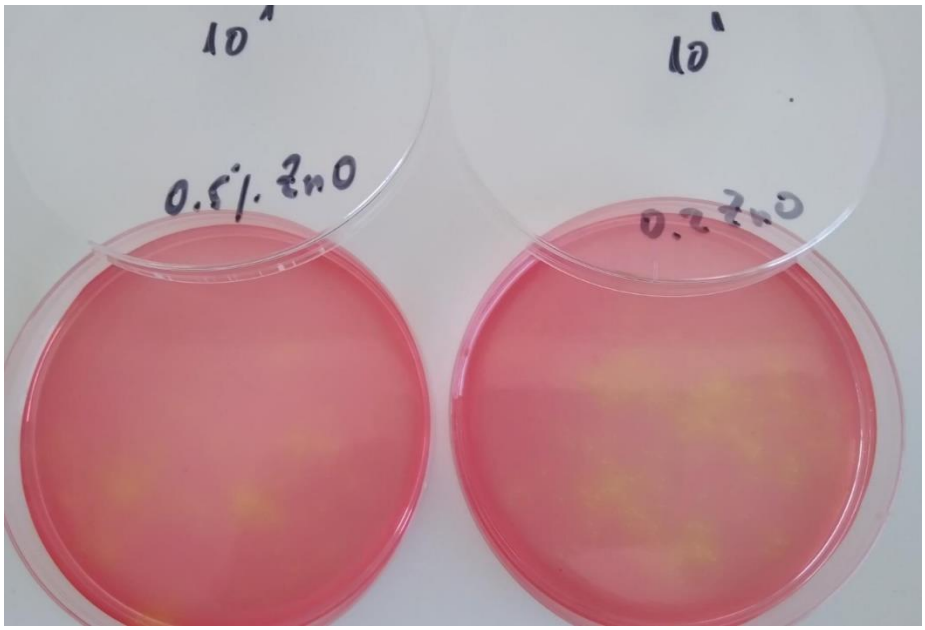

Figure 58 ZN/NC coated samples contaminated with *Staphylococcus aureus* after incubation

The samples coated with TI/NC showed upgrade of the WB varnish against *S. aureus* and *L. monocytogenes* on samples with 0.25 and 0.5% weight ratio, (Table 36, Figure 59).

Table 36 Testing of microbial contamination of samples by *Staphylococcus aureus* and *Listeria monocytogenes* (TI/NC)

	***Staphylococcus aureus* ATCC 25923**	***Listeria monocytogenes* ATCC 7644**
Sample	**$\log_{10}$ cfu/ml**	**$\log_{10}$ cfu/ml**
No coating	6.16 ± 0.42	5.77 ± 0.34
WB coating	5.23 0.95	6.59 ± 0.17
0.25%	4.97 ± 0.48	6.21 ± 0.27
0.5%	5.09 ± 0.18	5.3 ± 0.26
1%	5.56 ± 0.46	7.08 ± 0.08
Hybrid/T	5.74 ± 0.27	6.71 ± 0.36

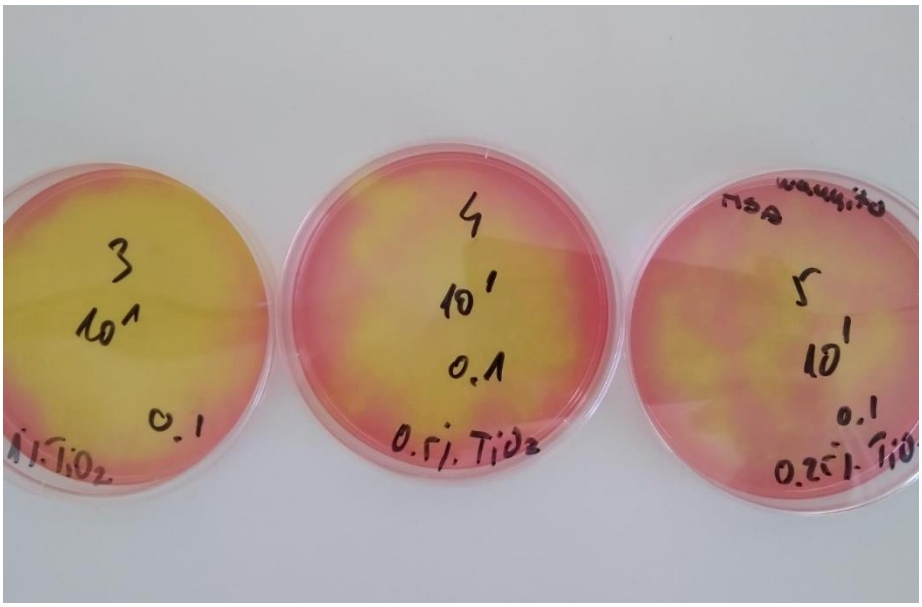

Figure 59 TI/NC coated samples contaminated with *Staphylococcus aureus* after incubation

The antimicrobial properties of the presented nanocomposite coating against *Citrobacter* spp. did not show any significant improvement. The ZN/NC (Table 37) and the TI/NC (Table 38) did not show any significant improvement of the WB against the *Citrobacter* spp., while Hybrid/Z showed the best result.

Table 37 Testing of microbial contamination by *Citrobacter* spp. (ZN/NC) – initial value was log10 cfu/ml = 7 per sample.

	Citrobacter spp
Sample	***log_{10} cfu/ml***
No coating	5.60
WB coating	5.69
0.25%	6.14
0.5%	6.34
1%	6.20
Hybrid/Z	5.30

Table 38 Testing of microbial contamination by *Citrobacter spp* (TI/NC) – initial value was log10 cfu/ml = 7 per sample.

	Citrobacter spp
Sample	***log_{10} cfu/ml***
No coating	5.60
WB coating	5.69
0.25%	5.69
0.5%	6.04
1%	5.95
Hybrid/T	6.23

After all tested bacteria and molds, the Hybrid/Z showed the best overall results. The SiO_2 has a proven antimicrobial mechanism, where on its surface presence of singlet oxygen and reactive oxygen fragments can be found that leads to disruption in the bacteria's cell membrane [179].

The ZN/NC and TI/NC showed improvement of the WB varnish on some tested microbes, but it has to be taken into account that the antimicrobial potential of nanoparticle compounds depends on the nanoparticle's size and crystal phase [180–182].

Table 39 Testing of microbial contamination of samples by *Yersinia enterocolitica* and *Penicillium* spp. (ZN/NC)

	Yersinia enterocolitica	***Penicillium* spp.**
Sample	**log_{10} cfu/ml**	**log_{10} cfu/ml**
No coating	<2	<2
WB coating	<2	<2
0.25%	<2	<2
0.5%	<2	<2
1%	<2	<2
Hybrid/Z	<2	<2

Table 40 Testing of microbial contamination of samples by *Yersinia enterocolitica* and *Penicillium spp*. (TI/NC)

	Yersinia enterocolitica	***Penicillium* spp.**
Sample	**log_{10} cfu/ml**	**log_{10} cfu/ml**
No coating	<2	<2
WB coating	<2	<2
0.25%	<2	<2
0.5%	<2	<2
1	<2	<2
Hybrid/T	<2	<2

The ZN/NC and TI/NC showed improvement of the WB varnish on some tested microbes, mainly *S. aureus* or *L. monocytogenes*. In the case of artificial inoculation of *Y. enterocolitica* and *Penicillium* spp. (Table 39 and Table 40), on control and experimental samples, no growth was observed. This clearly shows that the assessment of antimicrobial properties of nanocomposites depends on applied microbes and their (non) ability to growth on specific materials. On the other hand, *S. aureus* and *L. monocytogenes* are able to growth on different types of surfaces by biofilm formation, thus presenting the best indicator microorganisms for testing antimicrobial properties of applied nanocomposites.

ZN/NC supressed the growth of aerobic mesophilic bacteria to a greater extend compared to TI/NC. In terms of *S. aureus* and *L. monocytogenes,* both nanocomposites showed antimicrobial activity, therefore upgrade the commercial varnish in terms of cross contamination by handling of product (e.g. food packaging).

6 Comparison ZN/NC, TI/NC and Hybrids

To enable comparison between proposed coating compositions in this chapter most significant results which determine functionality of the coating are presented. The colorimetric values presented in Table 41 show that only the 0.25% ZN/NC did not exceed the ΔE_{ab}=5, which is designated border values in accordance with FOGRA PSO. Nevertheless, it can be noted that most problems occur at magenta (M) and (Y) where starting difference to the colour target was high. On the other hand, the closest colour difference for black (initial value is not close to the allowed colour difference) was achieved on the sample with highest TiO_2 weight ratio. From these results it could be noted that introduction of nanoparticles into the coating requests primary colours closer to the target CIE LAB values.

Table 41 Comparison of ΔE_{ab}

Sample	C	M	Y	K
Uncoated	1.97	3.74	4.28	3.05
WB	1.98	4.54	2.61	3.57
0.25% ZN/NC	1.54	4.51	3.78	2.74
0.5% ZN/NC	1.74	*5.18*	*5.29*	2.85
1% ZN/NC	1.35	4.43	*5.16*	2.92
Hybrid/Z	1.52	*5.66*	*5.07*	2.82
0.25% TI/NC	1.15	*5.47*	3.73	2.52
0.5% TI/NC	1.32	*6.95*	3.10	2.15
1% TI/NC	1.81	*6.88*	1.42	4.60
Hybrid/T	2.22	*6.03*	3.33	2.55

Table 42 Comparison of ΔE_{00} (0h and 30h AcA)

Sample	C	M	Y	K
WB	0.83	0.64	2.78	0.91
0.25% ZN/NC	0.46	0.56	2.55	0.33
0.5% ZN/NC	0.32	0.52	2.33	0.36
1% ZN/NC	0.60	0.53	2.06	0.96
Hybrid/Z	0.14	0.52	2.36	0.38
0.25% TI/NC	0.21	0.54	2.60	0.60
0.5% TI/NC	0.22	0.66	2.42	0.45
1% TI/NC	0.63	0.65	1.94	0.36
Hybrid/T	0.71	0.55	1.11	0.25

The colorimetric difference, ΔE_{00} between samples non-AcA samples and 30h AcA samples in comparison to WB can be seen in the Table 42. The smallest overall difference can be noted with Hybrid/Z and Hybrid/T. It can also be seen that with TI/NC, overall difference is slightly lower than with ZN/NC, but they are both capable to provide protection against UV radiation induced lightfastness.

In the Table 43, WVTR difference regarding the WB for both 0h and 30h AcA samples is shown. The smallest TI/NC weight ratio (0.25%) lowers the WVTR by 56%. Table 42 also shows that with increase of TiO_2 nanoparticles weight ratio, water permeability decreases significantly where the 0.5% TI/NC provided the best result (-63%). The second column showing results after 30h AcA was calculated also compared to the WB that was under UV induced AcA. The TI/NC also showed the better performance.

Table 43 WVTR comparison of samples compared to WB

Sample	0 h	30 h (AcA)
0.25% ZN/NC	-4%	-18%
0.5% ZN/NC	-29%	-32%
1% ZN/NC	-44%	-21%
Hybrid/Z	-46%	-49%
0.25% TI/NC	-56%	-21%
0.5% TI/NC	-63%	-43%
1% TI/NC	-61%	-43%
Hybrid/T	-46%	-49%

SFE of the interphase is close to zero for all samples, which is favourable for the optimal adhesion. Wetting coefficients are negative for all coatings but are closer to zero for the nanocomposite coatings with 0.25% ZN/NC and 0.25% TI/NC.

The highest work of the adhesion was achieved between the print and the coating with 1% TI/NC. Although wetting coefficients are negative for all investigated sample, they are closest to 0 at 0.25% ZN/NC and TI/NC. With SFE of the interphase for all investigated nanocomposites closer to zero than the WB, it could be expected good adhesion of them onto the prints.

Table 44 Adhesion comparison

	Adhesion parameters (mJm^{-2})		
Sample	γ_{12}	W_{12}	S_{12}
WB	1.13	66.64	-2.71
0.25% ZN/NC	0.06	66.65	**-1.97**
0.5% ZN/NC	0.12	67.25	-2.69
1% ZN/NC	0.19	69.27	-4.85
0.25% TI/NC	0.75	65.24	**-1.94**
0.5% TI/NC	0.17	69.26	-4.80
1% TI/NC	0.36	**70.12**	-6.04
Hybrid/Z	0.30	68.69	-4.49
Hybrid/T	0.62	68.92	-5.36

To better determine influence of the added NPs to WB, values in Table 45 represent stiffness in regard to WB. The stiffness increases with addition of the NPs but there is no visible dependence to the NP weight ratio (Table 45). After 30h AcA 0.5% TI/NC has the biggest increase of stiffness regarding AcA-WB.

Table 45 Comparison of stiffness/bursting strength change of nanocomposites compared to WB

	Stiffness		Bursting	
Sample	0 h	30 h	0 h	30 h
0.25% ZN/NC	12%	15%	4%	4%
0.5% ZN/NC	22%	22%	-2%	2%
1% ZN/NC	16%	19%	0%	5%
Hybrid/Z	11%	7%	3%	-2%
0.25% TI/NC	12%	21%	6%	0%
0.5% TI/NC	16%	30%	0%	5%
1% TI/NC	15%	20%	2%	4%
Hybrid/T	14%	16%	-2%	5%

On the other hand, it can be noted that the overall bursting strength of the sample is almost unchanged (Table 45). Although after coating, there was almost no change, it could be noted that after 30 h AcA almost all nanocomposites show higher bursting strength values than the WB, with exception of Hybrid/Z.

The antimicrobial activity is calculated to the values achieved on WB on three bacteria cultures. The negative values in Table 46 means better antimicrobial activity.

On *Aerobic mesophilic bacteria*, ZN/NC provided better bacteria inhibition than the TI/NC. In terms of other two, *Staphylococcus aureus* and *Listeria monocytogenes*, both nanocomposites show the ability to inhibit bacteria therefore upgrade the commercial varnish in terms of antimicrobial activity.

Table 46 Antimicrobial properties of NP compared to WB

Sample	*Aerobic mesophilic bacteria*	*Staphylococcus aureus ATCC 25923*	*Listeria monocytogenes ATCC 7644*
0.25% ZN/NC	**-22%**	9%	**-17%**
0.5% ZN/NC	**-6%**	**-2%**	**-6%**
1% ZN/NC	**-6%**	9%	**-12%**
Hybrid/Z	**-22%**	**-4%**	**-16%**
0.25% TI/NC	22%	0%	0%
0.5% TI/NC	4%	**-5%**	**-6%**
1% TI/NC	14%	**-3%**	**-24%**
Hybrid/T	**-3%**	10%	2%

7 Conclusion

Packaging industry as part of wider printing industry must find more sustainable solutions to cope with the new challenges. Coating applications is environmentally more suitable than the lamination as well as cheaper. The idea was to formulate new type of coating by upgrading a commercial varnish with nanoparticle compounds that have features that are desirable in the printed packaging. Due to their properties, compounds chosen for this research were ZnO, TiO_2 and SiO_2.

For the purpose of this research, nanocomposite coatings were prepared by mixing and homogenizing defined weight ratio of TiO_2 and ZnO (0.25, 0.50, 1%) and two hybrids, which included 0.5% wt SiO_2 and TiO_2/ZnO into the commercial waterbased varnish (WB). These nanocomposites were diluted with demineralized water due to the targeted viscosity (in accordance with the application technology – flexography). The coatings were then applied onto the prepared prints achieved in lithographic offset in accordance with Fogra PSO.

The coated print samples were characterized by obtaining SEM images and EDS spectra to detect possible agglomerates, determining colour coordinates value, mechanical and surface properties and evaluation of the antimicrobial activity. The analysed samples were put under the influence of light degradation (accelerated ageing (AcA) in Xenon chamber) for 30 hours.

The newly formed nanocomposite compositions can protect the printed paperboard packaging, with a relatively small effect on the colour. Although on some samples primary colours caused colour difference to the colour targets set by Fogra PSO above ΔE_{ab}=5, it must be taken into account that the initial values were close to the tolerance range (magenta was above ΔE_{ab} 4.5). Nevertheless, that means that usage of the proposed nanocomposites leads to better control of the printing and setting the primary colours closer to the colour targets, if printing in standardized mode. The results showed that ZN/NC have the initial colour difference to FOGRA PSO target values smaller than the TI/NC.

The results proved that ZN/NC and TI/NC did increase the resistance to AcA induced by the UV radiation, i.e. better preserved colour appearance. After 30h AcA, TI/NC showed higher resistance to UV radiation, where the ΔE_{00} values are slightly lower. Furthermore, it can be noted that increase of the nanoparticle's weight ratio will increase preservation of colour in the AcA process.

Both Hybrid/Z and Hybrid/T did upgrade the WB performance in terms of resistance to the AcA, where Hybrid/T showed better resistance to the lightfastness caused by the UV radiation. When compared to WB they both upgraded the system, where in terms of M and Y ink Hybrid/Z performed 19 and 14% better and Hybrid/T performed 15 and 60% better.

Regarding the mechanical properties, evaluation of the bursting strength and cardboard stiffness was performed. The results showed that including nanoparticles did not significantly changed the mechanical properties of the cardboard in the terms of busting strength but influenced sample's stiffness. Although not to great extent, the proposed nanocomposites caused increase of the bursting strength after AcA. In both sets (ZN/NC and TI/NC) there is no visible dependence between mechanical properties and weight ratio of nanoparticles.

The results showed that the highest work of the adhesion was achieved between the print and the coating with 1% TI/NC, but it is visible that even lower weight ratios of the nanoparticles will result with similar values (with exception of the 0.25%), higher than the one achieved at WB. From the results of the adhesion parameters, it could be concluded that increasing weight ratio of nanoparticles will decrease S_{12}, which leads to the conclusion that adhesion of the proposed coating will be worse than the WB, although this is partly compensated by decrease of interfacial tension and increase of the work of adhesion.

The incorporation of the nanoparticles in the polymer structure does not cause any significant changes in the IR spectra. For the samples made with the incorporation of the Hybrid systems, a significant changes and formation of new vibrational band at 1101 cm^{-1} can be noticed, with more pronounced peak in the case of Hybrid/T system. This can be attributed to the ester crosslinking which in the end can stabilize the whole polymer meaning it become more resilient to any possible change in its structure. In the case of TI/NC, no significant changes occurred in the IR spectra. This implies that WB is stabilized by the addition of nanoparticles.

The WVTR values decrease with the increase of the nanoparticles weight ratio, i.e. the barrier for water vapour increases significantly (ZN/NC). On the other hand, by TI/NC even the lowest weight ratio significantly increases barrier properties, but further addition of nanoparticles has lower influence. Furthermore, coatings containing SiO_2 decrease water permeability drastically (Hybrid/Z 44% and Hybrid/T by 46% compared to WB).

Results have showed that the AcA diminished influence of the nanoparticles on the water vapour transfer rate, i.e. the difference to the WB is lower. The results of the antimicrobial activity showed that the Hybrid/Z showed the best overall results. The ZN/NC and TI/NC

showed improvement of the WB varnish on some tested microbes (*Staphylococcus aureus*, *Yersinia enterocolitica*, *Listeria monocytogenes*, inoculation of Enterobacteria (*Citrobacter spp*.) in lyophilized form and mold of *Penicillium spp)*. But in the case of *Yersinia enterocolitica* and mold of *Penicillium spp* , the incorporation of proposed nanoparticles did not cause improvements in the antimicrobial activity. On *Aerobic mesophilic bacteria*, ZN/NC provided better bacteria inhibition than the TI/NC. In terms of other two, *Staphylococcus aureus* and *Listeria monocytogenes*, both nanocomposites show the ability to inhibit bacteria therefore upgrade the commercial varnish in terms of antimicrobial activity.

To summarize, all three hypotheses defined before research have been proved:

H1:

The addition of nanoparticles in commercial varnish will influence the properties of nanocomposites and of the coated printed samples. However, it will not create significant change of the sample colorimetric. – coating of printed cardboard packaging with prepared nanocomposites has relatively little effect on the printed colour. Only some coatings exceed the allowed tolerance $\Delta E_{ab} > 5$ and in that causes initial colorimetric value of WB (ΔE_{ab}) was close to the FOGRA PSO border value.

H2:

The addition of of nanoparticles in commercial varnish will lower the overall degradation caused by electromagnetic radiation while improving barrier properties of the packaging material. – coating with ZN/NC and TI/NC will increase resistance to accelerated ageing. Surface properties (mechanical resistance) as well barrier properties will not change significantly with age. On the other hand, the coating with proposed nanocomposites increased barrier to water vapour before, but also after AcA.

H3:

Coatings enriched with TiO_2 and ZnO nanoparticles with the help of the UV light will improve the antimicrobial properties of the packaging material. – NPs did upgrade the bacteria inhibition properties. After antimicrobial analysis on three know bacteria (*Aerobic mesophilic bacteria, Staphylococcus aureus* and *Listeria monocytogenes),* ZN/NC provided protection against all, where TI/NC did not work against *Aerobic mesophilic bacteria* at all.

The scientific contribution of this research can be seen in the researched and provided results of the nanocomposite's composition on its application in printing process. Moreover, this research provided information on optimal composition and weight ratios of presented nanocomposites in achieving designated protective features on the printed packaging surface. Furthermore, this research provided a new perspective on packaging functionality through antimicrobial properties.

To conclude, this research proved the benefits of nanoparticles addition to commercial varnish as it does not significantly influence colour, could be applied with known technologies but provides added value in terms of antimicrobial activity, resistance to colour change induced by UV radiation and improving barrier properties to water vapour.

Further research will focus on tailoring the nanocomposite composure (number of added nanoparticles) and incorporating the nanoparticles in the different varnish types as well as targeting primary colours to achieve coated prints in accordance to present printing standards.

8 Reference

[1] Antimicrobial Packaging Market - Growth, Trends, COVID-19 Impact, and Forecasts (2021 - 2026), (n.d.). https://www.mordorintelligence.com/industry-reports/antimicrobial-packaging-market (accessed April 15, 2021).

[2] DSM, Carbon Footprint Study for Industrial Coatings Applied on a Metal Substrate Focus on Powder Coatings, (2011) 24. https://www.dsm.com/content/dam/dsm/furniture/en_US/documents/20.-dsm-carbon-footprint--disclaimer.pdf.

[3] COVID-19: do I need to wash my shopping and groceries? | Patient, (n.d.). https://patient.info/news-and-features/covid-19-do-i-need-to-wash-my-shopping-and-groceries (accessed January 25, 2022).

[4] More bacteria are becoming resistant to antibiotics – here's how viruses and vaccines could help | Research and Innovation, (n.d.). https://ec.europa.eu/research-and-innovation/en/horizon-magazine/more-bacteria-are-becoming-resistant-antibiotics-heres-how-viruses-and-vaccines-could-help (accessed January 25, 2022).

[5] O.M. El-Feky, E.A. Hassan, S.M. Fadel, M.L. Hassan, Use of ZnO nanoparticles for protecting oil paintings on paper support against dirt, fungal attack, and UV aging, J. Cult. Herit. 15 (2014) 165–172. https://doi.org/10.1016/j.culher.2013.01.012.

[6] S.P. Krumdieck, R. Boichot, R. Gorthy, J.G. Land, S. Lay, A.J. Gardecka, M.I.J. Polson, A. Wasa, J.E. Aitken, J.A. Heinemann, G. Renou, G. Berthomé, F. Charlot, T. Encinas, M. Braccini, C.M. Bishop, Nanostructured TiO 2 anatase-rutile-carbon solid coating with visible light antimicrobial activity, Sci. Rep. 9 (2019) 1–11. https://doi.org/10.1038/s41598-018-38291-y.

[7] J. Salla, K.K. Pandey, K. Srinivas, Improvement of UV resistance of wood surfaces by using ZnO nanoparticles, Polym. Degrad. Stab. 97 (2012) 592–596. https://doi.org/10.1016/j.polymdegradstab.2012.01.013.

[8] M. Golik Krizmanić, PCL-ZnO nanoparticle funtional coating in terms of sunstrate protection (Funkcionalni premaz od PCL-a s dodatkom cinkovog oksida kao zaštita otisaka), University of Zagreb, 2020. http://library1.nida.ac.th/termpaper6/sd/2554/19755.pdf.

[9] R. Moya, A. Rodríguez-Zúñiga, J. Vega-Baudrit, A. Puente-Urbina, Effects of adding TiO2 nanoparticles to a water-based varnish for wood applied to nine tropical woods of Costa Rica exposed to natural and accelerated weathering, J. Coatings Technol. Res. 14 (2017) 141–152. https://doi.org/10.1007/s11998-016-9848-7.

[10] T. Cigula, T. Hudika, M. Katana, M. Golik Krizmanić, T. Tomašegović, The influence of PCL-ZnO coating composition on coated offset cardboard prints, (2020) 101–108. https://doi.org/10.24867/grid-2020-p8.

[11] T. Hudika, T. Cigula, M. Žličarić, M. Strižić Jakovljević, PCL-TiO2 nanocomposite to improve ageing of offset prints, (2020) 119–129. https://doi.org/10.24867/grid-2020-p10.

[12] D. Zvekic, V. Srdic, M. Karaman, M. Matavulj, Antimicrobial properties of ZnO nanoparticles incorporated in polyurethane varnish, Process. Appl. Ceram. 5 (2011) 41–45. https://doi.org/10.2298/pac1101041z.

[13] T. Cigula, T. Hudika, M. Vukoje, Modulation of water based commercial varnish by adding ZnO and SO2 nanoparticles to enhance protective function on printed packaging, in: 2. Int. Circ. Packag. Conf., ICP; FTPO Slovenia, Ljubljana, Slovenia, 2021: pp. 249–260.

[14] Z.Y. Wang, F.C. Liu, E.H. Han, W. Ke, S.Z. Luo, Effect of ZnO nanoparticles on anti-aging properties of polyurethane coating, Chinese Sci. Bull. 54 (2009) 3464–3472. https://doi.org/10.1007/s11434-009-0024-7.

[15] C.L. de Dicastillo, M.G. Correa, F.B. Martínez, C. Streitt, M.J. Galotto, Antimicrobial Effect of Titanium Dioxide Nanoparticles, Antimicrob. Resist. - A One Heal. Perspect. (2020). https://doi.org/10.5772/INTECHOPEN.90891.

[16] F. Golub, Influence of the amount of functional coatings on the properties of prints, University of Zagreb, 2019.

[17] T. Hudika, T. Cigula, M. Vukoje, Antimicrobial properties of TiO2 nanocomposite coating, in: Proc. 13th Int. Conf. Nanomater. - Res. Appl., 2021: pp. 351–358. https://doi.org/doi.org/10.37904/nanocon.2021.4345.

[18] D. Meng, X. Liu, Y. Xie, Y. Du, Y. Yang, C. Xiao, Antibacterial Activity of Visible Light-Activated TiO2 Thin Films with Low Level of Fe Doping, Adv. Mater. Sci. Eng. 2019 (2019). https://doi.org/10.1155/2019/5819805.

[19] R. Kumar, A. Umar, G. Kumar, H.S. Nalwa, Antimicrobial properties of ZnO nanomaterials: A review, Ceram. Int. 43 (2017) 3940–3961. https://doi.org/10.1016/j.ceramint.2016.12.062.

[20] P.J.P. Espitia, R.A. Batista, C.G. Otoni, N.F.F. Soares, Antimicrobial Food Packaging Incorporated with Triclosan: Potential Uses and Restrictions, Antimicrob. Food Packag. (2016) 417–423. https://doi.org/10.1016/B978-0-12-800723-5.00033-4.

[21] G. Fuertes, I. Soto, R. Carrasco, M. Vargas, J. Sabattin, C. Lagos, Intelligent Packaging Systems: Sensors and Nanosensors to Monitor Food Quality and Safety, J. Sensors. 2016 (2016). https://doi.org/10.1155/2016/4046061.

[22] Gloves Won't Reduce Your Risk of COVID-19 at the Grocery Store, (n.d.). https://www.healthline.com/health-news/wearing-gloves-while-grocery-shopping-doesnt-prevent-covid-19#Why-gloves-arent-medically-necessary (accessed September 14, 2021).

[23] C.D. Russell, C.J. Fairfield, Co-infections, secondary infections, and antimicrobial use in patients hospitalised with COVID-19 during the first pandemic wave from the ISARIC WHO CCP-UK study: a multicentre, prospective cohort study, The Lancet Microbe. 2 (2021) e354–e365. https://doi.org/10.1016/S2666-5247(21)00090-2.

[24] A History of Packaging | Ohioline, (n.d.). https://ohioline.osu.edu/factsheet/cdfs-133 (accessed January 25, 2022).

[25] The History of Packaging | Crawford Packaging Blog, (n.d.). https://crawfordpackaging.com/automation-and-innovations/history-of-packaging (accessed January 25, 2022).

[26] Introduction - Consumer Advertising During the Great Depression: A Resource Guide - Research Guides at Library of Congress, (n.d.). https://guides.loc.gov/consumer-advertising-great-depression (accessed January 25, 2022).

[27] Brief History of Polymers | MATSE 202: Introduction to Polymer Materials, (n.d.). https://www.e-education.psu.edu/matse202/node/4 (accessed January 25, 2022).

[28] The battle: Getting on the shelf. The war: Getting in the cart | Grocery Dive, (n.d.). https://www.grocerydive.com/news/grocery--the-battle-getting-on-the-shelf-the-war-getting-in-the-cart/535535/ (accessed October 6, 2021).

[29] D. Goodwin, D. Young, Protective packaging for distribution : design and development, (2011) 256.

[30] EUR-Lex - 32019L2161 - EN - EUR-Lex, (n.d.). https://eur-lex.europa.eu/legal-content/EN/TXT/?uri=CELEX:32019L2161 (accessed January 25, 2022).

[31] Primary, Secondary & Tertiary Packaging | Saxon Packaging, (n.d.). https://www.saxonpackaging.co.uk/difference-between-primary-secondary-tertiary-packaging/ (accessed September 30, 2021).

[32] Consumer rights directive | European Commission, (n.d.). https://ec.europa.eu/info/law/law-topic/consumer-protection-law/consumer-contract-law/consumer-rights-directive_en (accessed September 30, 2021).

[33] M. Cortina-Mercado, U. Del Este, P. Rico, Effect of Packaging Design in the Purchase Decision Process: a Comparison of Generations, Glob. J. Bus. Res. 11 (2017) 11–26. www.theIBFR.com.

[34] What is Tamper-Evident Packaging? | IPS Packaging & Automation, (n.d.). https://www.ipack.com/solutions/post/what-is-tamper-evident-packaging (accessed January 25, 2022).

[35] A special article about packaging optimization. It's useful in any business!, (n.d.). https://boxaroundtheworld.com/packaging-optimization/ (accessed January 25, 2022).

[36] What Is Packaging? Definition, Types, Functions, Types Of Packaging Material, (n.d.). https://www.geektonight.com/what-is-packaging/ (accessed September 30, 2021).

[37] 4 Reasons Why Package Optimization Also Benefits Your Supply Chain, (n.d.). https://www.globaltranz.com/package-optimization/ (accessed January 25, 2022).

[38] Primary, secondary and tertiary packaging: What's the difference? | CARTIER, (n.d.). https://www.emballagecartier.com/en/article/primary-secondary-and-tertiary-packaging-whats-the-difference/ (accessed January 25, 2022).

[39] Figure - organic-packaging-for-organic-tea, (n.d.). https://www.tripwiremagazine.com/wp-content/uploads/2012/06/organic-packaging-for-organic-tea.jpg (accessed May 18, 2022).

[40] A. Ybxoll, R. Janson, S.R. Bradbury, J. Langley, J. Wearn, S. Hayes, Openability: Producing design limits for consumer packaging, Packag. Technol. Sci. 19 (2006) 219–225. https://doi.org/10.1002/pts.725.

[41] The Importance of Secondary Packaging, (n.d.). https://www.alcaminow.com/blog/the-importance-of-secondary-packaging (accessed January 25, 2022).

[42] Primary, Secondary & Tertiary Packaging | Saxon Packaging, (n.d.). https://www.saxonpackaging.co.uk/difference-between-primary-secondary-tertiary-packaging/ (accessed March 8, 2021).

[43] K.L. Yam, The Wiley encyclopedia of packaging technology, 2010. https://doi.org/10.5860/choice.47-6003.

[44] P.J. Conway, M. Bale, Approximating the Effective Protection Coefficient without Reference to Technological Data Author (s): Patrick J . Conway and Malcolm Bale Source : The World Bank Economic Review , Vol . 2 , No . 3 (Sep ., 1988), pp . 349-363 Published by : Oxford Uni, 2 (2022) 349–363.

[45] What Are The Different Types Of Packaging Materials?, (n.d.). https://www.industrialpackaging.com/blog/what-are-packaging-materials (accessed January 26, 2022).

[46] W. Soroka, Fundamentals of Packaging Technology, 2nd ed., Institute of Packaging Professionals, Herndon (USA), 1999. https://doi.org/1566768624.

[47] K. Verghese, S. Lockrey, S. Clune, D. Sivaraman, Life cycle assessment (LCA) of food and beverage packaging, Woodhead Publishing Limited, 2012. https://doi.org/10.1533/9780857095664.4.380.

[48] D.L.T. Beynon, Plastics Packaging, Third Edit, Carl Hanser Verlag GmbH & Co. KG, 1972. https://doi.org/10.1111/j.1471-0307.1972.tb01123.x.

[49] M.R. Klimchuk, S.A. Krasovec, Packaging Design: Successful Product Branding from Concept to Shelf, illustrate, NYC (USA), 2006. https://doi.org/047172016X.

[50] C. Vasile, M. Sivertsvik, Food Packaging Manual, Special ei, MDPI, Basel (CH), 2019.

[51] M.J. Fabra, A. López-Rubio, J.M. Lagaron, Biopolymers for food packaging applications, 2014. https://doi.org/10.1533/9780857097026.2.476.

[52] Directive 94/62/EC on packaging and packaging waste — European Environment Agency, (n.d.). https://www.eea.europa.eu/policy-documents/directive-94-62-ec-on (accessed October 1, 2021).

[53] EC, Directive (EU) 2018/852 of the European Parliament and of the Council of 30 May 2018 amending Directive 94/62/EC on packaging and packaging waste, Off. J. Eur. Union. 2018 (2018) 141–154. https://eur-lex.europa.eu/legal-content/EN/TXT/PDF/?uri=CELEX:32018L0852.

[54] EUR-Lex - 31994L0062 - EN, Off. J. L 365 , 31/12/1994 P. 0010 - 0023; Finnish Spec. Ed. Chapter 15 Vol. 13 P. 0266 ; Swedish Spec. Ed. Chapter 15 Vol. 13 P. 0266 ; . (n.d.).

[55] A. Regattieri, G. Santarelli, The Important Role of Packaging in Operations Management, Oper. Manag. (2013). https://doi.org/10.5772/54073.

[56] Slade-Brooking, Catharine, Creating a Brand Identity: A Guide for Designers: (Graphic Design Books, Logo Design, Marketing), 1st ed., Laurence King Publishing, London, 2016.

[57] Wrapping up? How paper and board are back on track, (n.d.). https://www.allianz-trade.com/en_global/news-insights/economic-insights/wrapping-up-how-paper-and-board-are-back-on-track.html (accessed April 10, 2022).

[58] Paper Market Update, August 2021 | Quad, (n.d.). https://www.quad.com/resources/documents/paper-market-update-august-2021/ (accessed October 6, 2021).

[59] Freight jumped 11% in June to all-time high | American Trucker, (n.d.). https://www.trucker.com/equipment/press-release/21170458/freight-jumped-11-in-june-to-alltime-high (accessed October 6, 2021).

[60] Pulp & paper market size globally 2027 | Statista, (n.d.). https://www.statista.com/statistics/1073451/global-market-value-pulp-and-paper/ (accessed October 6, 2021).

[61] ISO - 85.060 - Paper and board, (n.d.). https://www.iso.org/ics/85.060/x/ (accessed October 7, 2021).

[62] F. of G. arts (UNIZG), General properties of paper/ (absorbency) Thickness-lecture, Zagreb, n.d.

[63] What Paper Grammage Do I Need?, (n.d.). https://www.bbpress.co.uk/news/what-paper-grammage-do-i-need (accessed October 6, 2021).

[64] What's The Difference: Cardboard Vs. Corrugated Cartons, (n.d.). https://inbound.betterpackages.com/blog/whats-the-difference-cardboard-vs.-corrugated-cartons (accessed April 26, 2022).

[65] Figure - corr. boxes, (n.d.). https://lana.hr/wp-content/uploads/2019/07/boxeslana.jpg (accessed May 18, 2022).

[66] O.A. El Seoud, M. Kostag, K. Jedvert, N.I. Malek, Cellulose Regeneration and Chemical Recycling: Closing the "Cellulose Gap" Using Environmentally Benign Solvents, Macromol. Mater. Eng. 305 (2020) 1–21. https://doi.org/10.1002/mame.201900832.

[67] H. Kipphan, Handbook Of Print media, 1st ed., Springer-Verlag Berlin Heidelberg, Berlin-Heidelberg, 2001. https://doi.org/10.1007/978-3-540-29900-4.

[68] ISO standard, ISO 12647-2:2013(en) Graphic technology — Process control for the production of half-tone colour separations, proof and production prints — Part 2: Offset lithographic processes, 2013.

[69] T. Hudika, I. Majnarić, T. Cigula, Influence of the Varnishing "Surface" Coverage on Optical Print Characteristics, Teh. Glas. 14 (2020) 428–433. https://doi.org/10.31803/tg-20191129104559.

[70] Lithography | Tate, (n.d.). https://www.tate.org.uk/art/art-terms/l/lithography (accessed March 10, 2022).

[71] Figure - offset press, (n.d.). https://i.pinimg.com/originals/28/61/36/2861363d8fbd4880b446a073ce32c365.jpg (accessed May 18, 2022).

[72] WATER-BASED PRINTING INK COMPOSITION - SIEGWERK DRUCKFARBEN AG & CO KGAA, (n.d.). https://www.freepatentsonline.com/WO2015165553.html (accessed April 15, 2022).

[73] Varnish | coating | Britannica, (n.d.). https://www.britannica.com/technology/varnish (accessed October 12, 2021).

[74] L. Simonot, M. Elias, Color change due to a varnish layer, Color Res. Appl. 29 (2004) 196–204. https://doi.org/10.1002/col.20008.

[75] D. Macinić, Utjecaj lakiranja na mehanička svojstva ambalaže, Univesrity of Zagreb, 2013.

[76] J. Bota, Optimisation of Coated Paperboard Packaging Properties According to Design, University of Zagreb, 2017.

[77] G. Petković, M. Vukoje, J. Bota, S. Pasanec Preprotić, Enhancement of Polyvinyl Acetate (PVAc) Adhesion Performance by SiO2 and TiO2 Nanoparticles, Coatings. 9 (2019) 707. https://doi.org/10.3390/coatings9110707.

[78] J.P. Kaiser, L. Diener, P. Wick, Nanoparticles in paints: A new strategy to protect façades and surfaces?, J. Phys. Conf. Ser. 429 (2013) 0–10. https://doi.org/10.1088/1742-6596/429/1/012036.

[79] R. Anselmann, Nanoparticles and nanolayers in commercial applications, J. Nanoparticle Res. 3 (2001) 329–336. https://doi.org/10.1023/A:1017529712314.

[80] V.G.L. Souza, A.L. Fernando, Nanoparticles in food packaging: Biodegradability and potential migration to food-A review, Food Packag. Shelf Life. 8 (2016) 63–70. https://doi.org/10.1016/j.fpsl.2016.04.001.

[81] K. El Bourakadi, F.-Z.S.A. Hassani, A.E.K. Qaiss, R. Bouhfid, Antimicrobial coated food packaging paper from agricultural biomass, in: Biopolym. Biocomposites from Agro-Waste Packag. Appl., Elsevier, 2021: pp. 35–63. https://doi.org/10.1016/b978-0-12-819953-4.00013-6.

[82] A. Hardy, D. Benford, T. Halldorsson, M.J. Jeger, H.K. Knutsen, S. More, H. Naegeli, H.

Noteborn, C. Ockleford, A. Ricci, G. Rychen, J.R. Schlatter, V. Silano, R. Solecki, D. Turck, M. Younes, Q. Chaudhry, F. Cubadda, D. Gott, A. Oomen, S. Weigel, M. Karamitrou, R. Schoonjans, A. Mortensen, Guidance on risk assessment of the application of nanoscience and nanotechnologies in the food and feed chain: Part 1, human and animal health, EFSA J. 16 (2018). https://doi.org/10.2903/J.EFSA.2018.5327.

[83] M.J. Hajipour, K.M. Fromm, A. Akbar Ashkarran, D. Jimenez de Aberasturi, I.R. de Larramendi, T. Rojo, V. Serpooshan, W.J. Parak, M. Mahmoudi, Antibacterial properties of nanoparticles, Trends Biotechnol. 30 (2012) 499–511. https://doi.org/10.1016/J.TIBTECH.2012.06.004.

[84] G. V. Vimbela, S.M. Ngo, C. Fraze, L. Yang, D.A. Stout, Antibacterial properties and toxicity from metallic nanomaterials, Int. J. Nanomedicine. 12 (2017) 3941–3965. https://doi.org/10.2147/IJN.S134526.

[85] E. Çerçi, H. Erdost, Stem cell, Ataturk Univ. Vet. Bilim. Derg. 14 (2019) 221–228. https://doi.org/10.17094/ataunivbd.483253.

[86] M.F. Yan, Zinc Oxide, Concise Encycl. Adv. Ceram. Mater. (1991) 523–525. https://doi.org/10.1016/B978-0-08-034720-2.50144-1.

[87] G. Fu, P.S. Vary, C.T. Lin, Anatase TiO 2 nanocomposites for antimicrobial coatings, J. Phys. Chem. B. 109 (2005) 8889–8898. https://doi.org/10.1021/jp0502196.

[88] J. Zhang, P. Zhou, J. Liu, J. Yu, New understanding of the difference of photocatalytic activity among anatase, rutile and brookite TiO2, Phys. Chem. Chem. Phys. 16 (2014) 20382–20386. https://doi.org/10.1039/C4CP02201G.

[89] Titanium dioxide: E171 no longer considered safe when used as a food additive | EFSA, (n.d.). https://www.efsa.europa.eu/en/news/titanium-dioxide-e171-no-longer-considered-safe-when-used-food-additive (accessed October 8, 2021).

[90] Titanium Dioxide Market Trends Analysis Report, 2021-2028, (n.d.). https://www.grandviewresearch.com/industry-analysis/titanium-dioxide-industry (accessed October 8, 2021).

[91] M. Younes, P. Aggett, F. Aguilar, R. Crebelli, B. Dusemund, M. Filipič, M.J. Frutos, P. Galtier, D. Gott, U. Gundert-Remy, G.G. Kuhnle, J.C. Leblanc, I.T. Lillegaard, P. Moldeus, A. Mortensen, A. Oskarsson, I. Stankovic, I. Waalkens-Berendsen, R.A. Woutersen, M. Wright, P. Boon, D. Chrysafidis, R. Gürtler, P. Mosesso, D. Parent-Massin, P. Tobback, N. Kovalkovicova, A.M. Rincon, A. Tard, C. Lambré, Re-evaluation of silicon dioxide (E 551) as a food additive, EFSA J. 16 (2018) 1–70. https://doi.org/10.2903/j.efsa.2018.5088.

[92] K.I. Lee, C.C. Su, K.M. Fang, C.C. Wu, C.T. Wu, Y.W. Chen, Ultrafine silicon dioxide nanoparticles cause lung epithelial cells apoptosis via oxidative stress-activated PI3K/Akt-mediated mitochondria- and endoplasmic reticulum stress-dependent signaling pathways, Sci. Rep. 10 (2020) 1–13. https://doi.org/10.1038/s41598-020-66644-z.

[93] Silicon Dioxide SiO2 for Optical Coating, (n.d.). https://materion.com/resource-center/newsletters/newsletter-archives/coating-materials-news-2000-to-2010/silicon-dioxide-sio2-for-optical-coating (accessed October 8, 2021).

[94] Novavit F 918 SUPREME BIO datasheet, Novavit. 61 (n.d.) 9797. https://flintgrp.com/media/4270/sf_process_ti_f918_e.pdf.

[95] TERRAWET® High Gloss Coating G 9/285 FoodSafe-040 | High Gloss | Matt & Gloss Coatings | Shop by product | Public Portfolio | ACTEGA Germany, (n.d.). https://www.actega.com/de/en/TERRAWET®-High-Gloss-Coating-G-9-285-FoodSafe-040/p/330114319 (accessed March 11, 2022).

[96] R.D. Crackling, Technical Datasheet High Gloss Coating G 9 / 285 FoodSafe Technical Datasheet High Gloss Coating G 9 / 285 FoodSafe, (2015) 50–52.

[97] E. Kampa, T. Dworak, C. Laaser, R. Vidaurre, European regulations, Green Sustain. Pharm. (2010) 253–277. https://doi.org/10.1007/978-3-642-05199-9_17.

[98] European Union, Commission Regulation (EU) No 10/2011 of 14 January 2011, Off. J. Eur. Union. (2011) 1–89. https://eur-lex.europa.eu/LexUriServ/LexUriServ.do?uri=OJ:L:2011:012:0001:0089:EN:PDF.

[99] Definition - Nanomaterials - Environment - European Commission, (n.d.). https://ec.europa.eu/environment/chemicals/nanotech/faq/definition_en.htm (accessed March 11, 2022).

[100] I. Khan, K. Saeed, I. Khan, Nanoparticles: Properties, applications and toxicities, Arab. J. Chem. 12 (2019) 908–931. https://doi.org/10.1016/j.arabjc.2017.05.011.

[101] Zinc oxide, NanoArc, ZN-0605, datasheet, Mater. Saf. Data Sheet. 4(2) (2012) 8–10. https://us.vwr.com/assetsvc/asset/en_US/id/16490607/contents.

[102] Titan dioxide, Sigma A., EC 2015-282-2, datasheet, Mater. Saf. Data Sheet. 4(2) (2012) 8–10. https://us.vwr.com/assetsvc/asset/en_US/id/16490607/contents.

[103] D.I.N.E.N. Iso, V. Unit, M. Safety, D. Sheet, E.I. Ag, AEROSIL ® 200 Hydrophilic fumed silica Characteristic physico - chemical data, 44 (2011) 44–45.

[104] Rapida 105 PRO – Best in Class Rapida 105 PRO : Ready for the future with even higher productivity, (n.d.).

[105] KBA, Figure of KBA 105/ https://www.koenig-bauer.com/fileadmin/user_upload/News/KBA-Sheetfed/2015/04-2015/15-023/F1_Seitenansicht_6_L_Final_CMYK_g.jpg, n.d. https://www.koenig-bauer.com/fileadmin/user_upload/News/KBA-Sheetfed/2015/04-2015/15-023/F1_Seitenansicht_6_L_Final_CMYK_g.jpg.

[106] Figure - up100h_cooled_p0500.jpg, (n.d.). https://www.hielscher.com/image/up100h_cooled_p0500.jpg (accessed May 18, 2022).

[107] DigiCap NX Patterning - TIFF Assembler Plus 4.1 - Kodak Workflow Documentation, (n.d.). https://workflowhelp.kodak.com/display/TAP41/DigiCap+NX+Patterning (accessed April 13, 2022).

[108] Figure - F1-700x700.jpg (700×700), (n.d.). https://www.igt.nl/wp-content/uploads/F1-700x700.jpg (accessed May 18, 2022).

[109] M. Features, K control coat e r, (n.d.).

[110] ISO 4892-2:2013(en), Plastics — Methods of exposure to laboratory light sources — Part 2: Xenon-arc lamps, (n.d.). https://www.iso.org/obp/ui/#iso:std:iso:4892:-2:ed-3:v1:en (accessed April 26, 2022).

[111] Figure Solarbox, n.d. https://www.n-wissen.com/images/02-SOLARBOX-1500-E-with-flooding.jpg.

[112] D. McMullan, Scanning electron microscopy 1928–1965, Scanning. 17 (2006) 175–185. https://doi.org/10.1002/sca.4950170309.

[113] K.C.A. Smith, C.W. Oatley, The scanning electron microscope and its fields of application, Br. J. Appl. Phys. 6 (1955) 391–399. https://doi.org/10.1088/0508-3443/6/11/304.

[114] Figure - JEOL JSM-6460, (n.d.). https://clms.cnsi.ucla.edu/cnsi/clms/equipment-image-display?image_id=965931&image_file_type=image/jpeg (accessed May 18, 2022).

[115] H.H. Momsen, Understanding Color, Printwear. 18 (2005) 32–36. https://doi.org/10.1002/9781119272946.ch10.

[116] Figure - Lab-color-space.jpg, (n.d.). https://images.linshangtech.com/product190119/Lab-color-space.jpg (accessed May 18, 2022).

[117] PSO certification | Fogra, (n.d.). https://fogra.org/en/certification/offset-printing/pso-certification (accessed March 14, 2022).

[118] Spectro-Densitometer - TECHKON - We measure color and more..., (n.d.). https://www.techkon.com/spectrodens-en.html (accessed March 14, 2022).

[119] G. Sharma, W. Wu, E.N. Dalal, The CIEDE2000 color-difference formula: Implementation notes, supplementary test data, and mathematical observations, Color Res. Appl. 30 (2005) 21–30. https://doi.org/10.1002/col.20070.

[120] ISO 12647/2-2013 and Fogra 51/52 | Print Future, (n.d.). http://printfuture.com/print-tribe/iso-126472-2013-and-fogra-5152/ (accessed April 11, 2022).

[121] Techkon, Density of Normal Inking in Offset Printing, 2000.

[122] G. Lychock, Dot Area, Dot Gain, and n-Factors, (1995) 1–9. https://www.xritephoto.com/documents/apps/public/whitepapers/Ga00005a.pdf.

[123] The Murray-Davies Equation: An Origin Story – CMYK History, (n.d.). https://cmykhistory.com/murray-davies-equation-origin-story/ (accessed June 17, 2022).

[124] British standard, BS 3110:1959; Methods for measuring the rub resistance of print, 2007.

[125] A. Timberlake, Bending resistance (stiffness) of paper and paperboard (Taber-type tester in basic configuration) (Revision of T 489 om-08), (2013).

[126] ISO - ISO 2493-1:2010 - Paper and board — Determination of bending resistance — Part 1: Constant rate of deflection, n.d.

[127] W.B. Tester, L & W Bendtsen Tester Lorentzen & Wettre Products | Paper Testing routine measuring with high precision , (n.d.).

[128] Figure Lorentzen & Wettre stiffness tester code 160, (n.d.). https://cdn.productimages.abb.com/9IBA222940_400x400.jpg.

[129] E. Applications, P. Spectroscopy, F. Group, P.M. Shameer, P.M. Nishath, Fourier Transform Infrared Spec- troscopy Exploration and enhancement on fuel stability of biodiesel Microbial Poly-3-Hydroxybutyrate and Related Copolymers Nanoparticle characterization tech- niques, (2019).

[130] How an FTIR Spectrometer Operates, (n.d.). https://chem.libretexts.org/Bookshelves/Physical_and_Theoretical_Chemistry_Textbook_Maps/Supplemental_Modules_(Physical_and_Theoretical_Chemistry)/Spectroscopy/Vibrational_Spectroscopy/Infrared_Spectroscopy/How_an_FTIR_Spectrometer_Operates (accessed March 15, 2022).

[131] Owens, Wendt, Rabel and Kaelble (OWRK) method | KRÜSS Scientific, (n.d.). https://www.kruss-scientific.com/en/know-how/glossary/owens-wendt-rabel-and-kaelble-owrk-method (accessed April 27, 2022).

[132] D.K. Owens, R.C. Wendt, Estimation of the surface free energy of polymers, J. Appl. Polym. Sci. 13 (1969) 1741–1747. https://doi.org/10.1002/app.1969.070130815.

[133] dpiMAX – Comprehensive software for contact angle meters of the OCA series - DataPhysics Instruments, (n.d.). https://www.dataphysics-instruments.com/products/oca/software/ (accessed

April 27, 2022).

[134] ASTM, ASTM D1653-13(2021); Standard Test Methods for Water Vapor Transmission of Organic Coating Films, 2021.

[135] VetBact, (n.d.). http://www.vetbact.org/?displayextinfo=97 (accessed March 27, 2022).

[136] J.Y. Park, K.S. Seo, Staphylococcus Aureus, Food Microbiol. Fundam. Front. (2022) 555–584. https://doi.org/10.1128/9781555819972.ch21.

[137] Brain Heart Infusion Broth, (n.d.). www.liofilchem.net (accessed March 27, 2022).

[138] Mannitol Salt Agar | Principle | Preparation | Interpretation, (n.d.). https://microbiologie-clinique.com/Mannitol-Salt-Agar.html (accessed March 27, 2022).

[139] Cefsulodin irgasan novobiocin (CIN) agar, Prog. Ind. Microbiol. 37 (2003) 428–430. https://doi.org/10.1016/S0079-6352(03)80039-5.

[140] S. Collection, Hippurate Hydrolysis Broth Intended Use : Specimen Collection and Handling : Warning and Precautions : Limitations :, (n.d.) 10–12.

[141] L. Dortet, L. Radoshevich, E. Veiga, P. Cossart, Listeria Monocytogenes, Encycl. Microbiol. (2021) 803–818. https://doi.org/10.1016/B978-0-12-801238-3.02297-2.

[142] T. Min, Listeria Chromogenic Agar Base according to Ottaviani and Agosti (ALOA) ISO Microbiological test, (2020) 15–16.

[143] Pathogen Safety Data Sheets: Infectious Substances – Citrobacter spp. - Canada.ca, (n.d.). https://www.canada.ca/en/public-health/services/laboratory-biosafety-biosecurity/pathogen-safety-data-sheets-risk-assessment/citrobacter.html (accessed March 27, 2022).

[144] Violet Red Bile Glucose Agar (VRBGA) - Selective solid media for microbiology, (n.d.). https://www.biotrend.com/en/buy/cat-violet-red-bile-glucose-agar-vrbga-5518.html (accessed March 27, 2022).

[145] Milipore, YGC Agar (Yeast Extract Glucose Chloramphenicol Agar FIL-IDF) YGC Agar (Yeast Extract Glucose Chloramphenicol Agar FIL-IDF) datasheet, 1992.

[146] M.A. Hubbe, R.A. Gill, Fillers for Papermaking: A Review of their Properties, Usage Practices, and their Mechanistic Role, BioResources. 11 (2016) 2886–2963. https://doi.org/10.15376/BIORES.11.1.2886-2963.

[147] S. GmbH&Co., Anti Set-off Powders for the Printing Industry, n.d.

[148] C.F. Klingshirn, ZnO: Material, physics and applications, ChemPhysChem. 8 (2007) 782–803. https://doi.org/10.1002/CPHC.200700002.

[149] A. Ragauskas, L.A. Lucia, Overview of the lightfastness of commercial printing inks : Understanding the mechanisms of color bleaching Instituteof Paper Scien c e and Technology IP ST Tech n ical Pa p er Series Number 7 01 Overview of the Lightfastness of Commercial Understanding, Inst. Pap. Sci. Technol. Atlanta - Tech. Pap. Ser. 701 (1998).

[150] C. Aydemir, S. Yenidoğan, Light fastness of printing inks: A review, J. Graph. Eng. Des. 9 (2018) 37–43. https://doi.org/10.24867/JGED-2018-1-037.

[151] G. Pfaff, Zinc oxide pigments, Phys. Sci. Rev. 6 (2021) 701–706. https://doi.org/10.1515/PSR-2020-0203/MACHINEREADABLECITATION/RIS.

[152] L. Majetic, Properties of PCL-coated imprints coated with Silica, University of Zagreb, 2020.

[153] Chroma - The Chroma of Color Explained in Plain English with Case Studies, (n.d.). https://thelandofcolor.com/chroma-explained-in-plain-english-with-case-studies/ (accessed

March 31, 2022).

[154] M. Vukoje, R. Kulˇ, K. Itri, Improvement in Thermochromic Offset Print UV Stability by Applying PCL Nanocomposite Coatings, (2022).

[155] G. Pfaff, Titanium dioxide pigments, Phys. Sci. Rev. 6 (2021) 679–696. https://doi.org/10.1515/PSR-2020-0199/HTML.

[156] S. Krishnan, A. Shriwastav, Application of TiO2 nanoparticles sensitized with natural chlorophyll pigments as catalyst for visible light photocatalytic degradation of methylene blue, J. Environ. Chem. Eng. 9 (2021) 104699. https://doi.org/10.1016/j.jece.2020.104699.

[157] T.N. Company, Brand Datasheet, (2015) 11475.

[158] R.A.I. Albattat, Z. Jamshidzadeh, A.K.R. Alasadi, Assessment of compressive strength and durability of silica fume-based concrete in acidic environment, Innov. Infrastruct. Solut. 5 (2020) 1–7. https://doi.org/10.1007/s41062-020-0269-1.

[159] W.M. Bundy, J.N. Ishley, Kaolin in paper filling and coating, Appl. Clay Sci. 5 (1991) 397–420. https://doi.org/10.1016/0169-1317(91)90015-2.

[160] S.Z. Erhan, M.O. Bagby, Vegetable-oil-based printing ink formulation and degradation, Ind. Crops Prod. 3 (1995) 237–246. https://doi.org/10.1016/0926-6690(94)00040-6.

[161] Y. Dou, F. Li, B. Tang, G. Zhou, Surface wettability tuning of acrylic resin photoresist and its aging performance, Sensors. 21 (2021). https://doi.org/10.3390/S21144866/S1.

[162] H. Ennaceri, L. Wang, D. Erfurt, W. Riedel, G. Mangalgiri, A. Khaldoun, A. El Kenz, A. Benyoussef, A. Ennaoui, Water-resistant surfaces using zinc oxide structured nanorod arrays with switchable wetting property, Surf. Coatings Technol. 299 (2016) 169–176. https://doi.org/10.1016/j.surfcoat.2016.04.056.

[163] W.-J. Li, E.-W. Shi, W.-Z. Zhong, Z.-W. Yin, W.-J. Li, E.-W. Shi, W.-Z. Zhong, Z.-W. Yin, Growth mechanism and growth habit of oxide crystals, JCrGr. 203 (1999) 186–196. https://doi.org/10.1016/S0022-0248(99)00076-7.

[164] N. Stevens, C.I. Priest, R. Sedev, J. Ralston, Wettability of photoresponsive titanium dioxide surfaces, Langmuir. 19 (2003) 3272–3275. https://doi.org/10.1021/la020660c.

[165] J.B. Rosenholm, Critical comparison of molecular mixing and interaction models for liquids, solutions and mixtures, Adv. Colloid Interface Sci. 156 (2010) 14–34. https://doi.org/10.1016/j.cis.2010.02.005.

[166] N. Dumitrascu, C. Borcia, Adhesion properties of polyamide-6 fibres treated by dielectric barrier discharge, Surf. Coatings Technol. 201 (2006) 1117–1123. https://doi.org/10.1016/j.surfcoat.2006.01.030.

[167] S. Grilj, M. Klanjšek Gunde, R. Szentgyörgyvölgyi, D. Gregor-Svetec, FT-IR and UV / VIS analysis of classic and recycled papers, Papíripar. (2012) 7–13.

[168] H.G. Leach, R.H., Pierce, R.J., Hickman, E.P., Mackenzie, M.J. and Smith, The Printing Ink Manual, Springer, 2007.

[169] T.V. Nguyen, P. Nguyen Tri, T.D. Nguyen, R. El Aidani, V.T. Trinh, C. Decker, Accelerated degradation of water borne acrylic nanocomposites used in outdoor protective coatings, Polym. Degrad. Stab. 128 (2016) 65–76. https://doi.org/10.1016/j.polymdegradstab.2016.03.002.

[170] J. Miklečić, S.L. Blagojević, M. Petrič, V. Jirouš-Rajković, Influence of TiO2 and ZnO nanoparticles on properties of waterborne polyacrylate coating exposed to outdoor conditions, Prog. Org. Coatings. 89 (2015) 67–74. https://doi.org/10.1016/j.porgcoat.2015.07.016.

[171] C. Ma, W.J. Koros, High-performance ester-crosslinked hollow fiber membranes for natural gas separations, J. Memb. Sci. 428 (2013) 251–259. https://doi.org/10.1016/j.memsci.2012.10.024.

[172] D. Raymand, A.C.T. van Duin, D. Spångberg, W.A. Goddard, K. Hermansson, Water adsorption on stepped ZnO surfaces from MD simulation, Surf. Sci. 604 (2010) 741–752. https://doi.org/10.1016/j.susc.2009.12.012.

[173] What Is The Ionic Charge Of Zinc (Zn)? | Science Trends, (n.d.). https://sciencetrends.com/what-is-the-ionic-charge-of-zinc-zn/ (accessed June 28, 2022).

[174] C.J. van Oss, M.K. Chaudhury, R.J. Good, Monopolar surfaces, Adv. Colloid Interface Sci. 28 (1987) 35–64. https://doi.org/10.1016/0001-8686(87)80008-8.

[175] S. Benkoula, O. Sublemontier, M. Patanen, C. Nicolas, F. Sirotti, A. Naitabdi, F. Gaie-Levrel, E. Antonsson, D. Aureau, F.X. Ouf, S.I. Wada, A. Etcheberry, K. Ueda, C. Miron, Water adsorption on TiO2 surfaces probed by soft X-ray spectroscopies: Bulk materials vs. isolated nanoparticles, Sci. Rep. 5 (2015) 1–11. https://doi.org/10.1038/srep15088.

[176] A. Nazari, S. Riahi, Corrigendum to " The effect of TiO2 nanoparticles on water permeability and thermal and mechanical properties of high strength self compacting concrete," Mater. Sci. Eng. A. 528 (2011) 3526. https://doi.org/10.1016/j.msea.2011.01.047.

[177] A. Hegyi, H. Szilagyi, E. Grebenişan, A.V. Sandu, A.V. Lăzărescu, C. Romila, Influence of TiO2 nanoparticles addition on the hydrophilicity of cementitious composites surfaces, Appl. Sci. 10 (2020). https://doi.org/10.3390/app10134501.

[178] Z. Zołek-Tryznowska, Additives for Ink Manufacture, Print. Polym. Fundam. Appl. (2015) 57–66. https://doi.org/10.1016/B978-0-323-37468-2.00004-X.

[179] N.A. Smirnov, S.I. Kudryashov, A.A. Nastulyavichus, A.A. Rudenko, I.N. Saraeva, E.R. Tolordava, S.A. Gonchukov, Y.M. Romanova, A.A. Ionin, D.A. Zayarny, Antibacterial properties of silicon nanoparticles, Laser Phys. Lett. 15 (2018) 105602. https://doi.org/10.1088/1612-202X/AAD853.

[180] S.Y. Yeo, H.J. Lee, S.H. Jeong, Preparation of nanocomposite fibers for permanent antibacterial effect, J. Mater. Sci. 38 (2003) 2143–2147. https://doi.org/10.1023/A:1023767828656.

[181] J. Jiang, G. Oberdörster, A. Elder, R. Gelein, P. Mercer, P. Biswas, Does nanoparticle activity depend upon size and crystal phase?, Nanotoxicology. 2 (2008) 33–42. https://doi.org/10.1080/17435390701882478.

[182] S.A. Kadhum, The effect of two types of nano-particles (ZnO & SiO2) on different types of bacterial growth, Biomed. Pharmacol. J. 10 (2017) 1701–1708. https://doi.org/10.13005/BPJ/1282.

Annex 1, List of shortcuts and acronyms (Sorted alphabetically)

CA - Contact angle

CAGR- Compound annual growth rate

CIELAB - International Commission on Illumination colour space model (L*a*b*) theory

*CIE L*a*b** - Colour space model L*a*b*

CMYK -Cyan, Magenta, Yellow, BlacK

EDS - Energy-dispersive X-ray spectroscopy

FOGRA PSO – Fogra's PSO "Process Standard Offset Printing"

FTIR - Fourier-transform infrared spectroscopy

Hybrid/T - SiO_2TiO_2 nanocoating

Hybrid/Z - SiO_2ZnO nanocoating

ISO - International Organization for Standardization

NCs - Nanocoatings

NPs - Nanoparticles

SEM -Scanning electron microscope

SFE - Surface free energy

SiO_2 - Silicon dioxide

SI/NC - Silicon dioxide nanocoating

TiO_2 - Titan dioxide

TI/NC - Titan dioxide nanocoating

OWRK - Owens, Wendt, Rabel and Kaelble method

RH – Relative humidity

Paper - Substrate

WB - Water based varnish

WVTR - Water-vapour transmission rate

ZnO - Zink oxid

ZN/NC - Zink oxid nanocoating

Annex 2 List of figures and tables

2.1 Tables

2.2 Figures

Annex 3 Survey used in preliminary research

1 - Vaš spol?

M/Ž

2 - Vaša dob?

18-25/ 25-35/ 35-50/ 50-60/ 60+

3 - Koje je Vaše formalno završeno obrazovanje?

Osnovna škola/ Srednja škola/ Viša škola/ Fakultet/ Doktorat

4 - Imate li djece?

Da/Ne

5 - Ukoliko je ambalaža oštećena utječe li to na Vašu odluku o kupnji?

Da/Ne

6 - Koji je Vaš stav kada vidite "oštećenu" ambalažu na polici dućana? Oštećeno po sljedećim kriterijima: izblijedjela slika, blago namreškana površina ambalaže, blago strukturalno oštećenje (oštećen kut ili rub pakiranja).

Mislim da je oštećen i proizvod/ Mislim da je proizvod sačuvan od vanjskog oštećenja ambalaže

7 - Ukoliko prilikom kupnje vidite "oštećenu" ambalažu na polici dućana, koja je Vaša reakcija? Oštećeno po sljedećim kriterijima: izblijedjela slika, blago namreškana površina ambalaže, blago strukturalno oštećenje (oštećen kut ili rub pakiranja).

Uzimam i kupujem jer mi je svejedno/ Uzimam i tražim popust/ Uzimam isti proizvod ali sačuvanog pakiranja/ Kupujem sličan proizvod, ali druge marke

8 - Prilikom kupnje jeftinijih proizvoda, smatrate li da ambalaža (pakiranje) reflektira i kvalitetu proizvoda (sadržaj pakiranja)?

Uopće se ne slažem/ Ne slažem se/ Ne znam/nemam mišljenje/ Slažem se/ U potpunosti se slažem

9 - Prilikom kupnje skupljih proizvoda, smatrate li da ambalaža (pakiranje) reflektira i kvalitetu proizvoda (sadržaj pakiranja)?

Uopće se ne slažem/ Ne slažem se/ Ne znam/nemam mišljenje/ Slažem se/ U potpunosti se slažem

10 - Prilikom kupnje jeftinijih proizvoda, koliko Vam je bitna ambalaža?

Bitno mi je jer reflektira kvalitetu / Bitno mi je jer kupujem cijeli "paket" (pakiranje i proizvod) / Nije mi bitno jer kupujem proizvod (sadržaj pakiranja)

11 - Prilikom kupnje skupljih proizvoda, koliko Vam je bitna ambalaža?

Bitno mi je jer reflektira kvalitetu / Bitno mi je jer kupujem cijeli "paket" (pakiranje i proizvod) / Nije mi bitno jer kupujem proizvod (sadržaj pakiranja)

12 - Ukoliko je ambalaža oštećena: u smislu izblijedjele slike ili slikovne informacije; smatrate li da je i proizvod (sadržaj pakiranja) oštećen?

Uopće se ne slažem/ Ne slažem se/ Ne znam/nemam mišljenje/ Slažem se/ U potpunosti se slažem

13 - Ukoliko je ambalaža oštećena: u smislu nabreškane površine pakiranja (usred djelovanja vlage npr.); smatrate li da je i proizvod (sadržaj pakiranja) oštećen?

Uopće se ne slažem/ Ne slažem se/ Ne znam/nemam mišljenje/ Slažem se/ U potpunosti se slažem

14 - Ukoliko je ambalaža oštećena: u smislu izgrebane površine pakiranja (mehaničkog oštećenja površine npr.); smatrate li da je i proizvod (sadržaj pakiranja) oštećen?

Uopće se ne slažem/ Ne slažem se/ Ne znam/nemam mišljenje/ Slažem se/ U potpunosti se slažem

15 - Ukoliko je ambalaža oštećena: u smislu strukturalne stabilnosti pakiranja (mehaničkog oštećenja djelovanja sile npr.); smatrate li da je i proizvod (sadržaj pakiranja) oštećen?

Uopće se ne slažem/ Ne slažem se/ Ne znam/nemam mišljenje/ Slažem se/ U potpunosti se slažem

16 - Da li zbog pandemije COVIDa imate povećanu zabrinutost o mikrobima (bakterijama, virusima, gljivicama) na površini ambalaže?

Imam (općenito)/ Nemam (općenito)/ Nemam mišljenje (svejedno mi je)/ Imam i brine me/ Imam i zaista sam zabrinut/a

17 - Ukoliko ambalaža proizvoda ima neki oblik mikrobne zaštite (poseban premaz) bi li Vam takav proizvod bio privlačniji?

Da znam, bio bi/ Ne bi/ Nemam mišljenje (svejedno mi je)

18 - Ukoliko ambalaža proizvoda ima neki oblik mikrobne zaštite (poseban premaz) bi li za taj proizvod bili spremniji platiti više?

Da/Ne/ Nemam mišljenje (svejedno mi je)

19 - Da li razmišljate o ekološkom aspektu ambalaže?

Da/Ne/ Nemam mišljenje (svejedno mi je)

20 - Da li ste za ekološki prihvatljiviju ambalažu spremni platiti više?

Da/Ne/ Nemam mišljenje (svejedno mi je)

Biography

Tomislav Hudika was born March 12th, 1990, in Zagreb, Croatia; where he finished School of Applied Arts and Design, with major in graphic design under supervision of late prof. Damir Brčić. Tomislav partook in many domestic and foreign design and digital illustration exhibitions during his school days. In 2009 he enrolled in the Faculty of Graphic Arts (GRF) in Zagreb, with undergraduate and graduate major in design of graphic products. After university degree, he moves to Basel (CH). In 2015 he was invited to European Patent Office as a patent examiner intern, but he chooses to return to Croatia instead. That year he employs himself in Denona printhouse as printing engineer. In 2018 he gets the job as a research assistant on a science project founded by Croatian Science Foundation (HRZZ) on GRF under doc. Tomislav Cigula's, phD, supervision where he currently works. His current scientific works is based on the printing varnish modulation with nanoparticles as well as work on intellectual property rights.

Published papers

[1] Cigula, Tomislav; Hudika, Tomislav; Tomašegović, Tamara; *Lightfastness, surface and interfacial properties of colour-printed paper substrates coated with PCL/ZnO and PCL/TiO_2 nanocomposites*//Surfaces and Interfaces, 27 (2021), 101522, 13 doi:10.1016/j.surfin.2021.101522

[2] Cigula, Tomislav; Hudika, Tomislav; Vukoje, Marina; *Modulation of water based commercial varnish by adding ZnO and Sio_2 nanoparticles to enhance protective function on printed packaging* // Proceedings of the 2nd International Conference on Circular Packaging / Karlovits, Igor (ur.). Slovenj Gradec: Pulp and Paper Institute, Faculty of Polymer Technology, 2021. str. 249-260 doi:10.5281/zenodo.5256586

[3] Cigula, Tomislav; Hudika, Tomislav; Donevski, Davor; *Color reproduction on varnished cardboard packaging by using lower ink coverages due to the gray component replacement image processing* // Color Research & Application, 47 (2021), 1; 172-181 doi:10.1002/col.22704

[4] Hudika, Tomislav; Cigula, Tomislav; Vukoje, Marina; *Antimicrobial properties of TiO_2 nanocomposite coating* // Proceedings 13th International Conference on Nanomaterials - Research & Application, Brno, 2021. 4345, 8 doi:10.37904/nanocon.2021.4345

[5] Hudika, Tomislav; Tomašegović, Tamara; Cigula, Tomislav; Prša, Marija; *Polycaprolactone primers with zinc oxide and silicon dioxide nanoparticles for paper substrates: Influence on the properties of cyan and magenta offset prints* // Coloration technology, 136 (2020), 5; 435-449 doi:10.1111/cote.12487

[6] Hudika, Tomislav; Cigula, Tomislav; Majnarić, Igor; *Influence of the Varnishing "Surface" Coverage on Optical Print Characteristics* // Tehnički glasnik - Technical journal, Vol. 14 No. 4, 2020. (2020), 428-433 doi:10.31803/tg-20191129104559

[7] Cigula, Tomislav; Hudika, Tomislav; Katana, Mihael; Golik Krizmanić, Marina; Tomašegović, Tamara; *The influence of PCL-ZnO coating composition on coated offset cardboard prints* // Proceedings - The Tenth International Symposium GRID 2020 / Dedijer, Sandra (ur.)., Novi Sad: University of Novi Sad, Faculty of technical sciences, Department of graphic engineering and design,, 2020. str. 101-108 doi:10.24867/grid-2020-p8

[8] Hudika, Tomislav; Cigula, Tomislav; Žličarić, Mihaela; Strižić Jakovljević, Maja; *PCL-TiO2 nanocomposite to improve ageing of offset prints* // Proceedings - The Tenth International Symposium GRID 2020 / Dedijer, Sandra (ur.)., Novi Sad: University of Novi Sad, Faculty of technical sciences, Department of graphic engineering and design,, 2020. str. 119-129 doi:10.24867/grid-2020-p10

[9] Donevski, Davor; Poljičak, Ante; Prša, Marija; Hudika, Tomislav; *Adjustable color transformation model* // Proceedings ELMAR-2019 / Muštra, Mario ; Vuković, Josip ; Zovko-Cihlar, Branka (ur.)., Zagreb: Faculty of Electrical Engineering and Computing, University of Zagreb, 2019. str. 69-72

[10] Cigula, Tomislav; Tomašegović, Tamara; Hudika, Tomislav; *Effect of the paper surface properties on the ink transfer parameters in offset printing* // Nordic pulp & paper research journal, 34 (2019), 4; 540-549 doi:10.1515/npprj-2019-0018

[11] Cigula, Tomislav; Tomašegović, Tamara; Hudika, Tomislav; Donevski, Davor; *Influence of the ink and substrate properties on the ink transfer in lithography* //

GRID2018 proceedings / Kašiković, Nemanja (ur.)., Novi Sad: Faculty of Technical Sciences, 2018. str. 45-50 doi:10.24867/grid-2018-p4

[12] Hudika, Tomislav; Tomašegović, Tamara; Cigula, Tomislav; Poljičak, Ante; *Analysis of the interactions in the "varnish - photopolymer" system* // GRID 2018 Proceedings / Kašiković, Nemanja (ur.)., Novi Sad: UNIVERSITY OF NOVI SAD, FACULTY OF TECHNICAL SCIENCES, 2018. str. 151-159 doi:10.24867/GRID-2018-p18

[13] Hudika, Tomislav; Modelling of the *line graphic on individualized typographic cut for the purpose of currency security protection*, 2015, graduate paper, Faculty of graphic arts, Zagreb

[14] Hudika, Tomislav; *Possibilities of image reproduction with polymer printing plate*, 2013., undergraduate paper, Faculty of graphic arts, Zagreb

[15] Hudika, Tomislav; Tomašegović, Tamara; Mahović Poljaček, Sanja; *Offset printing plates: alternative method for quality control* // GRID 2012 proceedings / Novaković, Dragoljub (ur.)., Novi Sad: Faculty of Technical Science, Department of Graphic Engineering and Design, 2012. str. 129-133